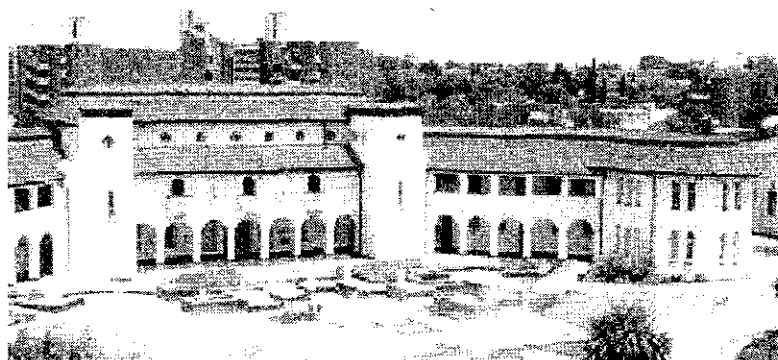
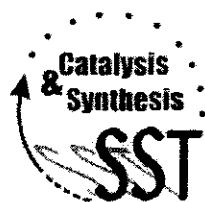


# THE METATHESIS ACTIVITY AND DEACTIVATION OF HETEROGENEOUS METAL OXIDE CATALYTIC SYSTEMS

D.J. Moodley  
Hons. B.Sc. (Natal)



Dissertation submitted in partial fulfilment  
of the requirements for the degree  
Magister Scientiae  
in  
Chemistry  
of the  
Potchefstroomse Universiteit vir Christelike Hoër Onderwys



Supervisor: Prof. H.C.M. Vosloo  
Co-supervisor: Dr. C. van Schalkwyk

October 2003  
Potchefstroom



Potchefstroomse Universiteit  
vir Christelike Hoër Onderwys

**PUKKE**



# TABLE OF CONTENTS

---

<b>LIST OF ABBREVIATIONS .....</b>	<b>V</b>
<b>1 INTRODUCTION AND AIM OF STUDY .....</b>	<b>1</b>
1.1 Background.....	1
1.2 Aim of Study .....	4
1.3 References .....	5
<b>2 THE OLEFIN METATHESIS REACTION.....</b>	<b>7</b>
2.1 Introduction .....	7
2.2 Industrial applications of olefin metathesis .....	9
2.3 Applications of olefin metathesis in organic chemistry .....	15
2.3.1 Synthesis of natural products.....	15
2.4 References .....	16
<b>3 MECHANISM OF METATHESIS AND SIDE REACTIONS.....</b>	<b>18</b>
3.1 Introduction .....	18
3.1.1 Transalkylidenation versus transalkylation .....	18
3.1.2 The metal carbene/metallacyclobutane mechanism .....	19
3.1.3 Formation of the metal carbene .....	20
3.1.4 Termination reactions of the metal carbene/metallacyclobutane intermediate ..	22
3.2 Mechanism of isomerization on $WO_3/SiO_2$ metathesis catalysts .....	23
3.3 Mechanism of coke formation on metal oxide catalysts .....	26
3.3.1 Introduction .....	26
3.3.2 Mechanism of coke formation from olefins .....	26
3.4 References .....	28
<b>4 CATALYST SYSTEMS .....</b>	<b>30</b>
4.1 Introduction .....	30
4.2 Homogeneous catalysts .....	31
4.3 Heterogeneous catalysts .....	32
4.3.1 Rhenium-based catalysts .....	32
4.3.2 Molybdenum-based catalysts .....	33
4.3.3 Tungsten-based catalysts .....	34
4.4 The $WO_3/SiO_2$ catalyst system.....	35
4.4.1 Structure and metathesis activity of $WO_3/SiO_2$ catalysts .....	35
4.4.2 Induction period.....	38
4.4.3 Factors affecting activity of $WO_3$ catalysts .....	39
4.4.4 Coke formation on tungsten-based catalysts .....	42
4.5 References .....	42

---

<b>5</b>	<b>EXPERIMENTAL</b> .....	<b>45</b>
5.1	Reagents .....	45
5.2	Apparatus.....	45
5.2.1	Percolation of feed .....	45
5.2.2	Metathesis Reactions .....	46
5.3	Analysis .....	48
5.3.1	Analysis of liquid product samples .....	48
5.3.2	Analysis of gaseous product samples .....	49
5.3.3	Data evaluation .....	49
5.4	Catalyst Preparation.....	52
5.4.1	Preparation of $\text{WO}_3/\text{SiO}_2$ catalysts with different tungsten loadings .....	52
5.4.2	Preparation of alkali doped $\text{WO}_3/\text{SiO}_2$ catalysts .....	52
5.4.3	Pretreatment of the $\text{WO}_3/\text{SiO}_3$ catalyst.....	52
5.5	Characterization techniques.....	53
5.5.1	X-Ray Diffraction (XRD).....	53
5.5.2	Surface area analysis .....	53
5.5.3	Laser Raman Spectroscopy (LRS) .....	53
5.5.4	Inductively coupled plasma-atomic emission spectroscopy (ICP-AES).....	53
5.5.5	Transmission electron microscopy (TEM) .....	54
5.5.6	Scanning electron microscopy (SEM).....	54
5.5.7	Thermogravimetry (TG) .....	55
5.5.8	Ultraviolet-visible (UV-Vis) spectroscopy.....	56
5.5.9	Water and carbonyl analysis.....	57
5.6	References .....	57
<b>6</b>	<b>RESULTS AND DISCUSSION</b> .....	<b>58</b>
6.1	Introduction .....	58
6.2	Influence of metal loading on catalyst structure and metathesis activity .....	60
6.2.1	Catalyst characterization.....	60
6.2.2	Influence of metal loading on the metathesis activity of the $\text{WO}_3/\text{SiO}_2$ catalyst using a 1-octene feed .....	64
6.2.3	Metathesis of 1-octene with the 8 wt% $\text{WO}_3/\text{SiO}_2$ catalyst.....	67
6.2.4	Metathesis of an industrial cut 1-heptene feed with the 8 wt% $\text{WO}_3/\text{SiO}_2$ catalyst.....	67
6.3	Influence of ionic modification of the catalyst with Alkali metal ions .....	68
6.3.1	Influence of doping with 0.1 wt% of alkali metal ions on metathesis activity and selectivity .....	67
6.3.2	The influence of the sequence of impregnation of alkali metal ions.....	70
6.3.3	The influence of alkali metal loading on metathesis activity and selectivity .....	70
6.4	Lifetime, regeneration and coking studies of the 8 wt% $\text{WO}_3/\text{SiO}_2$ catalyst .....	72
6.4.1	Lifetime and effect of regeneration of the catalyst.....	72
6.4.2	Characterisation of fresh, spent and regenerated catalysts .....	75
6.4.3	Location of coke on the catalyst.....	78
6.5	Factors effecting coke formation.....	81

---

6.5.1	Coke formation as a function of temperature .....	81
6.5.2	Coke formation as a function of space velocity .....	82
6.5.3	Coke formation as a function of time online .....	82
6.5.4	Influence of olefin content in feed.....	83
6.5.5	Influence of oxygenated components on coke formation on the 8 wt% WO <sub>3</sub> /SiO <sub>2</sub> catalyst .....	84
6.6	Influence of oxygenates on the 8 wt% WO <sub>3</sub> /SiO <sub>2</sub> catalyst.....	85
6.6.1	Influence of Lewis bases on the activity and selectivity of the 8 wt% WO <sub>3</sub> /SiO <sub>2</sub> catalyst .....	85
6.6.2	The influence of Brønsted acids on the activity and selectivity of the 8 wt% WO <sub>3</sub> /SiO <sub>2</sub> catalyst .....	87
6.6.3	The influence of oxygenates on the activity and selectivity of the 8 wt% WO <sub>3</sub> /SiO <sub>2</sub> catalyst when operating in the recycle mode .....	90
6.6.4	The influence of oxygenates on the colour of the product produced <i>via</i> metathesis over the 8 wt% WO <sub>3</sub> /SiO <sub>2</sub> catalyst .....	92
6.6.5	The influence of a fixed concentration of oxygenate on the colour of the product produced <i>via</i> metathesis over the 8 wt% WO <sub>3</sub> /SiO <sub>2</sub> catalyst .....	97
6.7	Summary of important results .....	99
6.8	References .....	100
<b>7</b>	<b>CONCLUSIONS .....</b>	<b>101</b>
7.1	Metathesis reactions over WO <sub>3</sub> /SiO <sub>2</sub> catalysts.....	101
7.2	The WO <sub>3</sub> /SiO <sub>2</sub> catalyst system.....	102
7.2.1	Introduction .....	102
7.2.1	Characterisation of WO <sub>3</sub> /SiO <sub>2</sub> catalysts with different WO <sub>3</sub> loadings.....	102
7.3	Factors that influence the WO <sub>3</sub> /SiO <sub>2</sub> catalyst.....	103
7.3.1	Influence of WO <sub>3</sub> loading on the metathesis activity and selectivity of an 8 wt% WO <sub>3</sub> /SiO <sub>2</sub> catalyst .....	103
7.3.2	Influence of metal loading on the stability of the catalysts .....	104
7.3.3	Influence of alkali metal doping on metathesis activity .....	104
7.3.4	Influence of alkali metal ion loading of metathesis activity.....	105
7.3.5	The influence of sequence of impregnation of alkali metal ions.....	106
7.4	Lifetime, regeneration and coking studies.....	107
7.4.1	Lifetime and effect of regeneration of the catalyst.....	107
7.4.2	Characterisation of fresh, spent and regenerated catalysts .....	108
7.4.3	Location of coke on the catalyst .....	108
7.4.4	Factors effecting coke formation.....	109
7.5	Influence of oxygenates on the activity and selectivity of the 8 wt% WO <sub>3</sub> /SiO <sub>2</sub> catalyst .....	111
7.5.1	Influence of Lewis bases on the activity and selectivity of the 8 wt% WO <sub>3</sub> /SiO <sub>2</sub> catalyst .....	111
7.5.2	Influence of Brønsted acids on the activity and selectivity of the 8 wt% WO <sub>3</sub> /SiO <sub>2</sub> catalyst .....	113
7.5.3	The influence of oxygenates on the activity and selectivity of the 8 wt% WO <sub>3</sub> /SiO <sub>2</sub> catalyst in the recycle mode.....	114
7.5.4	The influence of oxygenates on the colour of the product .....	114

---

7.6 Summary.....	116
7.7 References .....	117
<b>SUMMARY.....</b>	<b>119</b>
<b>OPSOMMING.....</b>	<b>121</b>
<b>ACKNOWLEDGMENTS .....</b>	<b>123</b>

## LIST OF ABBREVIATIONS

---

ADMET	Acyclic diene metathesis
CCD	Charged coupled device
DA	Detergent alcohol
$d_i$	Inner diameter
$d_o$	Outer diameter
EDS	Energy dispersive spectroscopy
EELS	Electron energy loss spectroscopy
EFTEM	Energy filtered transmission electron microscopy
ESR	Electron spin resonance
Et	Ethyl
FEAST	Further exploitation of advanced Shell technology
FCC	Fluid catalytic cracking
FID	Flame ionization detector
FT	Fischer-Tropsch
GC	Gas chromatograph
GIF	Gatan imaging filter
HDMS	Hexamethyldisilazane
HOMO	Highest occupied molecular orbital
HPLC	High pressure liquid chromatograph
HRSEM	High resolution scanning electron microscopy
HRTEM	High resolution transmission electron microscopy
ICP	Inductively coupled plasma
ICP-AES	Inductively coupled plasma-Atomic emission spectroscopy
<i>i</i> -olefin	Internal olefin
IR	Infra-red
LAB	Linear alkyl benzenes
LABS	Linear alkyl benzene sulphonates
LHSV	Liquid hourly space velocity (volume feed/volume catalyst.h <sup>-1</sup> )
LRS	Laser Raman spectroscopy
LUMO	Lowest unoccupied molecular orbital
Me	Methyl
MTBE	Methyl tert-butyl ether
OCT	Olefins conversion technology

---

Pr	Propyl
RCM	Ring-closing metathesis
ROM	Ring-opening metathesis
ROMP	Ring-opening metathesis polymerization
SHOP	Shell higher olefins process
SLO	Stabilized light oil
TEM	Transmission electron microscopy
TG	Thermogravimetry
UV-Vis	Ultra violet-visible
WHSV	Weight hourly space velocity (mass feed/mass catalyst.h <sup>-1</sup> )
XRD	X-ray diffraction

# 1 INTRODUCTION AND AIM OF STUDY

---

## 1.1 Background

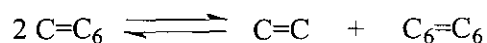
Most of the  $\alpha$ -olefin production in the world is ethene-based and results in the production of even numbered  $\alpha$ -olefins.<sup>1-3</sup> SASOL's Fischer-Tropsch (FT) process is based on synthesis gas ( $H_2$  and CO) and results in the production of a range of even and odd numbered  $\alpha$ -olefins.<sup>4</sup> Historically the odd numbered, low molecular weight  $\alpha$ -olefins (especially 1-heptene) are of low value. Olefin metathesis can play an important role in converting these low value olefins to higher value, longer chain olefins in the detergent range ( $C_{10}$ - $C_{13}$ ).<sup>5</sup>

When a linear olefin undergoes self-metathesis a longer chain symmetrical internal olefin and ethene is produced.<sup>6</sup> Double bond isomerization of the substrate olefin gives rise to internal isomers which can in turn undergo secondary metathesis to give a range of longer chain products. The case can be illustrated for 1-heptene as depicted in Scheme 1.1.

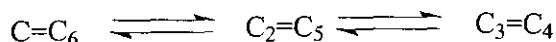
Scheme 1.1 depicts only secondary metathesis products which form when 2-heptene reacts with 1-, 2- and 3-heptene only. There are various other combinations which may occur, giving rise to a statistical distribution of products. A possibility may exist for isomerization of the internal olefin product and this will further complicate the product spectrum. It can be concluded that if a suitable catalyst system is used different longer chain internal olefins in the desired range ( $C_{10}$ - $C_{13}$ ) can be produced.

Olefins in the  $C_{10}$ - $C_{13}$  range can be converted to alcohols by a hydroformylation process, in which olefins react with synthesis gas to form aldehydes, which in turn are hydrogenated (Scheme 1.2).<sup>7</sup> By using the correct catalyst an internal olefin can be hydroformylated and hydrogenated to form a linear alcohol, because under the appropriate reaction conditions, isomerization of the double bond takes place, and  $\alpha$ -olefins can be formed before the hydroformylation step.<sup>8</sup>

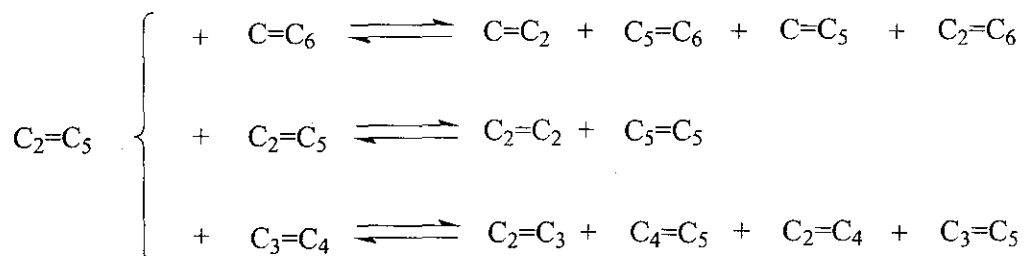
Primary metathesis:



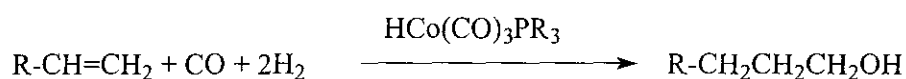
Double bond isomerization:



Secondary metathesis:



**Scheme 1.1** Role of double bond isomerization in 1-heptene metathesis (only carbon atoms and double bonds shown for simplicity).



**Scheme 1.2** The hydroformylation of an olefin to an alcohol.

An example of this technology is in the Shell Higher Olefin Process, where internal olefin fractions obtained from ethene are converted with synthesis gas to alcohols.<sup>9</sup> The alcohol mixtures formed consist of up to 80% linear compounds and are used in the plasticizer and detergent industries. These alcohols are important intermediates for a large number of chemical products, but over 95% of them are used in detergents.<sup>10</sup> To a lesser extent they are used directly as wetting, emulsifying, and foaming agents.

Internal olefins may also be used as feedstock for the alkylation of benzene to form linear alkyl benzene sulphonates (LABS). LABS are the most important synthetic materials in the surfactant industry. These are synthesized on an industrial scale by the alkylation of benzene with high molecular weight olefins (C<sub>10</sub>-C<sub>13</sub>).<sup>11</sup>

In order to commercialise a metathesis process that produces internal olefins from  $\alpha$ -olefins a number of factors need to be considered, e.g., the choice and selectivity of catalyst, lifetime and regeneration of the catalyst, resistance to poisons and fouling.

The catalyst of choice should not necessarily be highly selective to the primary metathesis products. It should allow an appreciable amount of isomerization to occur, since a range of olefins is desired as the product. However should it be required that the primary product selectivity be increased, it must be possible to fine tune the catalyst to achieve this outcome. Often the requirement for detergent range olefins is that the range peaks at the C<sub>12</sub> olefin.<sup>5</sup>

Industrial feeds often have many impurities and poisons present. It is well known that metathesis catalysts are sensitive to trace amounts of certain feed impurities, especially polar compounds. Water, air, carbon monoxide, acetone and methanol have been reported as catalyst poisons.<sup>12</sup> Feed purification is often necessary and may be costly. In addition autoxidation of olefinic feeds lead to formation of peroxides, which deactivate metathesis catalysts.<sup>13</sup> It is desirable to use catalysts which are less sensitive to catalyst poisons and that can be regenerated easily.

Metathesis is often accompanied by isomerization which is a reaction catalyzed by acid sites.<sup>14</sup> Side reactions on acid sites often lead to the formation of carbonaceous deposits on the catalyst. The build-up of these deposits eventually leads to deactivation of the catalyst.<sup>15</sup> Finding ways to limit carbon deposition is an important economic objective.

Regeneration of the classical transition metal oxide supported metathesis catalysts is achieved by burning of the carbonaceous material at 600 °C in air. Most of these catalysts can retain their activity after numerous regeneration cycles.<sup>12</sup>

The most common catalyst employed in industrial applications of olefin metathesis is the  $\text{WO}_3/\text{SiO}_2$  system which is used in processes such as the Neohexene Process and Olefins Conversion Technology (OCT).<sup>12,16</sup> The  $\text{WO}_3/\text{SiO}_2$  system is employed mostly for the metathesis of shorter chain olefins.<sup>17</sup> There are currently no commercial applications for this catalyst using longer chain olefins ( $\text{C}_6+$ ).

## 1.2 Aim of Study

In view of rising raw material and process costs it has become increasingly important to use a large proportion of lower olefin feed stocks in value adding processes. Olefins are of special importance as starting materials for synthesizing surfactants. Important examples include the alkylation of benzene with olefins to form alkyl aromatics and the hydroformylation of olefins to form oxo-alcohols. Olefin metathesis enables low molecular weight olefins to be converted to higher molecular weight olefins which can be used as surfactant raw materials.

The focus of this study will be on the investigation of the  $\text{WO}_3/\text{SiO}_2$  catalyst for the metathesis of an industrial cut 1-heptene or 1-octene feed to longer chain olefins. 1-Octene was used as a model feed for the industrial cut 1-heptene as it is cheaper and readily available.  $\text{WO}_3/\text{SiO}_2$  is a commercially used metathesis catalyst with appreciable isomerization activity.<sup>12,18</sup> Silica-supported tungsten oxide catalysts are less active for metathesis than their rhenium and molybdenum counterparts.<sup>19</sup> In order to obtain acceptable metathesis activity, much higher reaction temperatures (300-500 °C) have to be used for the  $\text{WO}_3/\text{SiO}_2$  system. High reaction temperatures also favour coke formation<sup>15</sup> which leads to catalyst deactivation.

The system has a high potential for practical applications in metathesis, mainly due to its low sensitivity to trace amounts of catalyst poisons and to coke formation at the elevated temperatures at which it is applied.<sup>19</sup> The online lifetime of this catalyst is greater than both the rhenium and molybdenum systems and it can also be regenerated continuously without any adverse effect on structure and activity.<sup>20</sup>

The aims and objectives of this study are:

- (a) the optimisation of the activity of the catalyst by choosing the appropriate metal loading;
- (b) to establish the influence of alkali metal ions on the metathesis and isomerization activity;
- (c) to investigate the effects of poisons on the catalyst and elucidating the deactivation mechanism;
- (d) to determine the location of the coke deposits on the catalyst by appropriate characterization techniques, studying factors that effect coke formation and reducing coke formation; and
- (e) to enhance the quality of the product obtained from the metathesis reaction by using suitable additives.

### 1.3 References

1. A. Wu (to Phillips Petroleum Co.), US Pat. 5210360, 1993 (11 May)
2. L. W. Hedrich (to Chevron Research and Tech. Co.), US Pat. 55345022, 1994 (6 September)
3. W. Keim (to Shell Dev. Co.), US Pat. 3686159, 1972 (22 August)
4. A. P. Steynberg, R. L. Espinoza, B. Jager, A. C. Vosloo, *Appl. Catal. A: Gen.*, 1999, **186**, 41
5. S. Warwel, G. Hachen, H. Kirchmeyer, H. Ridder, W. Winkelmuller, *Tenside Deterg.*, 1982, **19**, 321
6. R. L. Banks, D. S. Banasiak, P. S. Hudson, J. R. Norell, *J. Mol. Catal.*, 1982, **15**, 21
7. H. Bahrman, H. Bach in *Ullmann's Encyclopedia of Industrial Chemistry*, 5<sup>th</sup> Edition, M. Bohnet, C. J. Brinker (Eds.) Wiley-VCH, Electronic format, 2002
8. A. Lundeen, R. Poe, *Encycl. Chem. Process. Design*, 1972, **2**, 465
9. L. H. Slauch (to Shell Oil Co.), US Pat. 3239569, 1966 (1 March)
10. M. Sherwood, *Chem. Ind. (London)* 1982, 994
11. E. R. Freitas, C. R. Gum, *Chem. Eng. Prog.*, 1979, **75**, 73
12. G. C. Bailey, *Chem. Rev.*, 1969, **3**, 37; J. A. K. du Plessis, A. Spamer, H. C. M. Vosloo, *J. Mol. Catal. A: Chem.*, 1998, **133**, 181
13. M. Sibeijn, E. K. Poels, A. Bliet, J. A. Moulijn, *J. Am. Oil Chem. Soc.*, 1994, **71**, 553
14. B. Delmon, J. T. Yates, *Stud. Surf. Sci. Catal.*, 1989, **51**, 215
15. J. R. Rostrup-Nielsen, *Catal. Today*, 1997, **37**, 225
16. *European Chemical News*, 25 March 2002, p. 20
17. K. J. Ivin, J. C. Mol, *Olefin Metathesis and Metathesis Polymerization*, Academic Press (San Diego), 1997, p. 100
18. A. J. Van Roosmalen, J. C. Mol, *J. Catal.*, 1982, **78**, 17
19. J. C. Mol in *Handbook of Heterogeneous Catalysis*, Volume 5, G. Ertl, H. Knozinger, J. Weitkamp (Eds.), Wiley-VCH (Weinheim), 1997, p. 2395

20. L. F. Heckelsburg (to Phillips Petroleum Co.), US Pat. 3365513, 1968 (23 January)

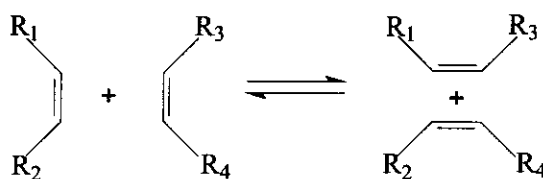
## 2 THE OLEFIN METATHESIS REACTION

---

### 2.1 Introduction

The catalytic metathesis of olefins is one of the most broadly applicable reactions of hydrocarbons to emerge in years.<sup>1</sup> The elegance of this reaction lies in the fact that the interconversion of olefins is the backbone of the petrochemical industry. Over the past few decades considerable interest has been shown by various research groups in this versatile reaction, despite these efforts only a few significant commercial applications have emerged.<sup>2,3</sup> Tighter environmental constraints combined with competitive economic forces and significant improvements in metathesis technology will improve the prospects for commercial applications of metathesis processes in the future.<sup>2</sup>

The metathesis of olefins was discovered independently by researchers at Du Pont, Standard Oil of Indiana and Philips Petroleum Company in the mid-1960's, during the development of olefin polymerization processes<sup>1,4,5</sup> The olefin metathesis reaction can be thought of as a reaction in which the carbon-carbon double bonds in an olefin are broken and then rearranged in a statistical fashion to form new olefins.<sup>6</sup> The reaction is essentially the interchange of carbon atoms between a pair of double bonds (Scheme 2.1).

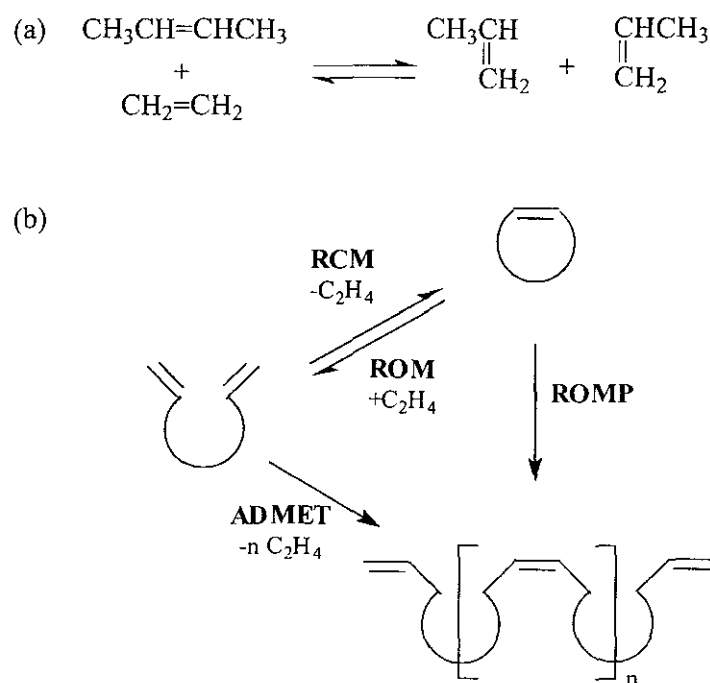


**Scheme 2.1** A generalised metathesis reaction

Olefin metathesis reactions do not occur spontaneously. They require a catalyst system containing a transition metal compound only or a transition metal complex in combination with a non-transition metal compound. One of the most intriguing features of the reaction

is the fact that metathesis can be catalyzed homogeneously as well as heterogeneously by catalysts containing the same elements.<sup>7</sup> The reactions are generally reversible and thermoneutral, and equilibrium can be attained in a matter of seconds.<sup>8</sup>

Olefin metathesis reactions can be divided into various categories (Scheme 2.2).<sup>9</sup>



**Scheme 2.2** The broad classes of metathesis reactions: (a) Exchange metathesis reaction, (b) Ring-opening metathesis polymerization (ROMP), Ring-closing Metathesis (RCM), Ring-opening metathesis (ROM) and Acyclic diene metathesis (ADMET).<sup>9</sup>

The forward reaction in Scheme 2.2a represents cross-metathesis between two different olefins and the exchange of the alkylidene moieties provides a route to propene. The reverse reaction is called self-metathesis and can be productive, giving rise to new products or degenerate, resulting in the formation of the original reactant olefins.

Ring-opening metathesis polymerization (ROMP) is the formation of unsaturated oligomers and solid polymers by the metathesis of cyclic olefins into a growing “living” polymer chain.<sup>10</sup> The forward reaction in Scheme 2.2b is an example of ring-closing

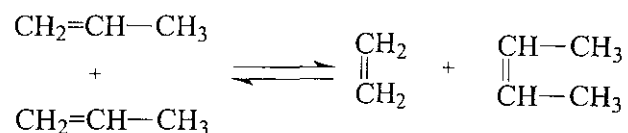
metathesis (RCM). RCM is an important preparative route for useful cyclic intermediates in organic chemistry.<sup>11</sup> The reverse reaction is termed ring-opening metathesis (ROM). Acyclic diene metathesis (ADMET) involves the formation of polymers *via* the metathesis of  $\alpha,\omega$ -dienes by the removal of ethene.

The metathesis reaction can be also extended to functionalised alkenes,<sup>12</sup> polyolefins<sup>13</sup> and alkynes.<sup>14</sup>

## 2.2 Industrial applications of olefin metathesis

### (a) The Phillips Triolefin Process<sup>1,10,15,16</sup>

The metathesis reaction was discovered at a time when the olefin market was over-supplied with propene. Thus the first commercial application in 1966 known as the Triolefin process, involved the conversion of propene into polymerization grade ethene and high purity butenes (Scheme 2.3). The process was operated with a sodium doped tungsten oxide on silica catalyst system. The process operated at a near equilibrium conversion (40-43%) and at a high selectivity (>95%), with the unconverted propene being recycled to the reactor. This process became outdated in 1972 when competing applications of propene had turned the propene oversupply into a shortage.



**Scheme 2.3** The Phillips Triolefin Process.

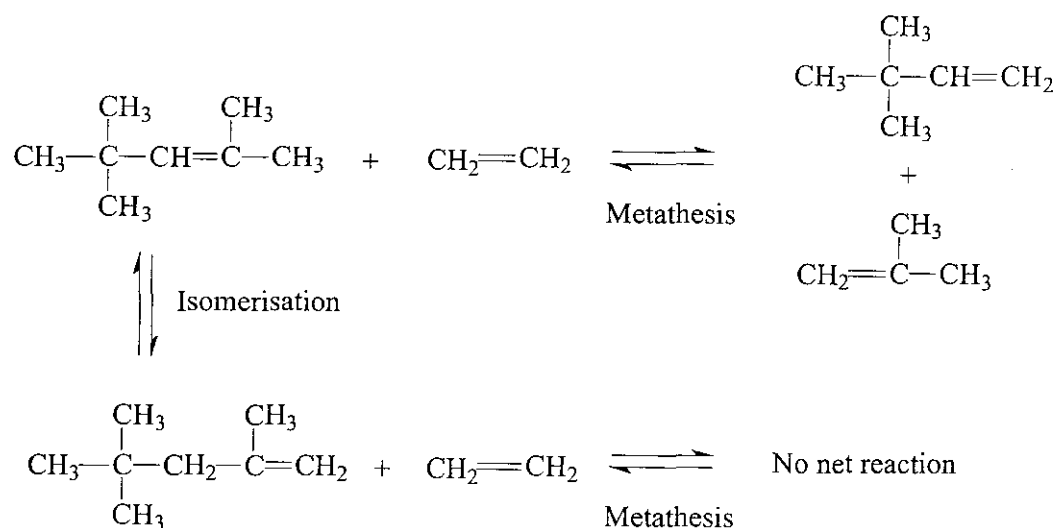
### (b) ABB Lummus' Olefins Conversion Technology (OCT)<sup>17</sup>

ABB Lummus Global has acquired the rights to use Phillips' technology. Since there will be an estimated shortfall of propene in the future, a "reverse" Triolefin process is applied to produce more propene. The key metathesis step is the reaction of ethene with 2-butene,

which occurs in a fixed bed reactor with a tungsten oxide catalyst that is continuously regenerated. As 2-butene is used up, 1-butene is isomerized to produce more 2-butene. Propene yield is 60% per pass and Lummus reports that they are able to substantially increase the propene-ethene ratio available from the steam cracker. Metathesis also bypasses the need for further purification, as product from the process usually exceeds polymer grade purity.

(c) The Phillips Neohexene Process<sup>16, 18</sup>

An application in the speciality chemicals sector is the Neohexene process in which diisobutene (2,4,4-trimethyl-2-pentene) is metathesized with ethene to produce neohexene (3,3-dimethyl-1-butene) and isobutene (Scheme 2.4).



Scheme 2.4 The synthesis of Neohexene.

The plant was constructed in Houston, Texas, in 1969 and the neohexene produced is used in the manufacture of synthetic musk perfume components. An isomerization catalyst, MgO is added to the  $\text{WO}_3/\text{SiO}_2$  system in order to isomerize the 2,4,4-trimethyl-2-pentene to 2,4,4-trimethyl-1-pentene. An average conversion of diisobutene of 65-70% and selectivity of about 85% are obtained.

(d) The Axens Meta-4 Process<sup>17</sup>

In the Axens Meta-4 process (Figure 2.1), fluid catalytic cracker (FCC) or steam cracker  $C_4$ 's are selectively hydrogenated to convert butadiene and 1-butene to 2-butene and isobutene is removed either in a methyl tert-butyl ether (MTBE) unit or by fractionation. The resulting 2-butene rich stream is fed to the metathesis unit with ethene, where the materials pass through a moving catalyst bed to give polymer grade propene. The Axens process uses a rhenium oxide catalyst that gives a 63% conversion rate per pass. The Chinese Petroleum Corporation has operated a 15 kg/h pilot plant for 8600 h in Taiwan. The low operating temperatures minimises catalyst fouling. The catalyst deactivation depends on feedstock purity and polymer formation rate. The lower the temperature, the lower the rate of polymer formation. Axens' catalyst retained excellent chemical and physical stability after 76 regenerations and the company says that the catalyst would last at least two years in an operational plant. Meta-4 can be coupled onto an existing cracker and easily brought on or off stream, depending on the demand.

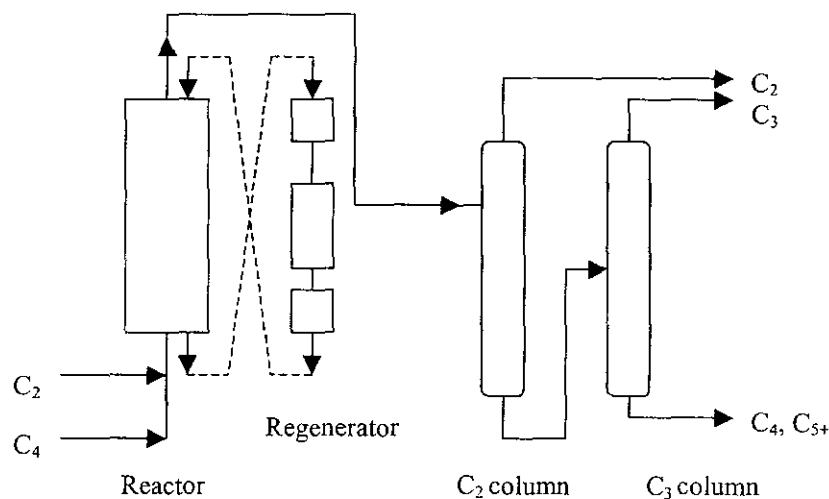


**Figure 2.1** Block diagram of the Axens Meta-4 Process.

(e) Shell Higher Olefin Process (SHOP)<sup>2, 4, 10, 19</sup>

Shell's commercial olefin process, incorporates an olefin metathesis stage to convert light and heavy byproducts from ethene oligomerization to linear internal detergent range olefins. In the commercial process (Figure 2.2), C<sub>4</sub>-C<sub>10</sub> and C<sub>20+</sub> fractions of α-olefins from the oligomerization step pass through a double bond isomerization unit to an olefin metathesis unit for conversion to C<sub>11</sub>-C<sub>14</sub> internal olefins. A feed purification system using conventional absorbents is ahead of the system. The double bond isomerization, cross-metathesis and purification steps take place at 100-125 °C, 10 bar and an alumina-supported cobalt molybdate catalyst is probably used.

(f) The Isoamylene Process<sup>1,2,10</sup>

Isoamylenes are readily produced *via* cross-metathesis of isobutylene and propene or 2-butene (Scheme 2.5). This application of metathesis, combined with conventional oxidative dehydrogenation and diene polymerization processes, provides a route for producing synthetic rubber (polyisoprene) from propene and butenes.



Scheme 2.5 Synthesis of isoamylene.

Technology for an isoamylene metathesis process using a WO<sub>3</sub>/SiO<sub>2</sub> catalyst has been developed in the laboratory and pilot plant. Although this application of metathesis has been demonstrated to be technically feasible, isobutylene has not been available in quantities required by an economically sized commercial plant.

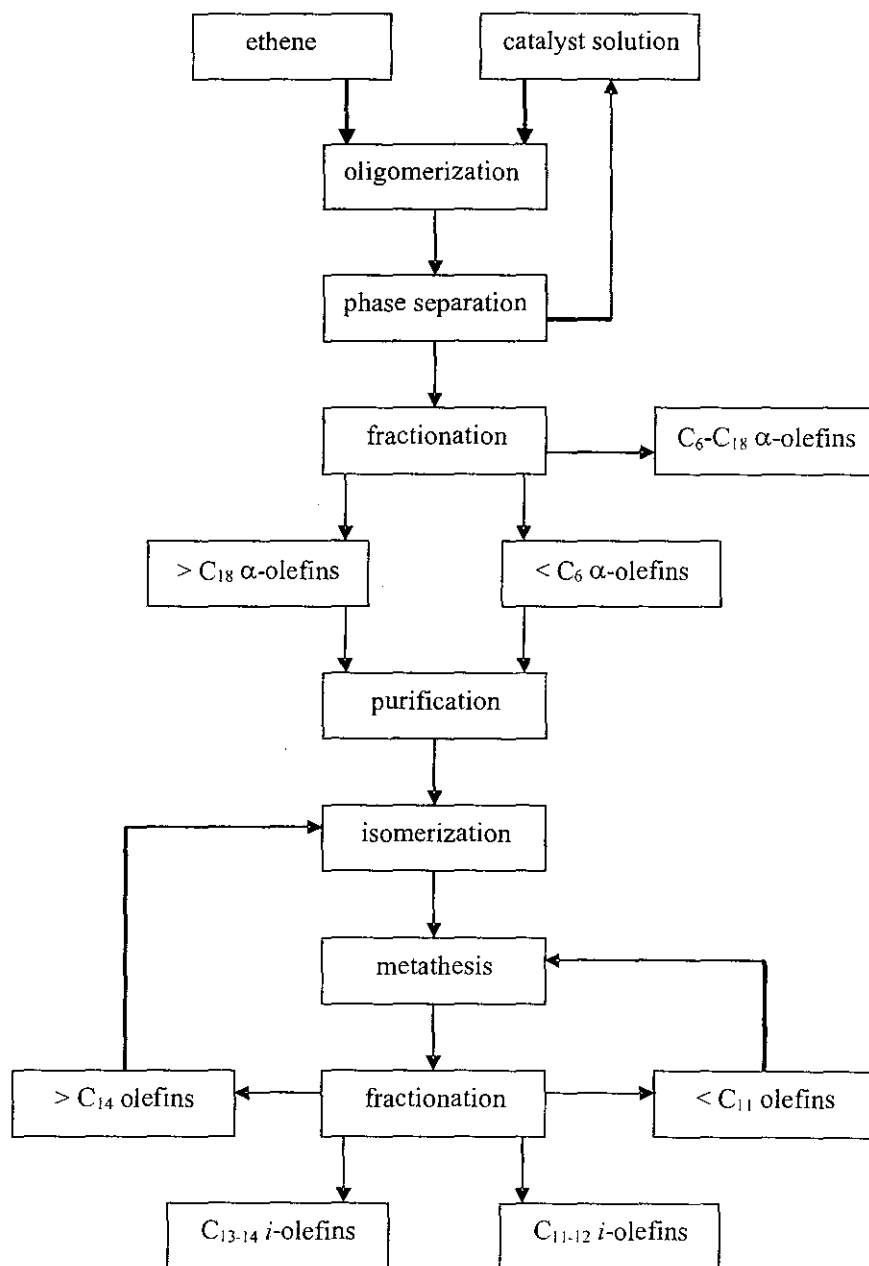
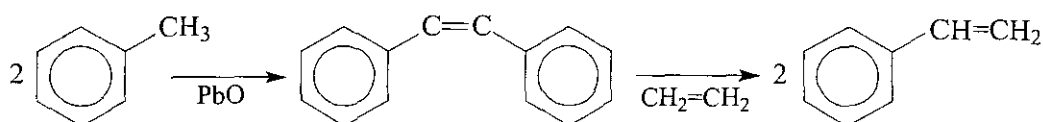


Figure 2.2 Block diagram of the Shell Higher Olefins Process (SHOP).

(g) Styrene from toluene<sup>6, 20, 21</sup>

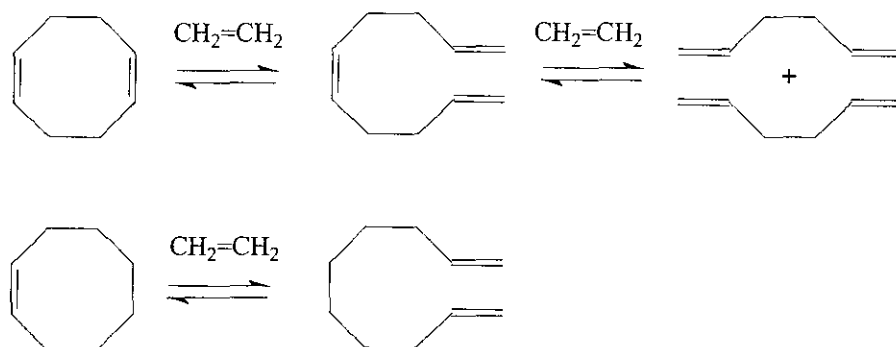
Olefin metathesis provides a potentially new industrial route to styrene, a key raw material of plastics-oriented polymers and styrene-butadiene rubber. In the first stage of the proposed two-stage process (Scheme 2.6), toluene is converted to stilbene over lead oxide. In the second step, purified stilbene is cleaved with ethene over a base treated  $\text{WO}_3/\text{SiO}_2$  catalyst. Monsanto have issued patents related to this scheme and results of laboratory studies of both stages have been reported by Gulf R&D.



**Scheme 2.6** Styrene from toluene process.

(h) The FEAST Process (Further Exploitation of Advanced Shell Technology)<sup>20, 22</sup>

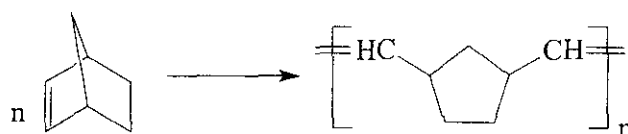
As with Phillips, Shell also applied olefin metathesis to the production of commodity and speciality olefins. A pilot metathesis unit in operation at Shell Research Laboratories in Amsterdam prepared numerous new compounds, predominantly by ethenolysis and isobutenolysis of butadiene and isoprene oligomers. In this way  $\alpha,\omega$ -dienes (1,5-hexadiene and 1,9-decadiene) were prepared from 1,5-cyclooctadiene and cyclooctene respectively (Scheme 2.7). Use was made of a promoted rhenium oxide on alumina catalyst. Interest in the products was sufficient to construct a plant in France in 1986.



**Scheme 2.7** The FEAST process for the production of  $\alpha,\omega$ -dienes.

(i) The Norsorex Process of CDF-Chimie<sup>20,23</sup>

The polymerization of norbornene to polynorbornene (Norsorex) has been carried out by CDF since 1976. The norbornene starting material is synthesised by the Diels-Alder reaction of ethene and cyclopentadiene. The homogeneous systems  $WCl_6/AlR_3/I_2$  or  $RuCl_3$  in  $BuOH/HCl$  are used as ROMP catalysts (Scheme 2.8). This material has thermoplastic behaviour and is used in noise and vibration dampening applications.



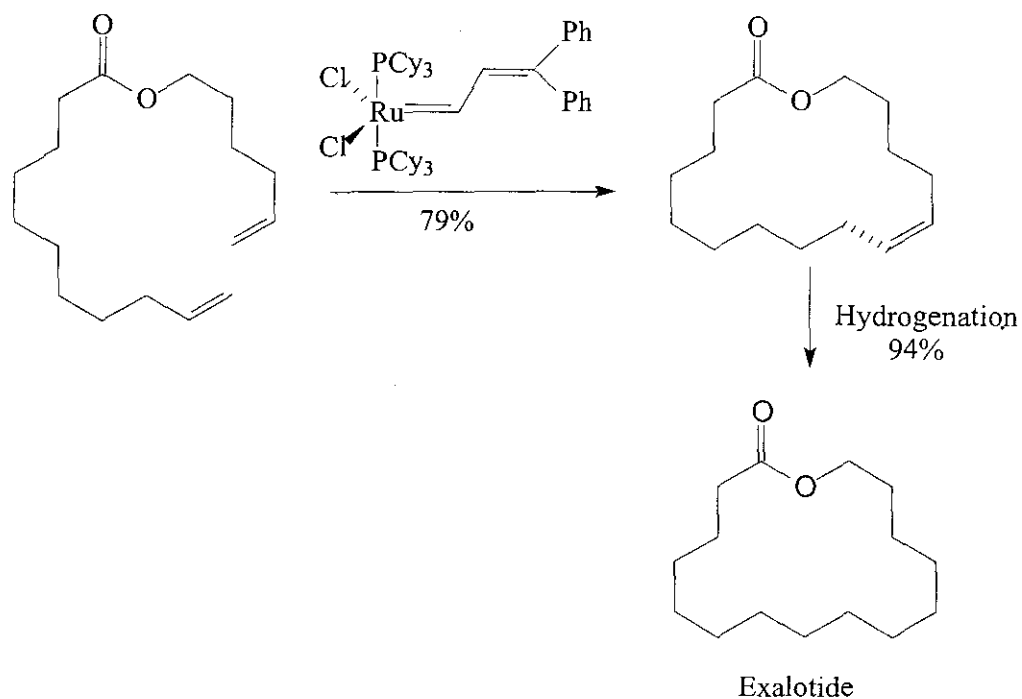
Scheme 2.8 The Norsorex Process.

## 2.3 Applications of olefin metathesis in organic chemistry

### 2.3.1 Synthesis of natural products<sup>10,24</sup>

The last few years have seen an explosion in applications of the olefin metathesis reaction in organic synthesis, particularly using RCM. Synthetic routes to natural products, biologically active agents and potentially important synthetic compounds have been reported. Fürstner and Langemann<sup>25</sup> have synthesized Exaltolide, a valuable musk odoured ingredient of *Archangelica officinalis* via metathesis and hydrogenation. Use was made of a ruthenium carbene catalyst for the ring-closing step (Scheme 2.9).

Pheromones have also been synthesised via metathesis. The sex pheromone of the common housefly, cis-9-tricosene was obtained in 95% purity from the cross-metathesis of 1-decene and 1-pentadecene.<sup>26</sup> The olefin metathesis reaction now forms an important part of the organic chemist's toolkit and will find increasing use, particularly for stereoselective ring-closing reactions.



Scheme 2.9 The synthesis of Exaltolide.

## 2.4 References

1. R. L. Banks, *Chemtech*, 1986, **16**, 112
2. P. H. Wagner, *Chem. Ind. (London)*, 1992, 331
3. H. S. Eleuterio, *J. Mol. Catal.*, 1991, **46** 55
4. R. Streck, *J. Mol. Catal.*, 1988, **46**, 305
5. H. Euleterio, *Chemtech*, 1991, **21**, 92
6. W. Grunert, *Indian. J. Technol.*, 1992, **30**, 113
7. R. L. Banks, G. C. Bailey, *Ind. Eng. Chem., Prod. Res. Dev.*, 1964, **3**, 170
8. A. Mortreux, F. Petit, *Industrial Applications of Homogeneous Catalysis*, D. Riedel Publishing (Dordrecht), 1988, p. 229
9. K. J. Ivin in *Olefin Metathesis and Polymerization Catalysts*, Y. Imamoglu (Ed.), Kluwer Academic Publishers (Netherlands), 1990, p. 1
10. K. J. Ivin, J. C. Mol, *Olefin Metathesis and Metathesis Polymerization*, Academic Press (San Diego), 1997, p. 397
11. J. J. Rooney, A. Stewart, *Catalysis (London)*, 1977, **1**, 277
12. J. C. Mol, *J. Mol. Catal.*, 1991, **65**, 145
13. E. A. Zeuch, W. B. Hughes, D. H. Kubicek, E. T. Kittleman, *J. Am. Chem. Soc.*, 1970, **92**, 528
14. F. Penella, R. L. Banks, G. C. Bailey, *J. Chem. Soc., Chem. Commun.*, 1968, 1548

15. R. L. Banks, *Chemtech*, 1974, 494
16. R. L. Banks in *Applied Industrial Catalysis*, Volume 3, B. E. Leach (Ed.), Academic Press (New York), 1984, p. 215
17. *European Chemical News*, 25 March 2002, p. 20
18. J. C. Mol, J. A. Moulijn in *Catalysis Science and Technology*, Volume 8, J. R. Anderson (Ed), Springer-Verlag (Berlin), 1987, p. 88
19. E. R. Freitas, C. R. Gum, *Chem. Eng. Prog.*, 1979, 75, 73
20. R. L. Streck, *Chemtech*, 1989, 19(8) 501
21. C. F. Hobbs (to Monsanto Company Inc.), US Pat. 4419527 (December 1983)
22. C. S. John, P. Chaumont, *J. Mol. Catal.*, 1988, 46, 317
23. G. Dall'Asta, G. Motroni, I. Motta, *J. Polym. Sci., Pt. A-1*, 1972, 10, 1601
24. K. J. Ivin, *J. Mol. Catal.*, 1998, 133, 1
25. A. Fürstner, K. Langemann, *J. Org. Chem.*, 1996, 61, 3942
26. W. J. Feast, V. C. Gibson in *The Chemistry of the Metal-Carbon Bond*, Volume 5, F. R. Hartley (Ed.), Wiley and Sons (New York), 1989, p. 200

### 3 MECHANISM OF METATHESIS AND SIDE REACTIONS

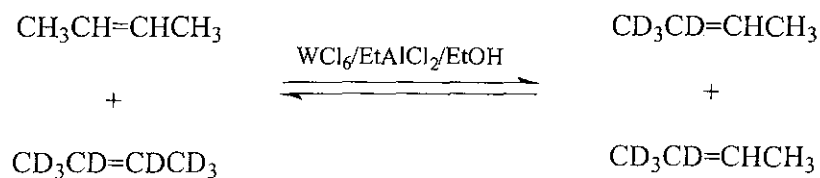
---

#### 3.1 Introduction

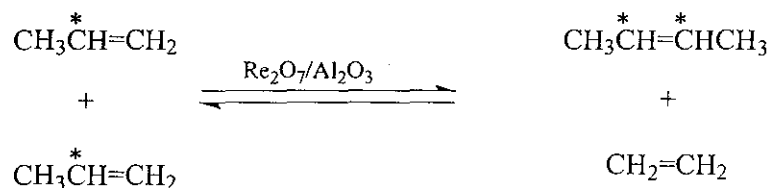
The basic question concerning the mechanism of olefin metathesis concerns the role of the catalyst and especially the transition metal.<sup>1</sup> At first it was thought that the two double bonds came together in the vicinity of the transition metal site and that the orbitals of the transition metal overlapped with those of the double bonds in such a way as to allow exchange to occur *via* a weakly held, cyclobutane-type complex. This pair wise mechanism was eventually discarded in favour of the metal carbene chain mechanism in which the propagating species is a metal carbene complex formed in some way from the catalyst/substrate system. The metal carbene mechanism for olefin metathesis is now universally accepted.<sup>2</sup>

##### 3.1.1 Transalkylidenation versus transalkylation

The first question, which arises about the mechanism of metathesis, is whether scission of the double bond occurs and thus whether the reaction is a transalkylidenation (exchange of alkylidene moieties) or a transalkylation (transfer of alkyl groups) process. Early work using <sup>14</sup>C- and deuterium-labeled propene and butene quickly established that two olefin bonds are switched between four carbon atoms and that the integrity of all other bonds remains intact.<sup>3</sup>



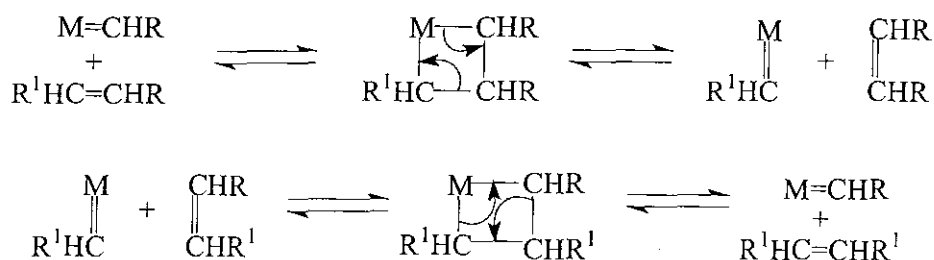
Mol *et al.*<sup>4</sup> obtained similar results for metathesis reactions using <sup>14</sup>C-labeled 2-propene over the heterogeneous Re<sub>2</sub>O<sub>7</sub>/Al<sub>2</sub>O<sub>3</sub> catalyst. No radioactivity was found in the ethene product, whereas 2-butene had twice the amount of radioactivity as the reactant propene:



From experimental evidence, it can then be concluded that olefin metathesis is a reaction in which C=C bonds are completely broken, leading to exchange of alkylidene moieties, i.e., a transalkylidenation process.

### 3.1.2 The metal carbene/metallacyclobutane mechanism

The understanding of the reaction mechanism is directly related to the role of the catalyst. The currently accepted mechanism for the metathesis reaction is the metal carbene or metallacyclobutane mechanism (Scheme 3.1). This mechanism was first proposed by Herrison and Chauvin.<sup>5</sup> The propagation reaction involves a transition metal carbene as the active species with a vacant coordination site at the transition metal. The olefin coordinates at this vacant site, and subsequently a metallacyclobutane intermediate is formed. The metallacycle is unstable and cleaves to form a new metal carbene complex and a new olefin.

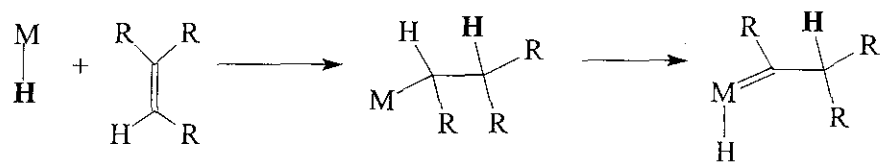


**Scheme 3.1** The metal carbene mechanism for olefin metathesis.

### 3.1.3 Formation of the metal carbene

It is established that coordinated carbenes are the initiating and propagating species for the olefin metathesis reaction. According to the catalyst type, several mechanisms have been suggested to account for the synthesis of the initial carbene.<sup>6,7</sup> These may include the following:

- (a) Formation of the metal carbene *via* a metal hydride (Scheme 3.2).<sup>8-10</sup>



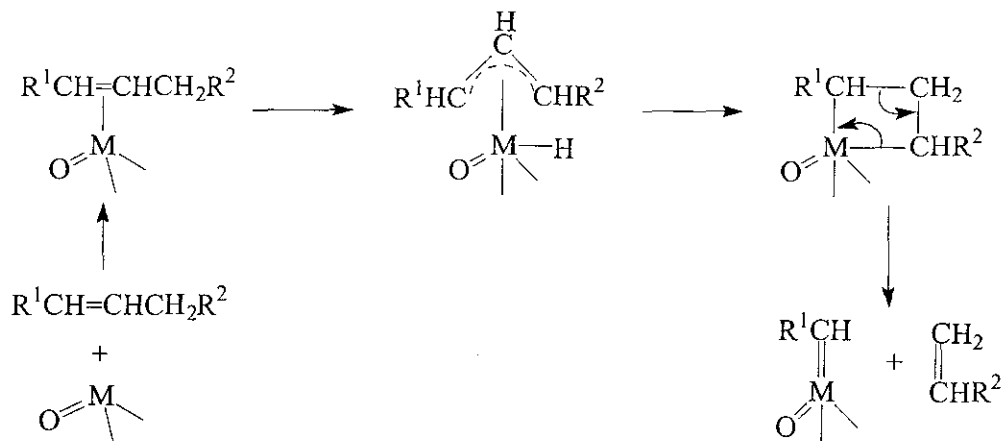
**Scheme 3.2** A metal hydride route to carbene formation.

The metal hydride mechanism involves the addition of a transition metal hydride to an olefin, followed by a  $\beta$ -hydrogen addition to form a metal alkyl complex. Subsequent  $\alpha$ -hydrogen elimination of the metal alkyl results in the initiating metal carbene complex. In this context it is significant to mention that trace amounts of protic solvents, e.g., ethanol often aid the metathesis reaction.<sup>11</sup> Rooney and co-workers<sup>12</sup> have suggested numerous sources of the original hydride and have spectroscopically detected metal hydrides. In heterogeneous catalyst systems the support can serve as the source and metal hydride is created *via* hydrogen migration from the support (Scheme 3.3).<sup>13</sup>



**Scheme 3.3** Hydrogen migration from the support to form a metal hydride.

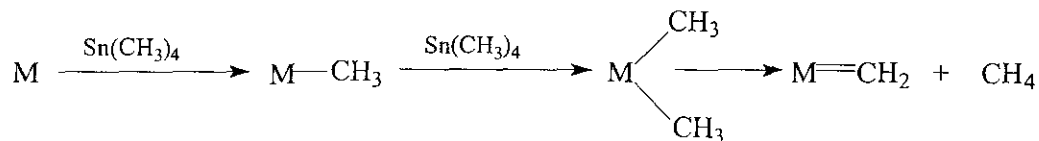
- (b) A second, more acceptable mechanism for the formation of the metal carbene is *via* a  $\pi$ -allyl species (Scheme 3.4).<sup>2,14</sup>



Scheme 3.4 Formation of a metal carbene *via* a  $\pi$ -allyl species.

The first step in the sequence is the formation of a  $\pi$ -allyl species. It is readily converted to a metallacyclobutane species *via* nucleophilic hydride attack on the central carbon of the  $\pi$ -allylic group. This type of initiation sequence demands the presence of at least three carbon atoms in the initiating olefin, i.e., the reactant olefin must contain an allylic hydrogen. It is significant that heterogeneous catalysts require pre-exposure to propene or butene before they catalyze the self-metathesis of deuterium labelled ethene.<sup>15</sup> The observation backs this mechanistic route for heterogeneous systems, without alkyl containing co-catalysts.

- (c) Formation of the metal carbene *via* carbene initiators (Scheme 3.5).<sup>2, 16</sup>



Scheme 3.5 The formation of a carbene with an alkyl tin co-catalyst.

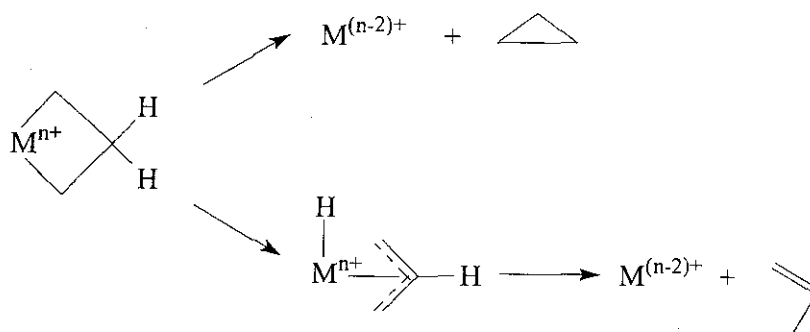
For simple olefins it is suggested that the co-catalyst activates the catalyst by generating the first carbene ligand. Methane is detected as a side product of the

reaction. This model of activation was demonstrated by Grubbs for both homogeneous<sup>17</sup> and heterogeneous<sup>18</sup> catalyst systems. In these cases it is presumed that the initiating carbene species is generated by alkylation of the metal by the alkyl metal compound, followed by  $\alpha$ -hydrogen elimination. Rhenium-based heterogeneous catalysts are often treated with  $R_4Sn$  or  $R_3Al$ , where  $R = Me, Et, Pr$ , etc. These co-catalysts also play a role in the initiation of the metal carbene.<sup>19</sup>

### 3.1.4 Termination reactions of the metal carbene/metallacyclobutane intermediate

Numerous reactions can lead to the termination of the metal carbene/metallacyclobutane intermediate and result in catalyst deactivation:<sup>1</sup>

- (a) Reductive elimination of the metallacyclobutane intermediate occurs to form cyclopropane or an olefin (Scheme 3.6).<sup>20</sup> After the metallacycle releases cyclopropane, the formal oxidation state of the metal decreases by two. As a result the fragment is coordinatively unsaturated. This is an intrinsic deactivation mechanism for some heterogeneous systems.<sup>21</sup>



**Scheme 3.6** The reductive elimination of the metallacycle.

- (b) Oxygen that is adsorbed on the surface of the catalyst can oxidize the carbene and terminate the existence thereof.<sup>22</sup>
- (c) Over-reduction with hydrogen, as well as with the olefin itself, can put the metal in a very low oxidation state, which is inactive towards metathesis.<sup>1</sup>

- (d) The metal carbene can react with itself to form a bridged di-metal and an olefin (Scheme 3.7), which terminates the active sites for metathesis.<sup>23</sup>



**Scheme 3.7** The reaction of carbene to form a di-metal.

- (e) Many varieties of polar and chemically active compounds have been reported as poisons that will deactivate the catalyst if present in the feed.<sup>24</sup> Aldehydes and ketones can deactivate the catalyst.<sup>25</sup> These Lewis bases contain a C=O bond and the available electron pairs on the oxygen atom can react with the metal carbene in a pseudo-Wittig type reaction as depicted in Scheme 3.8.<sup>26</sup>



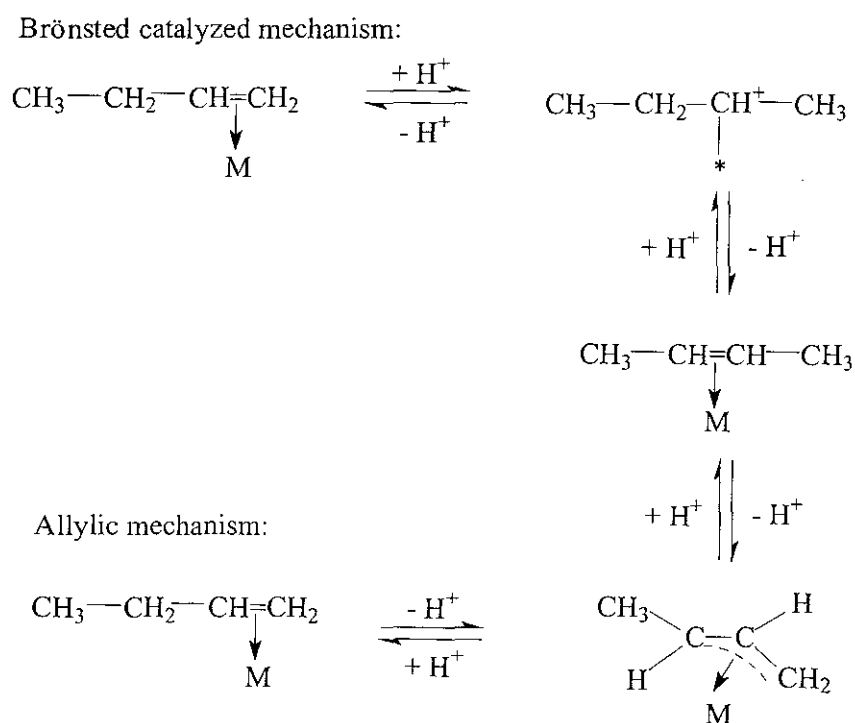
**Scheme 3.8** The reaction of a Lewis base with a metal carbene.

### 3.2 Mechanism of isomerization on $\text{WO}_3/\text{SiO}_2$ metathesis catalysts

Double bond isomerization is the main competing reaction with olefin metathesis over  $\text{WO}_3/\text{SiO}_2$  metathesis catalysts. Double bond isomerization results in products that facilitate secondary metathesis and lowers selectivity to the primary metathesis products.<sup>27</sup> In addition to double bond isomerization it is also possible to obtain skeletal isomerization on  $\text{WO}_3/\text{SiO}_2$  metathesis catalysts. Skeletal isomerization results in the formation of branched olefins from linear olefins.

Adsorption and reaction of olefins have been widely studied on a variety of oxide surfaces.<sup>28,29</sup> The metathesis of 1-butene on reduced oxide surfaces is also well understood.<sup>27, 30</sup> Ramani *et al.*<sup>31</sup> conducted studies on 1-butene adsorption on the  $\text{WO}_3/\text{SiO}_2$  catalyst and elucidated mechanisms for double bond isomerization.

Scheme 3.9 shows the possible ways that 1-butene interacts with oxide surfaces. If 1-butene adsorbs molecularly, it forms a  $\pi$ -complex on the surface, with the C=C bond coordinated to the supported cation (Lewis acid site). If Brønsted acid sites are present then protonation of 1-butene can occur, resulting in an alkoxide intermediate (carbenium ion) where the C=C character has been lost. Subsequent loss of a proton results in isomerization. If the first step involves C-H bond cleavage, an allylic intermediate is formed, with the resonant C-C-C bond coordinated to a supported metal atom. Subsequent protonation at a different carbon atom results in double bond isomerization. Thus there are two different mechanisms by which double bond isomerization of an olefin can occur, through the alkoxide or through the allylic intermediate. Both these double bond isomerization mechanisms have been observed on the  $\text{WO}_3/\text{SiO}_2$  catalyst.<sup>31</sup>

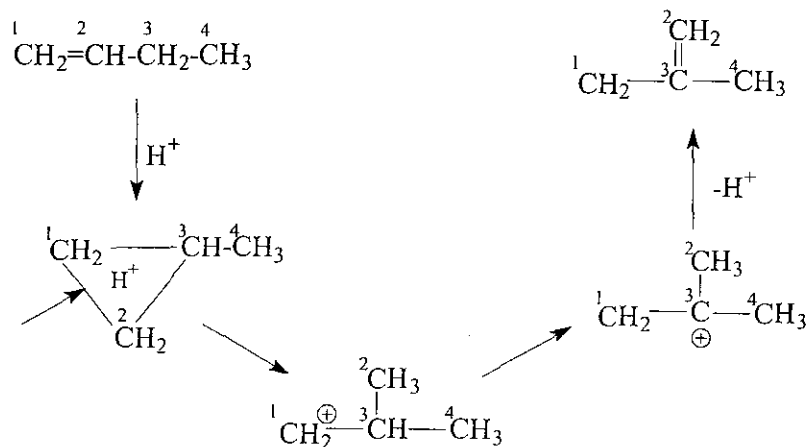


**Scheme 3.9** Double bond isomerization of butene over a  $\text{WO}_3/\text{SiO}_2$  catalyst.

Skeletal isomerization is catalyzed by a wide variety of catalysts.<sup>32</sup> In general it is thought that skeletal isomerization proceeds over Brønsted acid sites and therefore the most important factor seems to be catalyst acidity.<sup>33</sup> Acid sites that display intermediate acidity higher than that needed for *cis-trans* isomerization and double bond isomerization and lower than used in pyrolytic cracking are most suitable to give skeletal isomerization.<sup>34</sup>

Skeletal isomerization may occur by a bimolecular or monomolecular pathway:<sup>33</sup>

- In the bimolecular pathway two linear olefins may react to give a branched olefin and after isomerization and cracking, one branched olefin and one linear olefin is produced.
- The monomolecular pathway can be described using the skeletal isomerization of 1-butene (Scheme 3.10). In this pathway butene is isomerized over a Brønsted acid site, without the need of other butene molecules. The first step is the adsorption of the butene on the Brønsted site resulting in a covalently bonded alkoxy species. Proton transfer from the catalyst to the hydrocarbon then forms a cyclopropyl cation. This is followed by formed ring opening to give the primary carbocation, which leads to isobutene.



**Scheme 3.10** Monomolecular pathway for the skeletal isomerization of 1-butene.<sup>33</sup>

### 3.3 Mechanism of coke formation on metal oxide catalysts

#### 3.3.1 Introduction

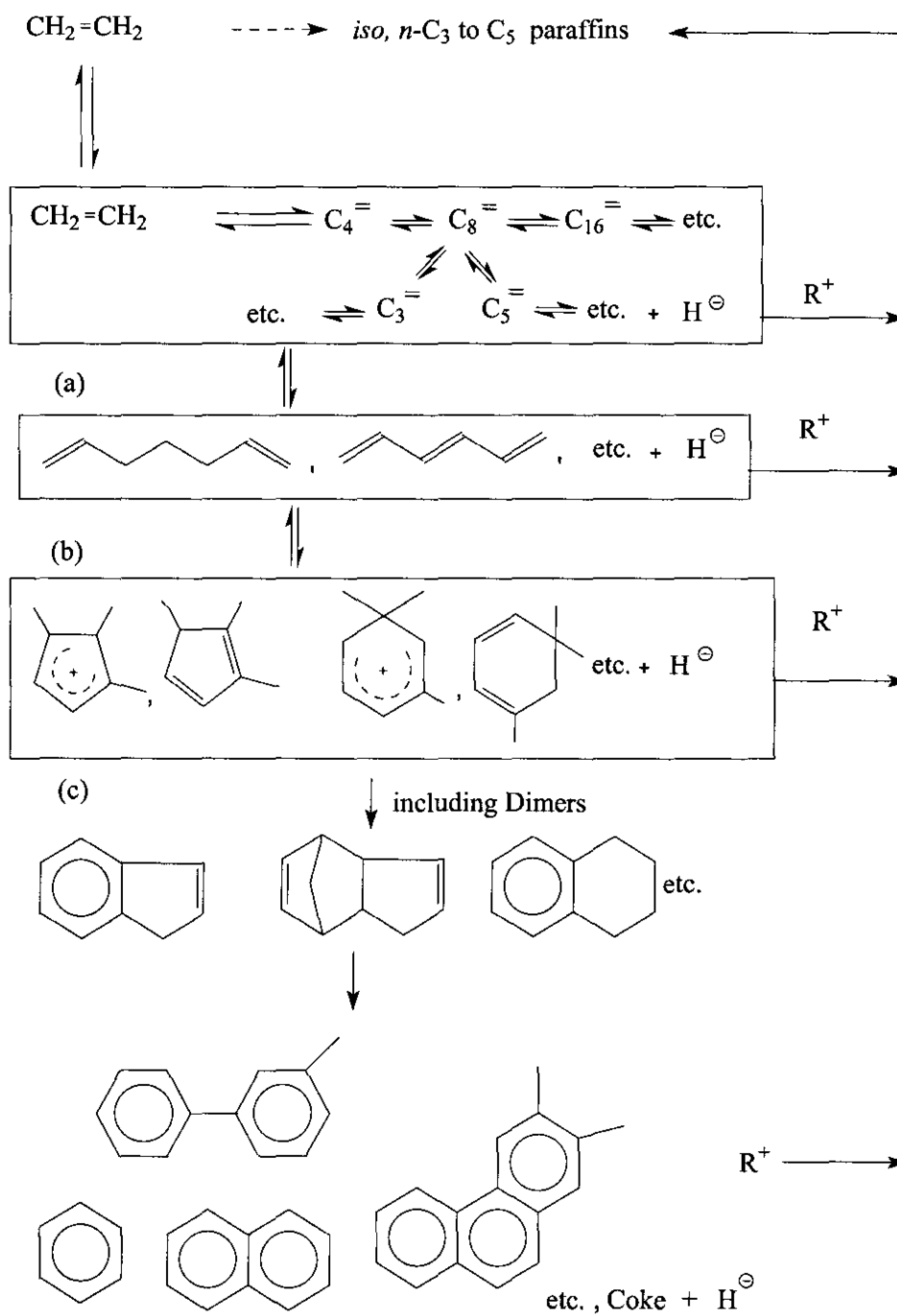
For catalytic reactions involving hydrocarbons, side reactions occur on the catalyst surface leading to the formation of carbonaceous residues (usually referred to as carbon or coke).<sup>35</sup> This type of physical deposition is one of the main causes of deactivation in high temperature processes.<sup>36</sup> The definitions of carbon and coke are somewhat arbitrary and by convention are related to their origin. Carbon is typically a product of CO disproportionation while coke is produced by the cracking or condensation of hydrocarbons.<sup>37</sup>

Coking decreases the activity (the rate of conversion of feedstock) of the catalyst. The loss of activity can be attributed to coke deposition by two mechanisms.<sup>38</sup> Firstly, the direct mechanism involves coke which is usually formed on the active sites which irreversibly adsorbs on the site and blocks the reactants. Secondly, coke may cause loss of activity by an indirect mechanism by depositing near the mouth of catalyst pores, narrowing the opening or completely blocking the pore mouth, and hence hindering diffusion or access of the reactants into pores.

Fouling by coke is generally a reversible process, being readily removed by gasification of the carbon with oxygen, carbon dioxide, steam or hydrogen at high temperatures. Finding ways to limit deactivation by coking and to regenerate the catalyst efficiently is an important economical objective.<sup>39</sup>

#### 3.3.2 Mechanism of coke formation from olefins

Coke formation on oxides is principally a result of cracking reactions involving coke precursors (typically olefins or aromatics) catalyzed by acid sites.<sup>38,40</sup> Dehydrogenation and cyclization of carbocation intermediates on acid sites lead to aromatics which react further to form higher molecular weight polynuclear aromatics which condense as coke. Step (a) in Scheme 3.11 illustrates the polymerization of olefins, step (b) illustrates



**Scheme 3.11** Coke-forming reactions of olefins and aromatics on oxide and sulphide catalysts: (a) polymerization of olefins; (b) cyclization from olefins; (c) formation of polynuclear aromatics.

cyclization from olefins and step (c) illustrates the chain reaction formation of polynuclear aromatics, which condense as coke on the surface. Because of the high stability of polynuclear carbocations, they can continue to grow on the surface for a relatively long time before a termination reaction occurs through the back donation of a proton. From this mechanistic scheme it is clear that olefins, benzene, benzene derivatives and polynuclear aromatics are precursors to coke formation.

### 3.4 References

1. K. J. Ivin, J. C. Mol, *Olefin Metathesis and Metathesis Polymerization*, Academic Press (San Diego), 1997, p. 7
2. J. C. Mol in *Handbook of Heterogeneous Catalysis*, Volume 5, G. Ertl, H. Knozinger, J. Weitkamp (Eds.), Wiley-VCH (Weinheim), 1997, p. 2387
3. N. Calderon, H. Y. Chen, K. W. Scott, *Tetrahedron Lett.*, 1967, 3327
4. J. C. Mol, J. A. Moulijn, C. Boelhouer, *Coll. Czech. Chem. Commun.*, 1963, 633
5. J. L. Herisson, Y. Chauvin, *Makromol. Chem.*, 1971, **141**, 161
6. M. F. Faron, R. L. Tucker, *J. Mol. Catal.*, 1980, **8**, 85
7. Y. Iwasawa, H. Kubo, H. Hamamura, *J. Mol. Catal.*, 1985, **28**, 191
8. R. L. Banks, *Chemtech*, 1979, 494
9. N. Calderon, J. P. Lawrence, E. A. Ofstead, *Adv. Organomet. Chem.*, 1979, **17**, 449
10. R. H. Grubbs, *Prog. Inorg. Chem.*, 1978, **24**
11. C. Masters, *Homogeneous Transition-metal Catalysis: A Gentle Art*, Chapman and Hall (London), 1981, p. 205
12. J. J. Rooney, D. T. Lavery, A. Stewart, *J. Catal.*, 1976, **45**, 110
13. E. A. Lambardo, M. Houalla, W. K. Hall, *J. Catal.*, 1978, **51**, 256
14. W. Grunert, *Indian J. Technol.*, 1992, **30**, 113
15. J. R. McCoy, M. F. Faron, *J. Mol. Catal.*, 1991, **66**, 51
16. J. A. Moulijn, J. C. Mol, *J. Mol. Catal.*, 1988, **46**, 1
17. R. H. Grubbs, C. R. Hoppin, *J. Chem. Soc., Chem. Commun.*, 1977, 634
18. R. H. Grubbs, S. J. Swetnick, *J. Mol. Catal.*, 1980, **8**, 25
19. R. Spronk, *Olefin Metathesis over Supported Rhenium Catalysts- Fundamental and Technological Aspects*, PhD thesis, University of Amsterdam, 1991
20. R. H. Grubbs in *Comprehensive Organometallic Chemistry*, Volume 8, G. Wilkinson, F. G. A. Stone, E. W. Abel (Eds.), Pergamon Press (Oxford), 1982, p. 533
21. J. C. Mol, *Catal. Today*, 1999, **51**, 289
22. G. C. Bailey, *Chem. Rev.*, 1969, **3**, 37
23. J. C. Mol, *Olefin Metathesis*, Academic Press (London), 1983
24. R. L. Banks in *Applied Industrial Catalysis*, Volume 3, B. E. Leach (Ed.), Academic Press (New York), 1984, p. 215
25. J. A. K. du Plessis, A. Spamer, H. C. M. Vosloo, *J. Mol. Catal. A: Chem.*, 1998, **133**, 181
26. G. C. Fu, R. H. Grubbs, *J. Am. Chem. Soc.*, 1993, **115**, 3800
27. A. J. van Roosmalen, J. C. Mol, *J. Mol. Catal.*, 1982, **78**, 17

28. G. Busca, V. Lorenzelli, *J. Chem. Soc., Faraday Trans. 1*, 1992, **88**, 2783
29. C. C. Chang, W. C. Conner, R. J. Kokes, *J. Phys. Chem.*, 1973, **77**, 1957
30. J. Engelhardt, J. Goldwasser, W. K. Hall, *J. Catal.*, 1981, **70**, 364
31. N. C. Ramani, D. L. Sullivan, J. R. Ekerdt, *J. Catal.*, 1998, **173**, 105
32. V. R. Choudary, *Ind. Eng. Chem., Prod. Res. Dev.*, 1977, **16**, 12
33. S. van Donk, J. H. Bitter, K. P. de Jong, *Appl. Catal. A: Gen.*, 2001, **212**, 97
34. J. P. Damon, B. Delmon, J. M. Bonnier, *J. Chem. Soc., Faraday Trans. 1*, 1977, **73(1)**, 372
35. M. Guisnet, P. Magnoux, *Appl. Catal. A: Gen.*, 2001, **212**, 83
36. D. L. Trimm, *Catal. Today*, 1999, **49**, 3
37. C. H. Bartholomew, *Appl. Catal. A: Gen.*, 2001, **212**, 17
38. E. E. Wolf, F. Alfani, *Catal. Rev. Sci. Eng.*, 1982, **24**, 239
39. J. R. Rostrup-Nielsen, *Catal. Today*, 1997, **37**, 225
40. B. C. Gates, J. R. Katzer, G. C. A. Schuit, *Chemistry of Catalytic Processes*, McGraw-Hill (New York), 1979, p.16

## 4 CATALYST SYSTEMS

---

### 4.1 Introduction

A large number of catalyst systems are known to catalyze the olefin metathesis reaction.<sup>1</sup> The systems may be either homogeneous or heterogeneous. The most important catalyst systems can be derived from transition metals from Group IV to VIII of the periodic table. The overwhelming majority of metathesis catalysts found so far contains one of the elements W, Mo or Re.<sup>2</sup> The important exceptions are the metathesis polymerization catalysts based on Ru, Rh, Ir and Os salts and complexes.<sup>3</sup>

Catalyst systems can be divided into three types:

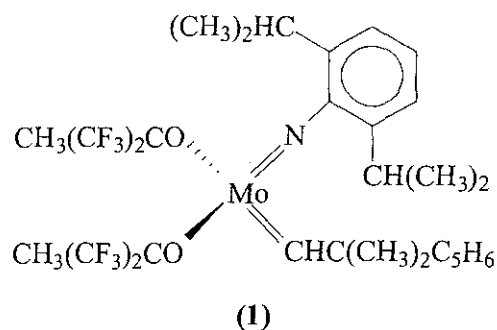
- (a) Those consisting of an actual metal carbene, such as  $W(=CPh_2)(CO)_5$ .
- (b) Those containing an alkyl or allyl group in one of its components such as  $Sn(CH_3)_4$  from which a carbene ligand can readily be generated.
- (c) Those neither having a carbene or an alkyl group in any component, e.g.,  $WO_3/SiO_2$ . In this case the carbene is generated by interaction with the reactant olefin.

For industrial applications it is preferred to use supported or heterogeneous catalysts.<sup>4</sup> Various refractory oxides and polymers have been used successfully as supports, with silica and alumina being the most commonly employed.<sup>5</sup> The most common method of preparing a supported catalyst is by impregnation of the support with a transition metal precursor solution, e.g., a  $MoO_3/SiO_2$  catalyst may be prepared by impregnation of the silica support with a solution of ammonium heptamolybdate then drying in air at 120 °C, followed by calcination at 550 °C.<sup>6</sup> Supported catalysts are activated by pretreatment in an appropriate gas ( $N_2$ , Ar, He) to clean the catalyst surface. The support often plays an integral role and there are indications that the interaction between the support and the transition metal contributes to the activity of the system.<sup>7</sup>

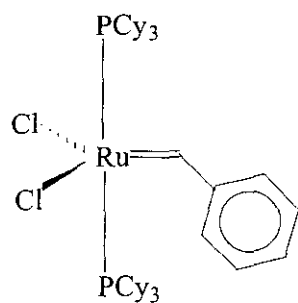
## 4.2 Homogeneous catalysts

A host of homogeneous catalyst systems that are active for the metathesis of acyclic olefins have been reported.<sup>8</sup> One of the first homogeneous catalyst systems was the  $WCl_6/EtAlCl_2/EtOH$  system, first reported by Calderon *et al.*<sup>9</sup> The system could metathesize 2-pentene to 2-butene and 3-hexene at room temperature and could also bring about the rapid ROMP of cyclooctene and cycloocta-1,5-diene.

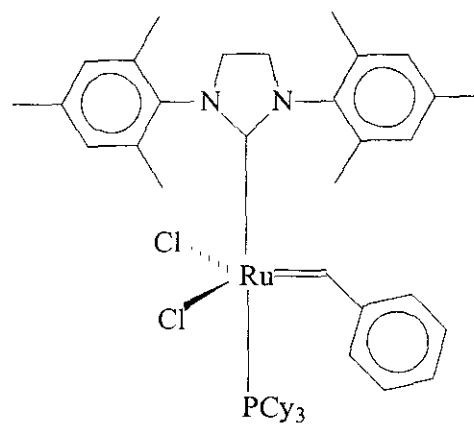
The most widely used homogeneous catalysts in recent times are the Grubbs- and Shrock-type carbene complexes.<sup>10,11</sup> These well defined carbene catalysts do not require co-catalysts or promoters. In the mid-1980's, Shrock developed highly reactive systems based on tungsten and then on molybdenum. The alkoxy imido molybdenum complex **(1)** is an example of a Shrock catalyst, which is highly active for a wide range of substrates.<sup>12</sup>



The ruthenium catalysts of Grubbs are credited with putting olefin metathesis in the forefront of organic synthesis.<sup>13</sup> The ruthenium catalysts have high preference for carbon-carbon double bonds and are reported to be indifferent to alcohols, amides, aldehydes and carboxylic acids. More importantly, their use does not require stringent conditions. The Grubbs first **(2)** and second **(3)** generation catalysts exhibit high reactivity in a variety of ROMP, RCM and cross metathesis reactions.<sup>14,15</sup>



(2)



(3)

### 4.3 Heterogeneous catalysts

Banks and Bailey<sup>16</sup> discovered the first heterogeneous catalyst, molybdenum hexacarbonyl on alumina, in 1964. Since then a plethora of other solid catalyst systems have been reported to be active for the metathesis of olefins.<sup>17</sup> A basic heterogeneous catalyst consists of a transition metal compound deposited on a high surface area support material. Important examples related to commercial applications are  $\text{Re}_2\text{O}_7/\text{SiO}_2\text{-Al}_2\text{O}_3$ ,  $\text{MoO}_3/\text{Al}_2\text{O}_3$  and  $\text{WO}_3/\text{SiO}_2$ .<sup>18</sup> Table 4.1 gives some typical examples of heterogeneous catalysts for the metathesis of propene. Pretreatment of the catalyst by heating it to a high temperature (120 °C for carbonyls and 550 °C for oxides) in a pure inert atmosphere is essential. Similarly the substrate olefin must be very pure to ensure a good catalyst lifetime.<sup>19</sup>

#### 4.3.1 Rhenium-based catalysts

Supported rhenium metathesis catalysts have been the subject of many studies.<sup>20</sup> These studies mainly deal with the  $\text{Re}_2\text{O}_7/\text{Al}_2\text{O}_3$  catalyst. The advantages of the system lie in its high activity and selectivity at relatively low temperatures (0-100 °C) and its ability to tolerate a variety of heteroatom-containing functional groups. The activity of the catalyst can be enhanced by using a tetra-alkyltin promoter.<sup>21</sup>

The performance of  $\text{Re}_2\text{O}_7/\text{Al}_2\text{O}_3$  catalysts can be improved by using a modified support, e.g., silica-alumina.<sup>22</sup> This results in a catalyst which is more active than one supported on  $\text{Al}_2\text{O}_3$  alone, especially at very low rhenium contents. The higher acidity of silica-alumina suggests that Brønsted acid sites may play a beneficial role in initiation of the metathesis reaction.<sup>23</sup> The enhanced acidity of the support however, results in the catalyst being more active for double bond isomerization than the  $\text{Re}_2\text{O}_7/\text{Al}_2\text{O}_3$  catalyst, although its selectivity can be improved by the addition of alkali metal ions, e.g., cesium.<sup>24</sup>

**Table 4.1** Examples of supported catalysts for the metathesis of propene.

Catalyst system	T/°C	Ref.
$\text{Re}_2\text{O}_7/\text{Al}_2\text{O}_3^a$	10-100	25
$\text{Re}_2\text{O}_7/\text{SiO}_2\text{-Al}_2\text{O}_3^a$	10-100	26
$\text{MoO}_3/\text{Al}_2\text{O}_3$	207	27
$\text{MoO}_3/\text{SiO}_2$	407	28
$\text{Mo}(\text{CO})_6/\text{Al}_2\text{O}_3$	60	25
$\text{Mo}(\pi\text{-C}_3\text{H}_5)_4/\text{Al}_2\text{O}_3$	0	29
$\text{WO}_3/\text{Al}_2\text{O}_3$	400	25
$\text{WO}_3/\text{SiO}_2$	487	28
$\text{WO}_3/\text{TiO}_2$	242	30
$\text{W}(\pi\text{-C}_3\text{H}_5)_4/\text{SiO}_2$	90	31

<sup>a</sup> activated with  $\text{R}_4\text{Sn}$  before use

### 4.3.2 Molybdenum-based catalysts

Supported molybdenum catalysts have received much attention as possible metathesis catalysts because they are already widely used in industrial chemical processes. The nature of the support and the molybdenum precursor compound, together with pretreatment conditions has an important influence on the ultimate metathesis activity.<sup>7</sup>

$\text{MoO}_3/\text{CoO}_3/\text{Al}_2\text{O}_3$  was the first oxide catalyst reported for olefin metathesis.<sup>16</sup> The catalyst was mainly used in hydrodesulphurization and the presence of cobalt resulted in

faster deactivation.<sup>32</sup> The  $\text{MoO}_3/\text{Al}_2\text{O}_3$  catalyst is presumed to be used in the SHOP process and therefore much research has been conducted on it. The metathesis of propene has been used as a probe for catalytic activity for molybdenum catalysts. The activity of  $\text{MoO}_3/\text{Al}_2\text{O}_3$  is highly dependent on the molybdenum content.<sup>33</sup> The activity is low for low Mo loadings but increases with increasing Mo loading and then passes through a maximum. The maximum activity is obtained at 2 Mo atoms/nm<sup>2</sup>.

Silica-supported  $\text{MoO}_3$  has similar behaviour to  $\text{MoO}_3$  supported on alumina. The activity of  $\text{MoO}_3/\text{SiO}_2$  for propene metathesis gradually increases when the activated catalyst is brought into contact with the reactant.<sup>34</sup> This phenomenon is termed catalyst break-in and illustrates that the reduction of  $\text{Mo}^{6+}$  is required for the catalyst to become active. The initial activity of the catalyst can be increased by prereduction in a reducing gas at elevated temperatures.

The catalytic activity of  $\text{MoO}_3/\text{SiO}_2$  depends on the Mo content.<sup>35</sup> The activity increases up to approximately 1 Mo atom/nm<sup>2</sup>, together with the formation of a monolayer of tetrahedrally and octahedrally coordinated Mo species. At higher molybdenum loading the activity decreases due to the formation of inactive crystalline  $\text{MoO}_3$ . Photoluminescence studies showed that the tetrahedrally coordinated  $\text{Mo}^{6+}$  species is reduced to the  $\text{Mo}^{4+}$  species through the loss of one ligand and that this 4+ species is the active precursor for metathesis.<sup>36</sup>

Photoreduction of  $\text{MoO}_3/\text{SiO}_2$  in CO with a laser beam of 308 nm and subsequent treatment with cyclopropane results in a high catalytic activity for propene metathesis.<sup>37</sup> Cyclopropane-treated CO-photoreduced catalysts bring about the metathesis of unsaturated fatty acid esters.<sup>38</sup>

### 4.3.3 Tungsten-based catalysts

Conventionally supported  $\text{WO}_3$  catalysts are chemically similar to  $\text{MoO}_3$  catalysts, but are less active for metathesis. In order to obtain an acceptable activity, much higher reaction temperatures have to be used than for other catalysts such as  $\text{MoO}_3/\text{Al}_2\text{O}_3$  and  $\text{Re}_2\text{O}_7/\text{Al}_2\text{O}_3$ .<sup>39</sup> The two most common types of tungsten oxide catalysts are  $\text{WO}_3/\text{SiO}_2$

and  $\text{WO}_3/\text{Al}_2\text{O}_3$ . More attention will be focused on the silica-supported catalyst, as this is the catalyst that will be employed for all experimental work in this study.  $\text{WO}_3/\text{SiO}_2$  has a high potential for practical applications in metathesis due to its low sensitivity to common poisons such as air, water and acetone and to coke formation at high temperatures at which it is employed.<sup>40</sup>  $\text{WO}_3/\text{SiO}_2$  is the most commonly used tungsten catalyst for propene metathesis.<sup>41</sup>

## 4.4 The $\text{WO}_3/\text{SiO}_2$ catalyst system

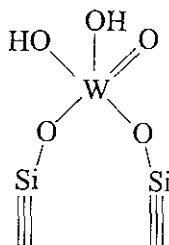
### 4.4.1 Structure and metathesis activity of $\text{WO}_3/\text{SiO}_2$ catalysts

Analogous to  $\text{MoO}_3/\text{SiO}_2$ , tungsten oxide on silica catalysts are composed of a surface phase and crystalline trioxide. Monolayer surface compounds are formed up to concentrations of approximately 1 W atom/nm<sup>2</sup>; whereas  $\text{WO}_3$  crystals are present at higher concentrations. XRD patterns of freshly activated catalyst show the presence of crystalline  $\text{WO}_3$  only if the catalyst contains more than 10 wt%  $\text{WO}_3$ .<sup>42</sup> Raman spectroscopy of  $\text{WO}_3/\text{SiO}_2$  catalysts show that the relative amounts of crystalline material increase with tungsten loading.<sup>28, 43-45</sup>

It has been proved extensively that  $\text{WO}_3$  crystals are not active in metathesis and as a consequence the catalytic sites have to be contained in the surface phase.<sup>28,46</sup> Even  $\text{WO}_3$  with a high surface area comparable to the supported catalyst is inactive for metathesis. Correlation between the amount of crystalline material and the catalytic activity suggests that active sites are located at the boundary between crystallites and silica.<sup>42</sup>

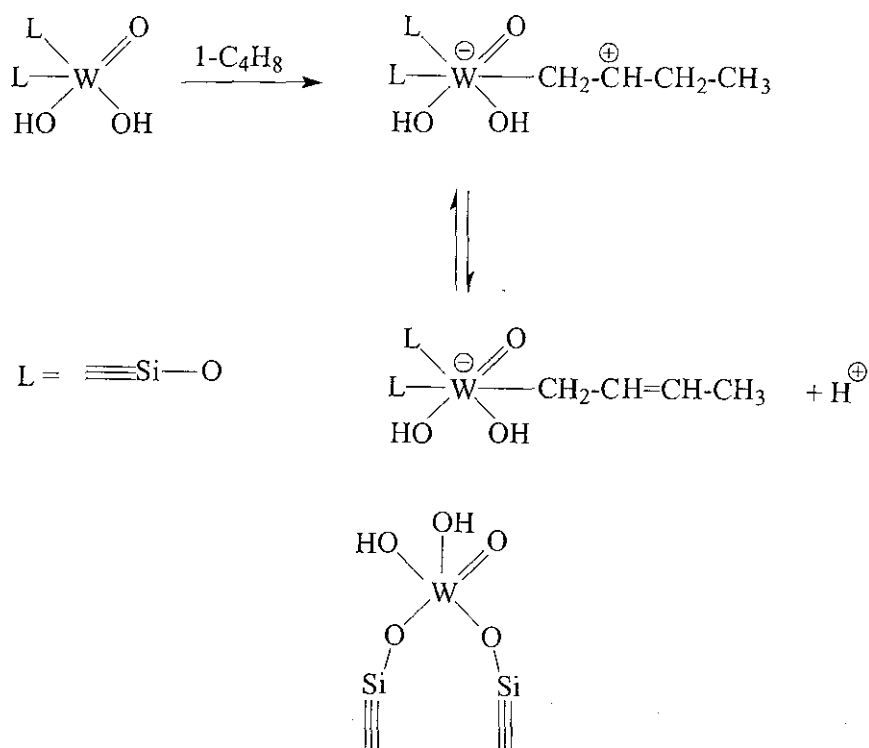
The configuration of the tungsten surface compound on dehydrated  $\text{WO}_3/\text{SiO}_2$  was postulated by Van Roosmalen *et al.*<sup>47</sup> and can be represented by Scheme 4.1.

According to a detailed study by Van Roosmalen *et al.*<sup>47, 48</sup> activated  $\text{WO}_3/\text{SiO}_2$  contains silanol groups with Lewis acidity. The  $\equiv\text{Si}-\text{O}$  bridges to the silica lattice are electron-withdrawing groups, due to the  $p_\pi-d_\pi$  back bonding between oxygen and silicon resulting in the Lewis acidity. In the presence of an olefin, the olefin can chemisorb onto the tungsten surface compound (Scheme 4.1) to form a Lewis acid-olefin complex (Scheme 4.2).

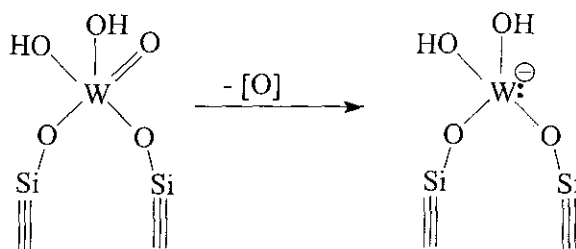


**Scheme 4.1** The configuration of the tungsten surface compound on dehydrated  $\text{WO}_3/\text{SiO}_2$ .

The generation of the active centres for metathesis activity was explained as proton donation by the Lewis acid site-olefin complexes (Scheme 4.2) to tetravalent tungsten. It was established from studies on  $\text{MoO}_3/\text{SiO}_2$  that the active site precursor for metathesis,  $\text{Mo}^{4+}$ , is formed *via* reduction of the tetrahedral dioxo  $\text{Mo}^{6+}$  species *via* loss of one oxygen ligand.<sup>49</sup> For  $\text{WO}_3/\text{SiO}_2$  this can be illustrated by Scheme 4.3.

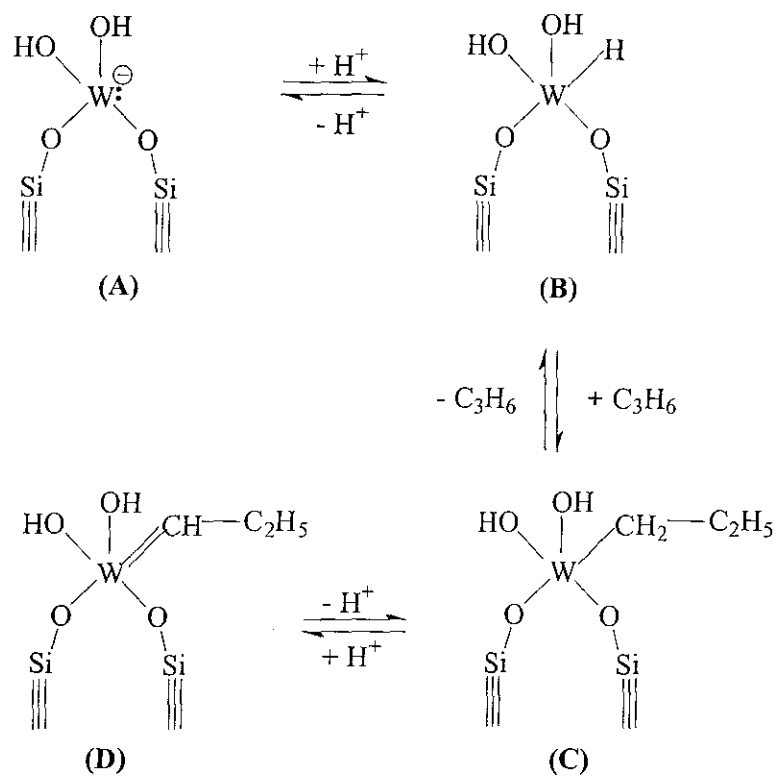


**Scheme 4.2** The interaction of 1-butene with the Lewis acid sites on activated  $\text{WO}_3/\text{SiO}_2$ .



**Scheme 4.3** Active site precursor is formed *via* elimination of an oxygen ligand.

For the initiation of metathesis on  $\text{WO}_3/\text{SiO}_2$  the following mechanism was proposed by Van Roosmalen *et al.*<sup>47,48</sup> (Scheme 4.4)



**Scheme 4.4** Initiation of metal carbene on  $\text{WO}_3/\text{SiO}_2$ .

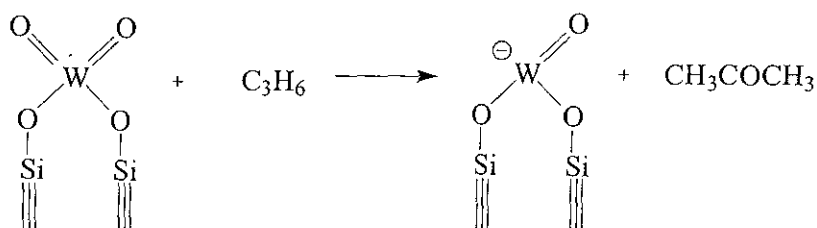
It was proposed that a proton originating from the Lewis acid-olefin complex (Scheme 4.2) reacts with the Lewis base (**A** in Scheme 4.4) to yield the tungsten hydride (**B** in Scheme 4.4). Adsorption of the olefin, in this case propene on the metal hydride, followed by  $\beta$ -

hydrogen addition results in the formation of **C** in Scheme 4.4. Back donation of a proton to the tungsten complex in Scheme 4.2 results in metal carbene formation necessary for initiation of further metathesis reactions (**D** in Scheme 4.4).

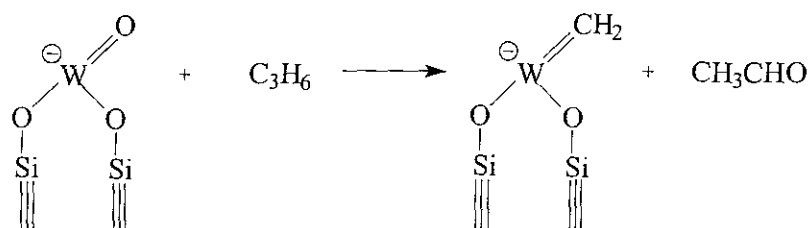
#### 4.4.2 Induction period

A distinctive feature of the  $\text{WO}_3/\text{SiO}_2$  catalyst is that if it is activated in air and then used without further treatment, the rate of metathesis builds up considerably over a period of minutes or hours as olefinic feed is passed through the system.<sup>50</sup> This phenomenon is known as catalyst break-in.<sup>51</sup> This break-in process is attributed to the formation of a steady state population of active sites, essentially exposed W ions in an appropriate oxidation state.<sup>52</sup> The necessary slight loss of oxygen is accompanied by the production of trace quantities of acetone and acetaldehyde, formed by the reaction of lattice oxygen from  $\text{WO}_3$  with propene.<sup>53</sup> This presumably occurs in two steps:

- (a) Initial reduction of the catalyst by propene yielding acetone and reduced metal oxide:



- (b) Subsequent to this, simultaneous formation of a metal carbene and acetaldehyde as a second step:



#### 4.4.3 Factors affecting activity of $\text{WO}_3$ catalysts

(a) *Effect of the support*

The two most common tungsten oxide catalysts are  $\text{WO}_3/\text{Al}_2\text{O}_3$  and  $\text{WO}_3/\text{SiO}_2$ .  $\text{WO}_3/\text{Al}_2\text{O}_3$  has a much lower activity than its silica-supported counterpart. This may be due to the stronger metal-support interaction which makes the tungsten difficult to reduce.<sup>54</sup> From a comparison of the activity of catalysts containing 6 wt%  $\text{WO}_3$  on different supports for propene metathesis at 402 °C, it follows that  $\text{WO}_3/\text{SiO}_2$  is most active followed by  $\text{WO}_3/\text{Al}_2\text{O}_3\text{-SiO}_2$  and  $\text{WO}_3/\text{Al}_2\text{O}_3$ .  $\text{TiO}_2$  gives the same order of activity as  $\text{Al}_2\text{O}_3$  and  $\text{ZnO}$  is the least favourable support.<sup>7,30,55</sup>

Andreini *et al.*<sup>30</sup> have found that the Brønsted acidity of the support does not seem to play a role in the metathesis reaction by evaluating several acidic supports for metathesis activity at different activation temperatures. They observed that for  $\text{Al}_2\text{O}_3$  and  $\text{Al}_2\text{O}_3/\text{SiO}_2$  the Brønsted acidity decreased with increasing activation temperature while metathesis activity increased. They suggested that the proton needed for the formation of the initial metal carbene (the intermediate in the metathesis reaction) is available from a Lewis site-olefin complex (Scheme 4.3) located on the transition metal ion.<sup>47</sup>

The nature of the support determines the Brønsted acidity and isomerization activity of the catalyst.<sup>56</sup> Pretreatment of a  $\text{WO}_3/\text{SiO}_2$  catalyst with hexamethyldisilazane (HDMS) at 250 °C has a remarkable effect on the activity, increasing it by 140 times for the metathesis of propene at 427 °C.<sup>57</sup> The same treatment of silica alone completely eliminates its capacity to isomerize trans-2-butene at 427 °C. It can be concluded that Brønsted acid groups poisoned by HDMS are not precursors for active sites for propene metathesis, but are responsible for isomerization activity instead.<sup>58</sup>

(b) *Effect of the WO<sub>3</sub> content*

For the WO<sub>3</sub>/Al<sub>2</sub>O<sub>3</sub> the relationship between activity and tungsten loading is analogous to the MoO<sub>3</sub>/Al<sub>2</sub>O<sub>3</sub> system.<sup>59</sup> The optimum activity is also obtained at 2 W atoms/nm<sup>2</sup>. For the WO<sub>3</sub>/SiO<sub>2</sub> catalyst the activity for propene metathesis is not a constant function of the tungsten content. Except for very low surface concentrations the activity decreases monotonically with the tungsten concentration.<sup>28</sup>

Several authors also state the importance of an optimum metal loading on the support for maximum metathesis activity. In the case of WO<sub>3</sub>/SiO<sub>2</sub> it was observed by Kerkhof *et al.*<sup>42</sup> that a composition of 20 wt% WO<sub>3</sub>/SiO<sub>2</sub> showed maximum activity with 1-butene as feed. IR-studies of adsorbed pyridine indicated Brønsted acid site formation on WO<sub>3</sub>/SiO<sub>2</sub> samples with high metal loadings.<sup>56</sup> For the reduction of side-reactions like isomerization it is therefore imperative to obtain optimum acidity necessary for maximum metathesis activity without inducing additional isomerization by adding extra unwanted Brønsted acidity. Several patents and publications claim to obtain equal activity with well dispersed low loading WO<sub>3</sub>/SiO<sub>2</sub> catalysts as with catalysts of appreciable higher tungsten content indicating the importance of obtaining a well dispersed catalyst.<sup>60-62</sup>

(c) *Effect of different activation/ pretreatment procedures*

There exists a correlation between the activity of WO<sub>3</sub>/SiO<sub>2</sub> catalysts and the activation temperature employed.<sup>50</sup> The effects of rate reduction by interphase mass transfer effects may be eliminated by activating the catalyst at high temperature (600 °C) for more than 2 h.<sup>63</sup> The break-in time may also be reduced by activating the catalyst in H<sub>2</sub> or CO. Activation at higher temperatures under inert gases greatly increases the break-in rate and activity.<sup>64</sup> Work done by Westhoff *et al.*<sup>65</sup> on the reduction process and its correlation with metathesis activity indicated that very short periods in a reducing atmosphere have maximum effect on catalyst activity. In their work they observed that pretreatment in H<sub>2</sub> at 600 °C and 1 bar H<sub>2</sub> pressure for periods between 1 to 10 min resulted in maximum

conversion of propene. This reduction period correlated to a tungsten oxide composition between  $\text{WO}_3$  and  $\text{WO}_{2.95}$ .

It has been shown that some intermediate nonstoichiometric oxidation state of tungsten oxide could be the most active one for propene metathesis, since pretreatment of the catalyst with nitrogen was found to be more beneficial than pretreatment with oxygen or hydrogen.<sup>64,66</sup>

d) *Effect of Additives*

The metathesis of propene on a  $\text{WO}_3/\text{SiO}_2$  catalyst is speeded up by the pretreatment of the catalyst with HCl but the product 2-butene undergoes considerable isomerization to 1-butene.<sup>67</sup> The effect of HCl can be attributed to a favourable modification of the metal d-orbital level as a result of the presence of new ligands.<sup>68</sup>

A  $\text{WO}_3/\text{SiO}_2$  catalyst can be promoted by adding minor amounts of elemental Na, S, Si, Mg, Ba, Zn or Sb to the catalyst and pretreating the admixture at elevated temperatures under an inert atmosphere.<sup>68</sup> The enhanced effect is due to the partial reduction of the supported tungsten catalyst by the additive.<sup>69</sup> Commercial applications where alkali metals have been used to reduce isomerization include sodium added to the  $\text{WO}_3/\text{SiO}_2$  catalyst developed for the Triolefin Process to limit the isomerization of butene.<sup>70</sup> Monsanto also issued patents related to using a potassium-doped, 8 wt%  $\text{WO}_3/\text{SiO}_2$  catalyst for their toluene to styrene process.<sup>71</sup> Using the alkali-doped catalyst resulted in a 96% selectivity towards styrene.

Combination of  $\text{WO}_3/\text{SiO}_2$  with MgO produces a dramatic increase in its metathesis activity, possibly caused by allyl radicals generated on the surface of the MgO. Addition of MgO also enhances the rate of isomerization.<sup>69,72</sup>

Banks<sup>73</sup> reported that the addition of ethene to a  $\text{WO}_3/\text{SiO}_2$  catalyst increases the conversion of propene at 400 °C five-fold.

e) *Effect of regeneration*

Regeneration of supported metal oxide metathesis catalysts usually occurs at 500-600 °C, using a controlled amount of oxygen to burn off accumulated coke.<sup>40</sup> Successful regeneration of a WO<sub>3</sub>/SiO<sub>2</sub> metathesis catalyst has been accomplished 110 times over a 1 year period, without any adverse effect on the structure and activity of the catalyst.<sup>74</sup>

Heckelsberg<sup>75</sup> demonstrated that the selectivity of the WO<sub>3</sub>/SiO<sub>2</sub> catalyst towards propene could be improved (with a slight drop in conversion) during the metathesis of 2-butene with ethene, after subsequent regeneration. This behaviour was also observed by Basur *et al.*<sup>53</sup> They concluded that a change in the catalyst structure facilitates this decrease in conversion and increase in selectivity. IR and Electron spin resonance (ESR) spectroscopy studies indicated that at least some of the WO<sub>3</sub> that was reduced to a lower state during the reaction could not readily be re-oxidized to W<sup>6+</sup> during regeneration and thus appeared to be in a stabilized non-stoichiometric state.<sup>53,76</sup>

#### 4.4.4 Coke formation on tungsten-based catalysts

Due to the high reaction temperatures employed with a WO<sub>3</sub>/SiO<sub>2</sub> metathesis catalyst, coke formation is favoured. Although the amount of feed converted to coke is usually very small; the accumulation of coke on a catalyst in a continuous process can be appreciable because of the high flow rates. For the Trioolefin Process an accumulation of 27 wt% coke over a 48 h period with propene feed at a WHSV of 20 h<sup>-1</sup> was reported.<sup>77</sup>

## 4.5 References

1. K. J. Ivin, J. C. Mol, *Olefin Metathesis and Metathesis Polymerization*, Academic Press (San Diego), 1997, p. 12
2. W. Grunert, *Indian J. Technol.*, 1992, **30**, 113
3. K. J. Ivin in *Olefin Metathesis and Polymerization Catalysts*, Y. Imamoglu (Ed.), Kluwer Academic Publishers (Netherlands), 1990, p. 1
4. B. C. Gates, J. R. Katzer, G. C. A. Schuit, *Chemistry of Catalytic Processes*, McGraw-Hill (New York), 1979, p. 79

5. J. C. Mol, J. A. Moulijn, *Adv. Catal.*, 1975, **24**, 131
6. B. Zhang, Y. Li, Q. Lin, D. Jin, *J. Mol. Catal.*, 1988, **46**, 229
7. J. C. Mol in *Handbook of Heterogeneous Catalysis*, Volume 5, G. Ertl, H. Knozinger, J. Weitkamp (Eds.), Wiley-VCH (Weinheim), 1997, p. 2387
8. J. C. Mol in *Applied Homogeneous Catalysis with Organometallic Compounds*, Volume 1, B. Cornils, W. A. Hermann (Eds.), Wiley & Sons (New York), 1998, p. 318
9. N. Calderon, H. Y. Chen, K. W. Scott, *Tetrahedron Lett.*, 1967, 3327
10. R. H. Grubbs, S. T. Nguyen, L. K. Johnson, J. W. Ziller, *J. Am. Chem. Soc.*, 1992, **114**, 3974
11. R. R. Shrock, *J. Organomet. Chem.*, 1986, **300**, 249
12. R. R. Shrock, J. S. Murdzek, G. C. Bazan, J. Robbins, M. DiMare, M. O'Regan, *J. Am. Chem. Soc.*, 1990, **112**, 3815
13. A. M. Rouhi, *Chem. Eng. News*, 23 December 2002, **80**, 29
14. R. H. Grubbs, S. Chang, *Tetrahedron*, 1998, **54**, 4413
15. R. H. Grubbs, S. T. Nguyen, J. W. Ziller, *J. Am. Chem. Soc.*, 1993, **115**, 7858
16. R. L. Banks, G. C. Bailey, *Ind. Eng. Chem., Prod. Res. Dev.*, 1964, **3**, 170
17. J. C. Mol, *Olefin Metathesis*, Academic Press (London), 1983, p. 13
18. J. C. Mol, *Chemtech*, 1983, 250
19. A. Mortreux, F. Petit, *Industrial Applications of Homogeneous Catalysis*, D. Riedel Publishing (Dordrecht), 1988, p. 229
20. J. C. Mol in *Olefin Metathesis and Polymerization Catalysts*, Y. Imamoglu (Ed.), Kluwer Academic Publishers (Netherlands), 1990, p. 247
21. J. C. Mol, *J. Mol. Catal.*, 1991, **65**, 145; R. Spronk, *Olefin Metathesis over Supported Rhenium Catalysts- Fundamental and Technological Aspects*, PhD thesis, University of Amsterdam, 1991
22. M. Sibeijn, R. Spronk, J. A. R. van Veen, J. C. Mol, *Catal. Lett.*, 1991, **8**, 20
23. J. C. Mol, *Catal. Today*, 1999, **51**, 289
24. J. A. K. du Plessis, A. Spamer, H. C. M. Vosloo, *J. Mol. Catal. A: Chem.*, 1998, **133**, 175
25. E. S. Davie, D. A. Whan, C. Kemball, *J. Catal.*, 1972, **24**, 272
26. A. Andreini, X. Xu, J. C. Mol, *Appl. Catal.*, 1986, **27**, 31
27. R. Thomas, J. A. Moulijn, *J. Mol. Catal.*, 1986, **98**, 70
28. R. Thomas, J. A. Moulijn, V. H. J. de beer, J. Medema, *J. Mol. Catal.*, 1980, **8**, 161
29. Y. Iwasa, H. Ichinose, S. Ogasawara, *J. Chem. Soc., Faraday Trans. 1*, 1981, **77**, 1763
30. A. Andreini, J. C. Mol, *J. Chem. Soc., Faraday Trans. 1*, 1985, **81**, 1705
31. A. N. Startsev, B. N. Kuznetsov, V. A. Shmachkov, D. I. Kochubey, A. L. Chuvilin, Y. I. Yermakov, *J. Mol. Catal.*, 1988, **46**, 209
32. J. Engelhardt, *React. Kinet. Catal. Lett.*, 1982, **21**, 7
33. O. V. Klimov, A. N. Startsev, *React. Kinet. Catal. Lett.*, 1990, **41**, 135
34. M. Anpo, M. Kondo, Y. Kubokawa, C. Louis, M. Che, *J. Chem. Soc., Faraday Trans. 1*, 1988, **84**, 2771
35. R. Thomas, J. A. Moulijn, *J. Mol. Catal.*, 1982, **15**, 157
36. T. Ono, M. Kondo, Y. Kubokawa, *Chem. Express*, 1986, **1**, 181
37. J. C. Mol, *Catal. Lett.*, 1994, **23**, 113
38. M. Y. Berezin, V. M. Ignatov, P. S. Belov, I. V. Elev, B. N. Shelimov, V. B. Kazansky, *J. Mol. Catal.*, 1989, **55**, 126
39. G. C. Bailey, *Chem. Rev.*, 1969, **3**, 37
40. R. L. Banks in *Applied Industrial Catalysis*, Volume 3, B. E. Leach (Ed.), Academic Press (New York), 1984, p. 215

41. J. Smith, W. Mowat, D. A. Whan, E. A. V. Ebsworth, *J. Chem. Soc., Dalton Trans.*, 1974, 1742
42. F. P. J. M. Kerkhof, R. Thomas, J. A. Moulijn, *Rec. Trav. Chim. Pays-Bas*, 1977, **96**, M121
43. R. Thomas, J. A. Moulijn, F. P. J. M. Kerkhof, *Rec. Trav. Chim. Pays-Bas*, 1977, **96**(ii), M134
44. A. Anderson, *Spectr. Lett.*, 1976, **9**(ii), 809
45. D. S. Kim, M. Ostromecki, I. E. Wachs, *Catal. Lett.*, 1995, **33**, 209
46. N. Tsuda, T. Mori, N. Kosaka, Y. Sakai, *J. Mol. Catal.*, 1985, **28**, 183
47. A. J. van Roosmalen, J. C. Mol, *J. Mol. Catal.*, 1982, **78**, 17
48. A. J. van Roosmalen, M. C. G. Hartmann, J. C. Mol, *J. Catal.*, 1980, **66**, 112
49. T. Ono, M. Anpo, Y. Kubokawa, *J. Phys. Chem.*, 1986, **90**, 4780
50. A. Andreini, J. C. Mol, *J. Colloid Interface Sci.*, 1981, **84**, 57
51. R. F. Baddour, M. Moddel, R. L. Goldsmith, *J. Phys. Chem.*, 1970, **74**, 1787
52. S. G. Gangwal, J. Fathikalajahi, G. B. Wills, *Ind. Eng. Chem., Prod. Res. Dev.*, 1977, **16**, 234
53. A. G. Basrur, S. R. Patwardan, S. N. Vyas, *J. Catal.*, 1991, **127**, 86
54. W. Grunert, R. Feldhaus, K. Anders, *React. Kinet. Catal. Lett.*, 1988, **36**, 195
55. R. L. Banks, *Prepr. Am. Chem. Soc., Div. Petr. Chem.*, 1979, **24**, 399
56. A. J. van Roosmalen, D. Koster, J. C. Mol, *J. Phys. Chem.*, 1980, **84**, 3075
57. A. J. van Roosmalen, J. C. Mol, *J. Phys. Chem.*, 1978, **82**, 2748
58. A. J. van Roosmalen, J. C. Mol, *J. Chem. Soc., Chem. Commun.*, 1980, 704
59. R. Thomas, J

## 5 EXPERIMENTAL

---

### 5.1 Reagents

The feed materials used were; 1-octene (98%, Aldrich), n-heptane (99%, Aldrich) and an industrial cut heptene feed (C<sub>7</sub> SLO, SASOL) consisting of 75% 1-heptene, 15% n-heptane and 10% branched paraffins and olefins.<sup>1</sup> All feed materials were percolated through a bed of activated, neutral aluminium oxide (Brockmann I, Aldrich) prior to use in reactions. The feed was then degassed thoroughly with nitrogen and stored under a nitrogen atmosphere.

2-Pentanone (99%), hexanal (98%), butanal (98%), butanol (99%) and ethyl acetate (99%) were obtained from Aldrich and used without further purification.

Silica gel (Davisil™, grade 646) with a surface area of 300 m<sup>2</sup>/g and a pore volume of 1.15 cm<sup>3</sup>/g from Aldrich was dried in an oven at 120 °C for 12 h prior to use. Ammonium metatungstate hydrate ((NH<sub>4</sub>)<sub>6</sub>H<sub>2</sub>W<sub>12</sub>O<sub>40</sub>), Aldrich), sodium nitrate (NaNO<sub>3</sub>, Merck), potassium nitrate (KNO<sub>3</sub>, Merck), and cesium nitrate (CsNO<sub>3</sub>, Merck) were used as obtained from the supplier.

### 5.2 Apparatus

#### 5.2.1 Percolation of feed

Metathesis catalysts are sensitive to oxygenated components in the feed stream.<sup>2</sup> It is known that alumina can be used to remove commonly found oxygenates in hydrocarbon streams.<sup>3</sup> Feed used in the metathesis reactions was percolated through a bed of alumina (activated, neutral, 150 mesh, 58 Å) before use (100 g Al<sub>2</sub>O<sub>3</sub>/ 1000 mL feed). The set-up for the percolation column is shown in Figure 5.1. After percolation the feed was purged with nitrogen for at least 5 min before being stored under a blanket of nitrogen. A gentle stream of nitrogen was bubbled through the feed for the duration of all reactions. Ideally

olefinic feed streams should be stored in cool, dark conditions as heat and light catalyze the formation of peroxides, which may act as catalyst poisons.<sup>4</sup>

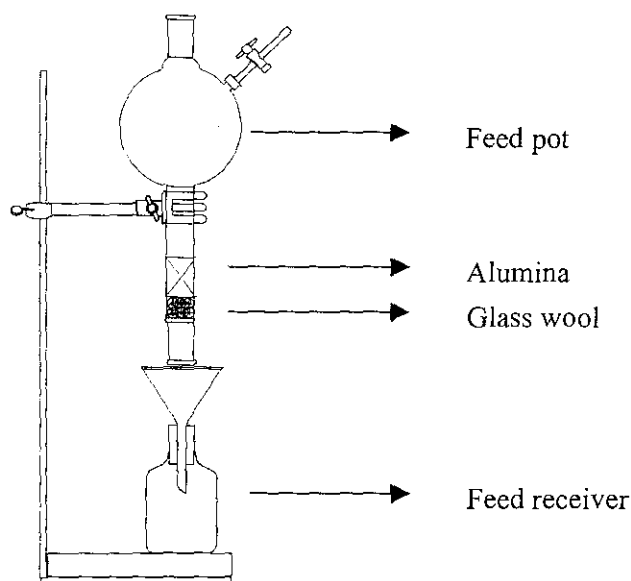


**Figure 5.1** Set-up of percolation column.

### 5.2.2 Metathesis Reactions

All reactions were performed in a bench scale demonstration unit, which consisted of a tubular fixed bed reactor (25.4 mm inner diameter), work-up columns and recycle lines (Figure 5.1). The reactor system could be operated in one of two modes:

(a) *Recycle mode*

The feed is pumped *via* an HPLC pump into the reactor, loaded with the desired amount of catalyst. The products are fed to Column 1, which is set at 220 °C, where separation of the heavy olefin product (C<sub>10</sub>-C<sub>15</sub>) occurs. The heavy product is drained at Purge 1. The light olefin products (C<sub>5</sub>-C<sub>9</sub>) and gases (C<sub>2</sub>-C<sub>4</sub>) pass overhead to Column 2 at 30 °C where separation of the light products occurs. The light fraction is recycled *via* a HPLC pump to the reactor. The feed to recycle ratio employed is 1:5.6. The separated gases then pass through a glass sampling bomb

and through a wet gas flow meter into a venting system. Samples of all three products are taken (liquids from Purge 1, 2 and gaseous product) and therefore an accurate mass balance is maintained. Only results with mass balances of  $100 \pm 3\%$  were accepted.

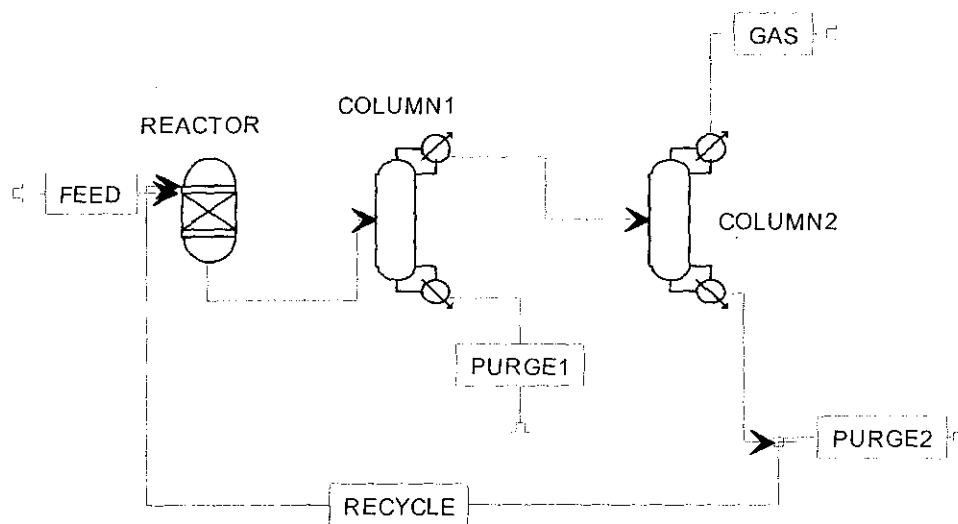


**Figure 5.2** Column 1: Reboiler = 220 °C, Column 2: Condenser = 34 °C. Recycle line = 25 °C, Reactor temperature = 460 °C, LHSV = 16 h<sup>-1</sup> (including a recycle loop of C<sub>5</sub>-C<sub>9</sub> at a feed to recycle ratio of 1:5.6), Reactor pressure = 0.1 atm (gauge).

(b) *Once through mode*

For once-through mode studies the feed is pumped into the reactor *via* a HPLC pump. The liquid product collects in Column 1 (room temperature), which acts as drain pot for the reactor. The sampling of liquid products is done at Purge 1. The gaseous product passes overhead through the glass sampling bomb, the wet gas flow meter and into a venting system.

## 5.3 Analysis

### 5.3.1 Analysis of liquid product samples

The liquid samples were analysed using a gas chromatograph (GC) equipped with a flame ionisation detector (FID). The analysis conditions are given in Table 5.1 with a typical chromatogram of a reaction mixture in Figure 5.3 and the compounds in Table 5.2.

**Table 5.1** Conditions for gas chromatographic analysis of liquid samples.

Injector	Split-injector at 250 °C
Head pressure	180 kPa (gauge)
Split ratio	1:100
Carrier gas	N <sub>2</sub> (20 ml (STP)/min)
Column	HP-PONA (l= 50 m; d <sub>o</sub> = 0.2 mm; d <sub>i</sub> = 0.5µm)
Temperature program	Initial: 50 °C for 2 min Heating rate: 12 °C/min Final: 270 °C for 10 min
Detector	FID at 300 °C
Fuel gas	H <sub>2</sub> at 40 ml (STP)/min
Air	400 ml (STP)/min

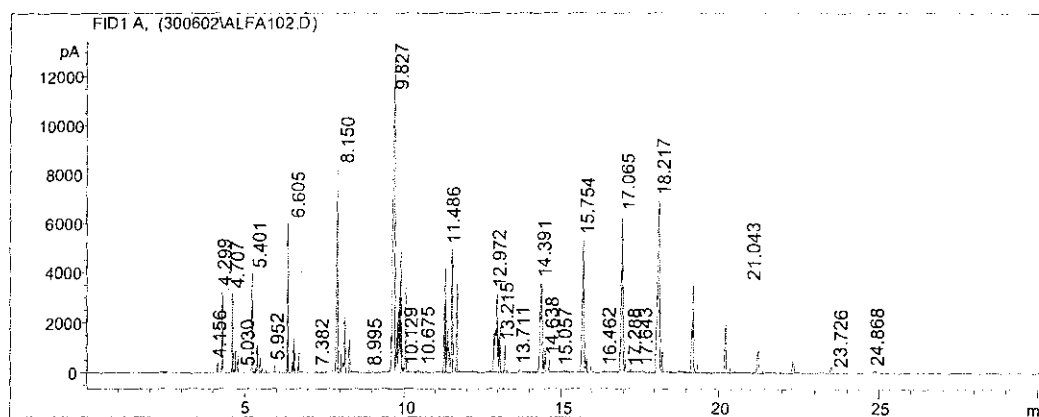


**Figure 5.3** Typical gas chromatogram of a liquid product sample from a once through mode reaction with a WO<sub>3</sub>/SiO<sub>2</sub> catalyst using 1-octene as feed.

**Table 5.2** Retention times of compounds in the liquid product sample in Figure 5.3.

Product compound	Retention time (min)	Product compound	Retention time (min)
Ethene	4.156	Linear C <sub>10</sub>	12.972
Propene	4.299	Branched C <sub>11</sub>	13.215
C <sub>4</sub> isomers	4.707	Linear C <sub>11</sub>	14.391
C <sub>5</sub> isomers	5.952	Branched C <sub>12</sub>	14.638
Branched C <sub>7</sub>	7.382	Linear C <sub>12</sub>	15.754
Linear C <sub>7</sub>	8.150	Branched C <sub>13</sub>	16.462
Branched C <sub>8</sub>	8.995	Linear C <sub>13</sub>	17.065
Linear C <sub>8</sub>	9.827	Branched C <sub>14</sub>	17.288
Linear C <sub>9</sub>	11.486	Linear C <sub>14</sub> *	18.217

\* Primary metathesis product

### 5.3.2 Analysis of gaseous product samples

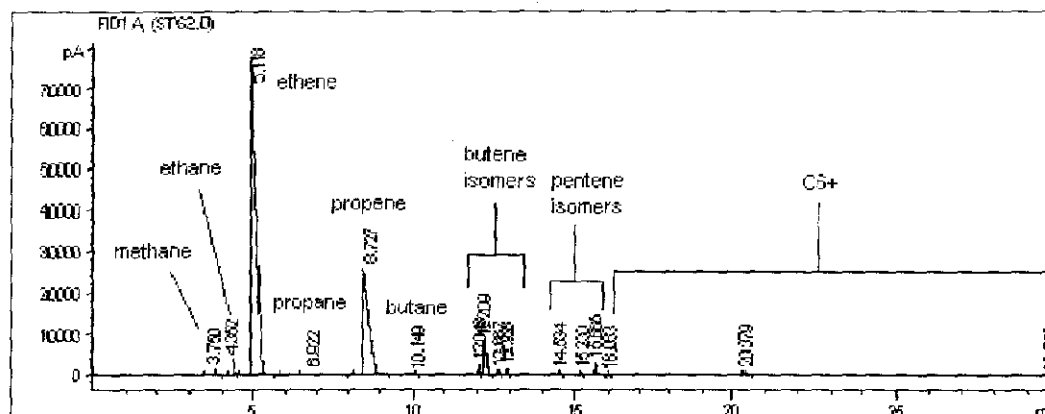
The gaseous samples were analysed using a gas chromatograph (GC) equipped with a flame ionisation detector (FID). The analysis conditions are given in Table 5.3. A typical chromatogram for a gaseous sample is shown in Figure 5.4. The main gaseous products obtained are ethene (primary metathesis product) and propene (secondary metathesis product).

### 5.3.3 Data evaluation

The amount of 1-octene/1-heptene converted was calculated on the basis of the mass of feed ( $m_{\text{feed}}$ ) pumped in and the mass of 1-octene/1-heptene collected as a liquid. The liquid was collected over a period of time hence the product mass flow rate can be determined. In the case of 1-octene feed, the mass fraction of 1-octene ( $w_{1\text{-octene}}$ ) in these samples can be easily determined from the GC analysis since the molecular response factor for olefins is approximately 1.<sup>5</sup>

**Table 5.3** Conditions for gas chromatographic analysis of gaseous samples.

Injector	Split-injector at 220 °C
Head pressure	30 kPa (gauge)
Split ratio	1:5
Carrier gas	N <sub>2</sub> (20 ml (STP)/min)
Column	HP-PLOT Al <sub>2</sub> O <sub>3</sub> "S" deactivated, capillary column (l= 50 m; d <sub>o</sub> = 0.53 mm; d <sub>i</sub> = 15 μm)
Temperature program	Initial: 50 °C for 2 min Heating rate: 10 °C/min Final: 180 °C for 10 min
Detector	FID at 300 °
Fuel gas	H <sub>2</sub> at 40 ml (STP)/min
Air	400 ml (STP)/min
Make-up	N <sub>2</sub> at 25 ml (STP)/min

**Figure 5.4** Typical gas chromatograph of gaseous product from a once through mode reaction with a WO<sub>3</sub>/SiO<sub>2</sub> catalyst using 1-octene as feed.

$$w_{\text{1-octene liquid sample}} = \left( \frac{A_{\text{1-octene}}}{\sum A_i} \right) \times 100 \text{ wt\%}$$

where:

$A_{\text{1-octene}}$  = peak area of 1-octene in GC-trace of liquid sample,

$\sum A_i$  = sum of all peak areas in GC-trace of liquid sample.

Thus, the conversion can be determined from:

$$X_{\text{1-octene}} = 100 \times \left( 1 - \frac{w_{\text{1-octene}} \times m_{\text{product}}}{m_{\text{feed}}} \right) \text{ wt\%}$$

where:

$m_{\text{feed}}$  = mass flow rate of feed pumped,

$m_{\text{product}}$  = mass flow rate of product.

The yield of the various product compounds (or carbon number fraction) can be determined in a similar manner from the GC-trace of the liquid sample, since the weight fraction of a component in the liquid sample ( $w_i$ ) is given by:

$$w_i = \left( \frac{A_i}{\sum A_i} \right) \times 100 \text{ wt\%}$$

Hence the yield for a given component ( $Y_i$ ) is given by:

$$Y_i = 100 \times \left( \frac{w_i \times m_{\text{product}}}{m_{\text{feed}}} \right) \text{ wt\%}$$

The selectivity for a given component ( $S_i$ ) is then defined as:

$$S_i = \frac{Y_i}{X_{\text{1-octene}}}$$

## 5.4 Catalyst Preparation

### 5.4.1 Preparation of $\text{WO}_3/\text{SiO}_2$ catalysts with different tungsten loadings

The desired wt%  $\text{WO}_3/\text{SiO}_2$  catalyst was prepared by wet impregnation of the silica support with an aqueous solution of ammonium metatungstate hydrate of appropriate concentration.<sup>6</sup> The mixture was stirred for 2 h and the excess water was then removed by evaporation at 80 °C under reduced pressure. The sample was dried in an oven at 110 °C for 12 hours. The temperature was then raised at a rate of 1 °C/min to 250 °C. This temperature was maintained for 2 h and then raised by 3 °C/min to 550 °C. The final step was a calcination at 550 °C for 8 h under an air atmosphere.

### 5.4.2 Preparation of alkali doped $\text{WO}_3/\text{SiO}_2$ catalysts

The 8 wt%  $\text{WO}_3/\text{SiO}_2$  catalyst was prepared as discussed in the previous section and was impregnated with an aqueous solution of 0.1 wt% of the metal in the form of a  $\text{NaNO}_3$ ,  $\text{KNO}_3$  or  $\text{CsNO}_3$  salt. The mixture was stirred for 2 h and the excess water was then removed by evaporation at 80 °C. Drying and calcination procedures were identical to those mentioned above for the preparation of the  $\text{WO}_3/\text{SiO}_3$  catalyst. Catalysts with different potassium loadings, i.e., 0.05, 0.1 and 0.5 wt%  $\text{K}^+$  were also prepared according to the above-mentioned procedure. For the reversal of the impregnation procedure, silica was first impregnated with the desired potassium nitrate concentration followed by the normal drying and calcination procedures as mentioned above. This was then followed by the impregnation of the potassium containing support with the correct ammonium metatungstate hydrate concentration. Drying and calcination procedures were identical to those mentioned above for the preparation of the  $\text{WO}_3/\text{SiO}_3$  catalyst.

### 5.4.3 Pretreatment of the $\text{WO}_3/\text{SiO}_3$ catalyst

Pretreatment of the  $\text{WO}_3/\text{SiO}_3$  catalyst with nitrogen gives the best activity.<sup>7</sup> The catalyst was pretreated *in situ* at 550 °C for 12 hours under a constant nitrogen flow. The temperature was decreased to the desired reaction temperature, under nitrogen and kept constant for the duration of the reaction

## 5.5 Characterization techniques

### 5.5.1 X-Ray Diffraction (XRD)

Samples were analyzed with a Siemens Diffrac 500 XRD. X-ray source: Co K $\alpha$ . Operation conditions: 40 kV and 25 mA. The system had a coupled scan:  $\theta / 2\theta$ . Crystallite size determinations were done from the line width of the peak at  $2\theta = 33.5^\circ$  using the Shadow software and with the aid of the Scherrer equation.

### 5.5.2 Surface area analysis

The specific surface area, the pore volume and the pore diameter of the different catalysts were determined by the BET-method on a Tristar (Micromeritics) instrument. Measurements were performed with nitrogen as adsorbate at  $-196^\circ\text{C}$ , after pre-treatment of the samples at  $200^\circ\text{C}$  under nitrogen flow for 12 h.

### 5.5.3 Laser Raman Spectroscopy (LRS)

The laser spectroscopy apparatus consisted of an Ar<sup>+</sup> laser delivering incident radiation tuned to 514 nm. The Raman spectra were recorded in the  $180^\circ$  configuration on a System 1000 Renishaw Raman spectrometer equipped with a Leica microscope. During the measurements a magnification of 50 was used. A Renishaw CCD detector was used. Powdered samples were analysed and the spectra were recorded under ambient conditions.

### 5.5.4 Inductively coupled plasma-atomic emission spectroscopy (ICP-AES)

Tungsten determinations on the supported WO<sub>3</sub>/SiO<sub>2</sub> catalysts were done by ICP-AES on a Perkin Elmer Optima 4300 DV spectrometer. The tungsten concentration was measured at 207.912 nm. In a typical analysis 0.2 g of catalyst was mixed with mixture of HNO<sub>3</sub>, HCl and HF (volumetric ratio 2:1:1) and digested in a microwave oven. Water was added after the solution had cooled down to make it up to 100 ml. The tungsten content was subsequently measured by ICP-AES and then calculated based on the dilution factor used.

### 5.5.5 Transmission electron microscopy (TEM)

TEM-analysis was done on a Phillips CM 200 microscope using 200 kV accelerator speed. An Oxford EDS detector utilizing Link ISIS software was used for energy dispersive spectroscopy (EDS) analysis. EDS analyses were performed in 100 s counting time at 100 kV accelerating voltage for TEM. For each sample, a minimum of three X-rays were obtained to characterize elemental tungsten. The samples were ground and suspended in methanol using an ultrasonic bath before analysis.

HRTEM (High resolution TEM) measurements were performed on a JEOL 2010 HRTEM with a point resolution of 1.9 Å. In order to avoid possible contamination, the sample powder was directly mounted on the TEM grid without using any solvent.

EFTEM was done at the University of New Mexico, using a JEOL 2010F microscope coupled with a Gatan Imaging Filter. TEM coupled with electron energy loss spectroscopy (EELS) has been used for the characterization of coke in catalysts. An advantage of EELS is that information on the chemical state of the element can be obtained allowing distinction for example, between graphitic and amorphous carbon. A fairly recent development in electron microscopy is the advent of imaging filters e.g. Gatan imaging filter (GIF).<sup>8</sup> These allow images to be recorded using electrons that have lost a certain amount of energy *via* interaction with the solid. Since the energy loss spectrum of a material contains a signature of all the chemical species present, it is actually possible to “tune” in to certain elements and obtain an elemental map. These filters therefore provide a powerful analytical tool for elemental mapping in TEM. This energy filtered transmission electron microscopy (EFTEM) technique can be used to create a carbon map of coked catalysts.

### 5.5.6 Scanning electron microscopy (SEM)

The morphology of the samples was studied by a high resolution JEOL JSM-6000L scanning electron microscope (HRSEM) operated at 20 kV.

### 5.5.7 Thermogravimetry (TG)

Coke levels (wt%) were determined by TG using a Mettler Toledo Star system. The catalyst sample (26 mg) was first treated at 900 °C in a Nitrogen flow to remove volatiles and then air to determine the mass loss due to carbon deposits. The conditions for the TG program are shown in Table 5.4. A typical TG curve for a coked catalyst is shown in Figure 5.5.

**Table 5.4** The operating conditions for the TG program.

Step	Temperature/°C	Time/min	Gas	Flow rate/ml.min <sup>-1</sup>
1	30	3	N <sub>2</sub>	100
2	30-110	3	N <sub>2</sub>	100
3	110	3	N <sub>2</sub>	100
4	110-900	15	N <sub>2</sub>	100
5	900	20	N <sub>2</sub>	100
6	900	50	Air	100

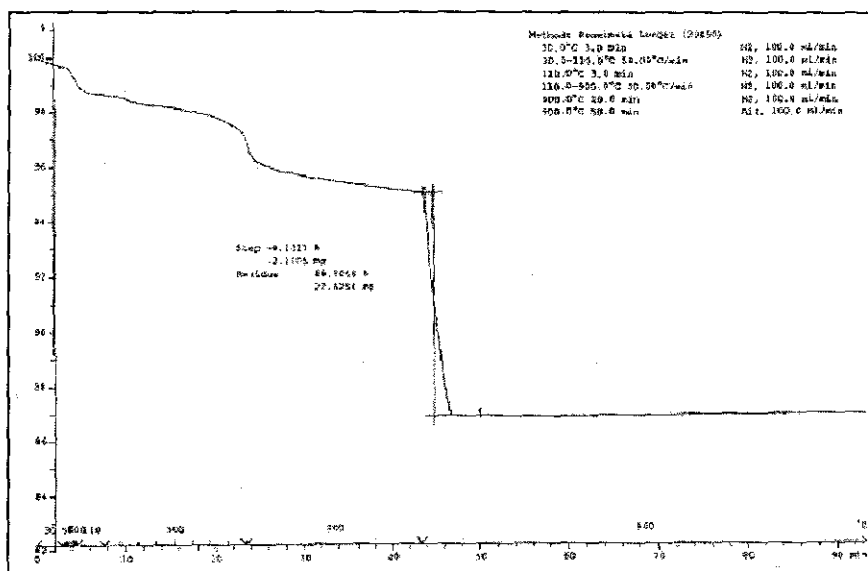


**Figure 5.5** A typical TG curve for a coked 8 wt% WO<sub>3</sub>/SiO<sub>2</sub> catalyst.

### 5.5.8 Ultraviolet-visible (UV-Vis) spectroscopy

UV-Vis absorption measurements of the product were recorded on a Varian Cary 1E UV-Visible Spectrophotometer using a quartz cell with a path length of 2 mm. The final metathesis product containing mostly C<sub>10</sub>-C<sub>13</sub> internal olefins is yellow. A 20 mL sample was percolated through neutral alumina to remove the colouration. Both the yellow and colourless products were analysed by UV-Vis spectroscopy. The percolated product has an absorption maximum at 250 nm, typical of higher olefins. The unpercolated product has an adsorption maximum in the same region, since it too contains the same olefins. In order to prevent any interference from olefinic material a wavelength of 370 nm was chosen for absorption measurements of the coloured product. This wavelength also falls in visible region of the electromagnetic spectrum where yellow is known to absorb.

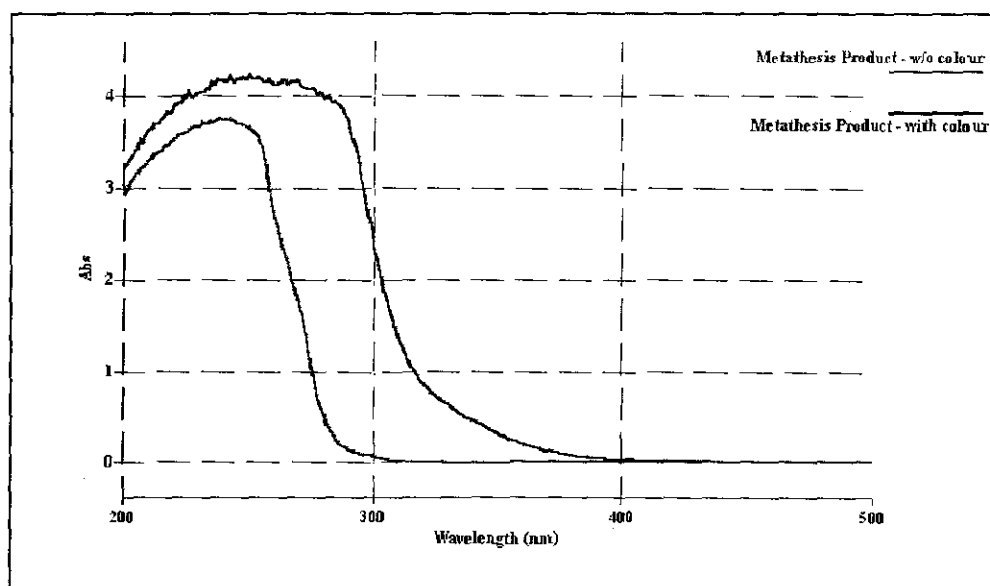


**Figure 5.6** The absorption spectra of the yellow and percolated (colourless) metathesis product.

### 5.5.9 Water and carbonyl analysis

Water analysis was done by colorimetry using a Metro-ohm colorimetric apparatus. Samples were analysed as is. The carbonyl content analysis was done by the Sasol Chemical Industries lab using an internal method, SAOW D.150 at 40 °C. The method involves the derivatization of carbonyls with an acidic solution of DNPH (2,4-dinitrophenylhydrazine) to form the corresponding hydrazones, which, upon reaction with sodium hydroxide, forms a wine-red colour and are quantified by means of UV-detection at 517 nm.

### 5.6 References

1. D. J. Moodley, C. van Schalkwyk, *SASTECH Internal Bulletin 7/01* (Confidential), August 2001
2. R. L. Banks in *Applied Industrial Catalysis*, Volume 3, B. E. Leach (Ed.), Academic Press (New York), 1984, p. 220; J. A. K. du Plessis, A. Spamer, H. C. M. Vosloo, *J. Mol. Catal. A: Chem.*, 1998, **133**, 175
3. P. Johnson, *Proceedings of the 7<sup>th</sup> World Petrochemical Congress*, 1967, p. 247
4. M. Sibeijn, E. K. Poels, A. Bliet, J. A. Moulijn, *J. Am. Oil Chem. Soc.*, 1994, **71**, 553
5. I. A. Fowles, *Gas Chromatography*, John Wiley & Sons (Chichester), 1995, p. 141
6. A. G. Basrur, S. R. Patwardan, S. N. Vyas, *J. Catal.*, 1991, **127**, 86
7. S. J. Choung, S. W. Weller, *Ind. Eng. Chem., Prod. Res. Dev.*, 1983, **22**, 662
8. A. K. Datye in *Handbook of Heterogeneous Catalysis*, Volume 2, G. Ertl, H. Knözinger, J. Weitkamp (Eds.), Wiley-VCH, (Weinheim), 1997, p. 234

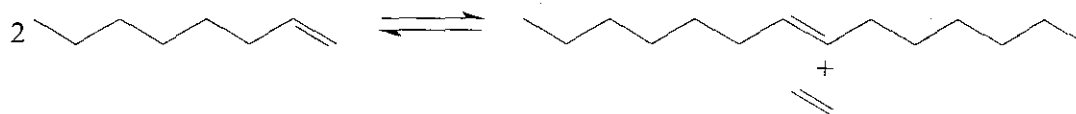
## 6 RESULTS AND DISCUSSION

---

### 6.1 Introduction

Olefin metathesis can be a valuable tool for the conversion of low value  $\alpha$ -olefins to longer chain internal olefins.<sup>1</sup> The internal olefins in the C<sub>10</sub>-C<sub>13</sub> range have applications as precursors to detergent range alcohols in the olefin and surfactant market.<sup>2</sup>

The WO<sub>3</sub>/SiO<sub>2</sub> catalyst is an active catalyst for the metathesis of  $\alpha$ -olefins at high temperatures.<sup>3</sup> Factors that influence the catalytic activity and selectivity, lifetime, product quality and coking were investigated. Evaluation of the catalyst was done using both 1-octene and an industrial 1-heptene cut. The primary metathesis products with a 1-octene feed are 7-tetradecene and ethene:

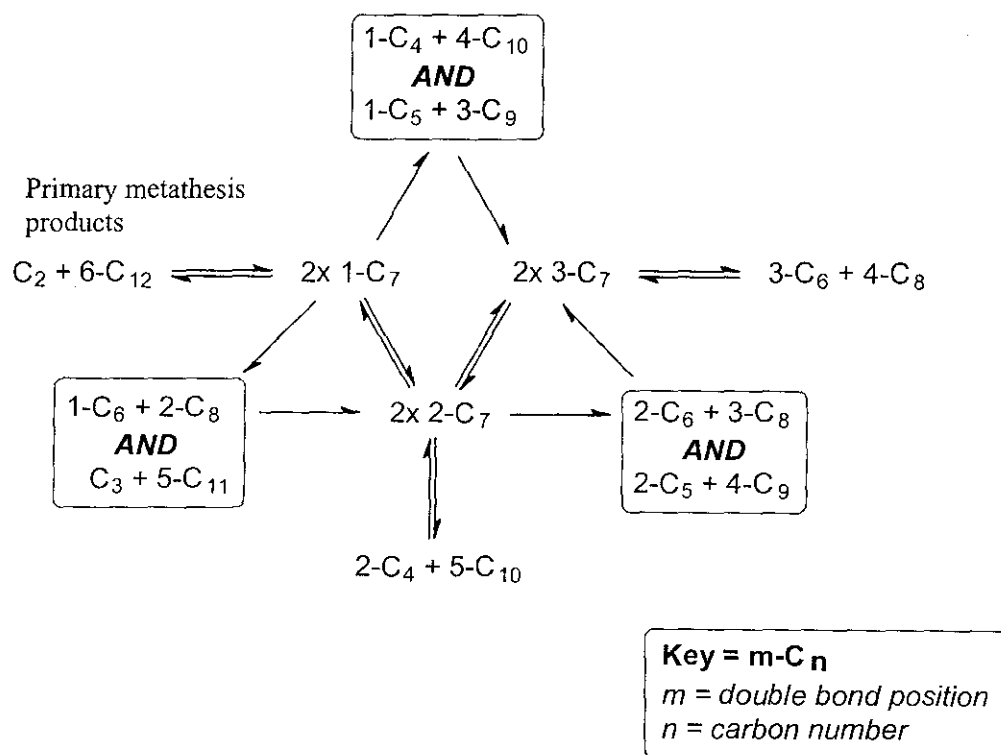


Similarly, the primary metathesis products with a 1-heptene feed are 6-dodecene and ethene.

The WO<sub>3</sub>/SiO<sub>2</sub> metathesis catalyst however requires relatively high reaction temperatures for maximum activity and this results in a mixture of products. It is well known that WO<sub>3</sub>/SiO<sub>2</sub> catalysts have substantial isomerization activity; as a consequence isomerization and metathesis of the feed will occur resulting in a distribution of products.<sup>4</sup> This product distribution is explained in Scheme 6.1 using 1-heptene (an industrial 1-heptene cut) as the substrate.

This product spectrum was formulated by assuming that the metathesis reaction proceeds *via* a metal carbene chain mechanism, that any non-symmetrical olefin can coordinate in two different ways with the active carbene and that only isomerization of the feed gives rise to the formation of secondary metathesis products. This scheme however just

indicates the formation of linear secondary metathesis products. It is also possible that skeletal isomerization of the feed occurs resulting in the formation of methyl branched metathesis products in the same range as indicated by the linear products illustrated in Scheme 6.1.



Scheme 6.1 **Formation of metathesis products via metathesis and isomerization of an industrial 1-heptene feed. Linear secondary metathesis products are indicated in the boxes.**

For the  $WO_3/SiO_2$  catalyst the following were investigated:

1. Influence of the metal loading on the  $SiO_2$  support.
2. Influence of ionic modification with alkali ions.
3. Lifetime, regeneration and coking studies.
4. Factors that influence coke formation.
5. Effect of oxygenates on the catalyst.

## 6.2 Influence of metal loading on catalyst structure and metathesis activity

The influence of tungsten loading on the structure, activity and the selectivity of the catalyst was investigated. Catalysts with different tungsten metal loading were prepared, i.e., 3, 4.5, 6, 7, 10, 15 and 20 wt%  $\text{WO}_3/\text{SiO}_2$ . These were characterised and then tested for metathesis activity with a percolated 1-octene feed stream.

### 6.2.1 Catalyst characterization

The actual loading of tungsten on the catalyst was determined by ICP and the results are tabulated in Table 6.1. Surface area analyses (Table 6.2) indicated a decrease in both surface area and pore volume with increasing tungsten loading. Crystallite size analyses, determined by XRD, indicated an increase in crystallite size with increasing loading. Crystallite size determinations could however only be done for catalysts with loadings of 8 wt% or more. For lower loadings the crystallite sizes were too small to determine.

To further explore the influence of the metal loading on the catalyst and the catalyst structure, XRD analyses were done (Figure 6.1). Only the diffraction pattern of the support was observed for low tungsten loadings indicating the presence of very small crystallites or an amorphous surface compound. From loadings of about 7 wt%  $\text{WO}_3$  upward it was possible to observe crystalline  $\text{WO}_3$ . A catalyst with 20 wt%  $\text{WO}_3$  showed the presence of extremely crystalline  $\text{WO}_3$  material.

Figure 6.2 shows the Raman spectra of the  $\text{WO}_3/\text{SiO}_2$  catalyst under ambient conditions. The spectrum possesses weak Raman bands due to the surface tungsten oxide species on  $\text{SiO}_2$  at 966-973 ( $\nu_s$  (W=O)) and 329.6  $\text{cm}^{-1}$  ( $\nu_b$  (W=O)).<sup>5</sup> The ( $\nu_s$  (W=O)) band is especially noticeable at low  $\text{WO}_3$  loadings (3 to 6 wt%  $\text{WO}_3$ ). However the Raman spectra of the  $\text{WO}_3/\text{SiO}_2$  catalysts also exhibits very strong Raman bands due to crystalline  $\text{WO}_3$  at 802-811, 700-718 and 271  $\text{cm}^{-1}$ , which are assigned to the symmetric stretching mode of the W-O bond, bending mode of the W-O bond and the deformation mode of the W-O-W bonds respectively.<sup>6</sup> These Raman bands also shift to the right (to lower wave numbers) with increasing tungsten loading, indicating a change in the physical environment of the crystalline  $\text{WO}_3$  molecules. On the catalysts with higher  $\text{WO}_3$  loadings the surface

tungsten oxide species on SiO<sub>2</sub> may be present but is probably obscured by the very strong Raman bands of crystalline WO<sub>3</sub>. A summary of the Raman bands of the different catalysts is shown in Table 6.3.

**Table 6.1** Quantification of weight percentage tungsten oxide present in the catalyst by ICP analyses.

Catalyst	wt% WO <sub>3</sub> ICP analyses
3 wt% WO <sub>3</sub> /SiO <sub>2</sub>	2.8
4.5 wt% WO <sub>3</sub> /SiO <sub>2</sub>	5.0
6 wt% WO <sub>3</sub> /SiO <sub>2</sub>	6.1
7 wt% WO <sub>3</sub> /SiO <sub>2</sub>	6.8
8 wt% WO <sub>3</sub> /SiO <sub>2</sub>	8.0
10 wt% WO <sub>3</sub> /SiO <sub>2</sub>	11.5
15 wt% WO <sub>3</sub> /SiO <sub>2</sub>	14.2
20 wt% WO <sub>3</sub> /SiO <sub>2</sub>	18.0

**Table 6.2** Summary of catalyst BET surface areas and crystallite sizes by XRD.

Catalyst	Surface Area (m <sup>2</sup> /g)	Pore Volume (cm <sup>3</sup> /g)	Avg. Pore Size (nm)	Crystallite Size (Å)
3 wt% WO <sub>3</sub> /SiO <sub>2</sub>	282	1.08	13.7	-
4.5 wt% WO <sub>3</sub> /SiO <sub>2</sub>	279	1.05	14.1	-
6 wt% WO <sub>3</sub> /SiO <sub>2</sub>	274	1.04	14.1	-
7 wt% WO <sub>3</sub> /SiO <sub>2</sub>	267	1.03	14.0	-
8 wt% WO <sub>3</sub> /SiO <sub>2</sub>	257	0.98	15.6	126.0
10 wt% WO <sub>3</sub> /SiO <sub>2</sub>	251	0.99	13.9	134.1
15 wt% WO <sub>3</sub> /SiO <sub>2</sub>	245	0.94	14.0	141.3
20 wt% WO <sub>3</sub> /SiO <sub>2</sub>	234	0.85	14.2	151.0

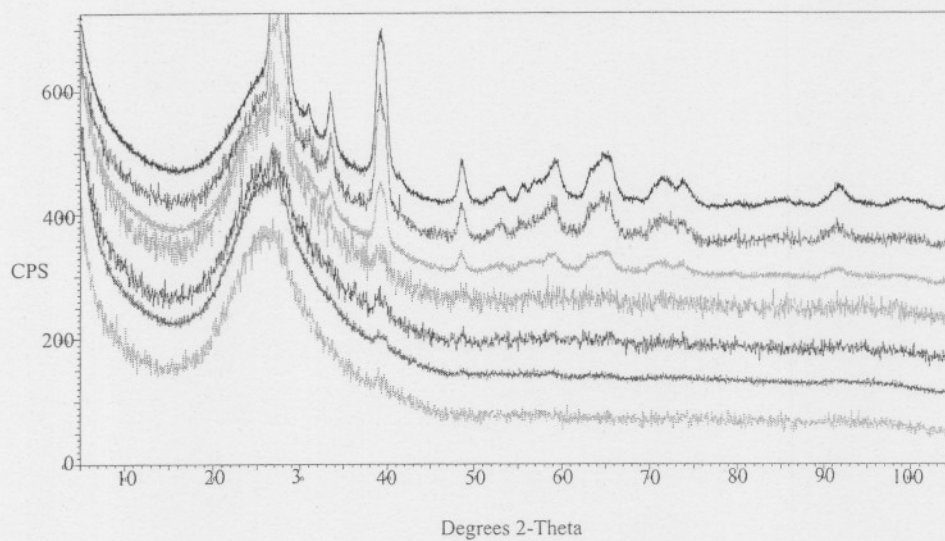


**Figure 6.1** XRD patterns of catalysts with 3, 4.5, 6, 8, 15 and 20 wt%  $\text{WO}_3$  on  $\text{SiO}_2$  (Spectra arranged from lowest loading at bottom to highest loading at top).

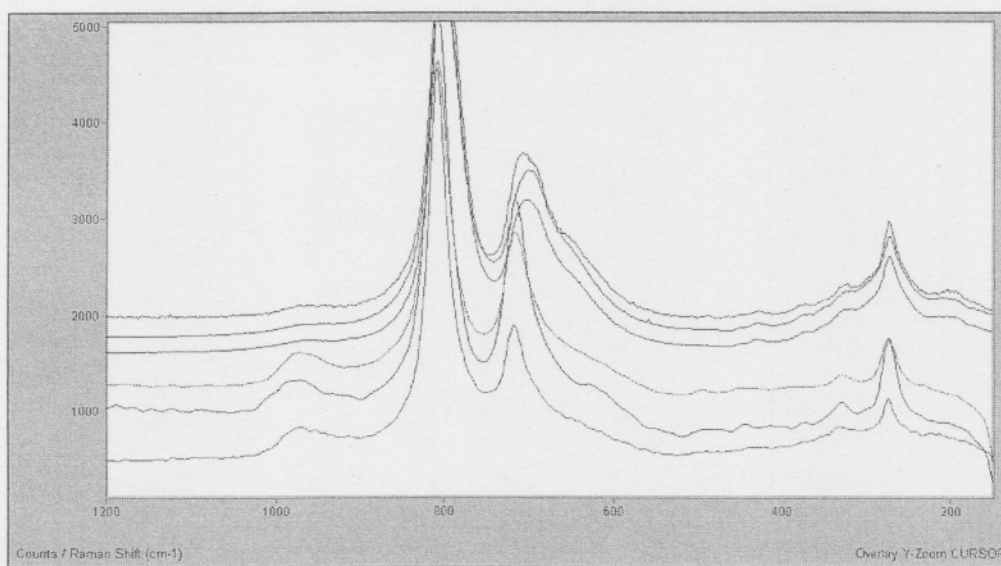


**Figure 6.2** Raman Spectra of the catalysts with 3, 4.5, 6, 8, 15 and 20 wt%  $\text{WO}_3$  on  $\text{SiO}_2$  (Spectra arranged from lowest loading at bottom to highest loading at top).

**Table 6.3** A summary of the Raman bands for the  $\text{WO}_3/\text{SiO}_2$  catalysts of different  $\text{WO}_3$  loadings.

Catalyst	$\nu_s (\text{W}=\text{O})/\text{cm}^{-1}$	$\nu_s (\text{W}-\text{O})/\text{cm}^{-1}$	$\nu_b (\text{W}-\text{O})/\text{cm}^{-1}$	$\nu_d (\text{W}-\text{O})/\text{cm}^{-1}$
3 wt% $\text{WO}_3/\text{SiO}_2$	977.3	809.7	719.1	272.3
4.5 wt% $\text{WO}_3/\text{SiO}_2$	976.4	808.2	717.1	271.3
6 wt% $\text{WO}_3/\text{SiO}_2$	975.6	807.9	716.9	269.9
8 wt% $\text{WO}_3/\text{SiO}_2$	973.5	805.9	714.8	269.9
15 wt% $\text{WO}_3/\text{SiO}_2$	967.3	805.9	714.8	269.9
20 wt% $\text{WO}_3/\text{SiO}_2$	965.2	805.9	708.6	269.9

$\nu_s$  – stretching mode,  $\nu_b$  – bending mode,  $\nu_d$  – deformation mode

The TEM micrographs of the 3, 7 and 20 wt%  $\text{WO}_3/\text{SiO}_2$  samples are illustrated in Figures 6.3-6.5. Large particles were observed on the 20 wt%  $\text{WO}_3/\text{SiO}_2$  catalyst. The crystallites showed dark features that were attributed to tungsten (confirmed by EDS). In the 3 wt%  $\text{WO}_3/\text{SiO}_2$  sample almost all the particles appeared to be uniform and the large crystallites of tungsten were not observed. The intermediate sample had mostly small and uniform particles but a few larger particles could be observed as well.

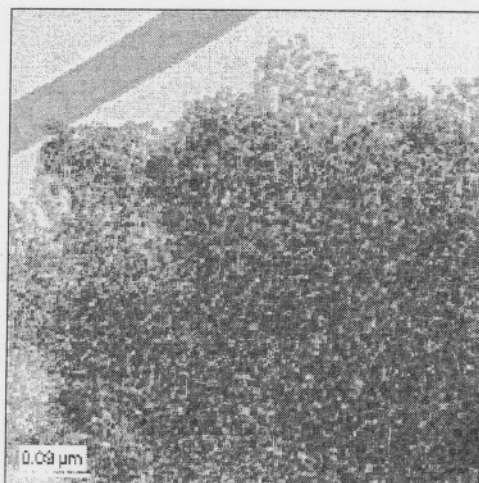


**Figure 6.3** TEM micrograph of catalyst with 3 wt%  $\text{WO}_3$  on  $\text{SiO}_2$ .

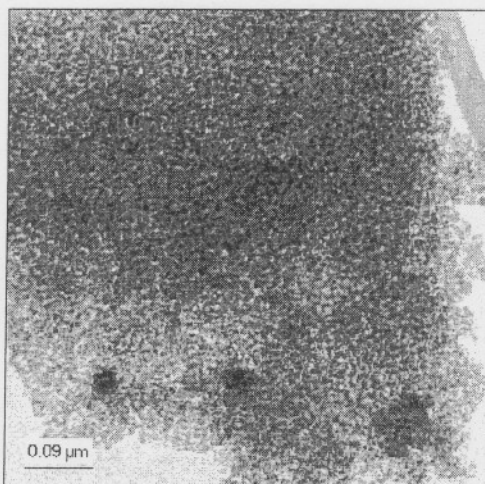


Figure 6.4 TEM micrograph of catalyst with 7 wt%  $\text{WO}_3$  on  $\text{SiO}_2$ .

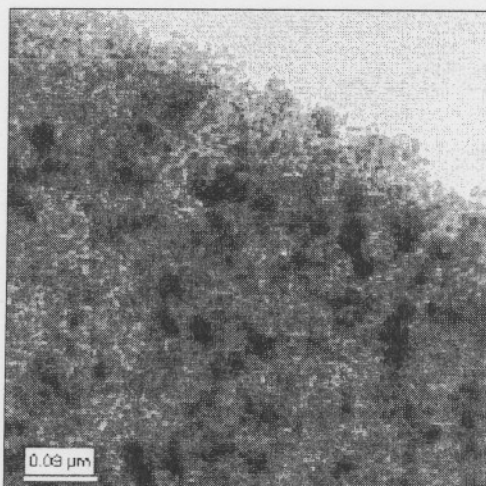


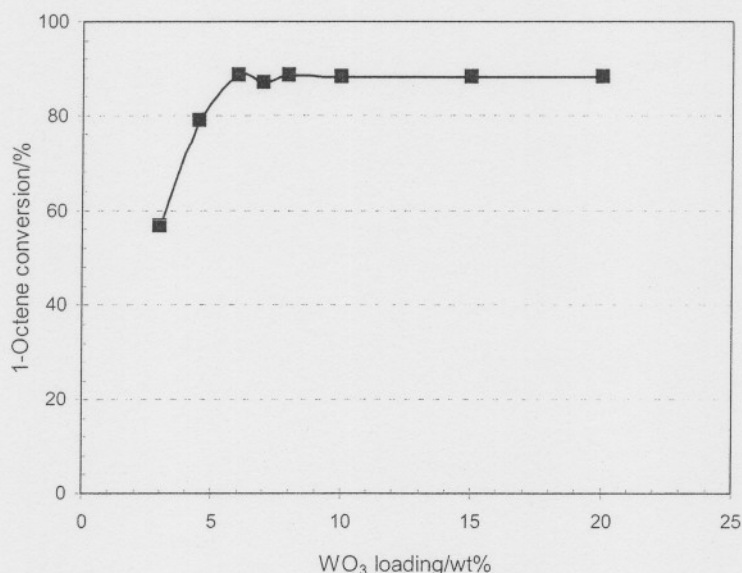
Figure 6.5 TEM micrograph of catalyst with 20 wt%  $\text{WO}_3$  on  $\text{SiO}_2$ .

### 6.2.2 Influence of metal loading on the metathesis activity of the $\text{WO}_3/\text{SiO}_2$ catalyst using a 1-octene feed

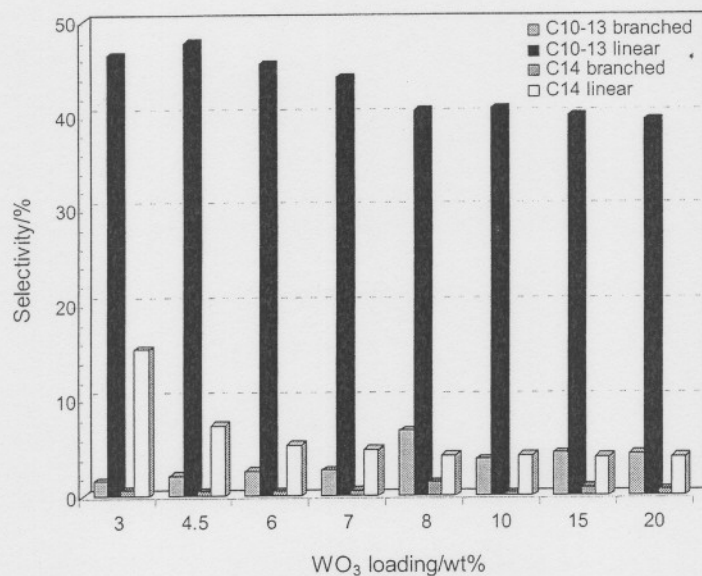
Metathesis reactions were performed with all the catalysts in the once through mode. Standard reaction conditions were 460 °C, 5.6  $\text{h}^{-1}$  LHSV and atmospheric pressure. Percolated 1-octene was used as feed in all cases. All reactions were terminated after 8 h online and the averages of conversion and product selectivities over this 8 h period were calculated.

Figure 6.6 indicates the relationship between  $\text{WO}_3$  loading and conversion. An increase in conversion of 1-octene with increasing  $\text{WO}_3$  loading is observed up to a loading of 6 wt%. Conversion stabilises with further addition of  $\text{WO}_3$  and it does not seem as if a further increase in tungsten loading has any significant effect on the conversion. The relationship between product selectivity and tungsten loading is illustrated in Figure 6.7. From the results it is clear that selectivity to the primary metathesis product 7-tetradecene (linear  $\text{C}_{14}$ ) is high at lower  $\text{WO}_3$  loadings. Selectivity to the linear  $\text{C}_{10}$ - $\text{C}_{13}$  metathesis products is also very high at low loadings but in both instances selectivity to the linear metathesis products slowly declines with increasing  $\text{WO}_3$  loading and stabilises from 8 wt%. Selectivity to branched products increase with loading and as with the rest of the products selectivity stabilises from 8 wt%  $\text{WO}_3$ .

An interesting observation regarding the lifetime of the different catalysts was that catalysts with lower loadings of  $\text{WO}_3$  (3 to 7 wt%) deactivated faster with time online as can be observed in Figure 6.7. In comparison  $\text{WO}_3$  loadings of 8 wt% and more did not show any deactivation and the conversion remained relatively constant over the 8 h period. It was decided to conduct all future experiments on the 8 wt% catalyst as this catalyst did not show signs of deactivation during the 8 h screening period.



**Figure 6.6** Influence of  $\text{WO}_3$  loading on 1-octene conversion over a  $\text{WO}_3/\text{SiO}_2$  metathesis catalyst (Reaction conditions: 460 °C, 5.6 h<sup>-1</sup> LHSV).



**Figure 6.7** Influence of WO<sub>3</sub> loading on product selectivity of WO<sub>3</sub>/SiO<sub>2</sub> metathesis catalysts. (Reaction conditions: 460 °C, 5.6 h<sup>-1</sup> LHSV).

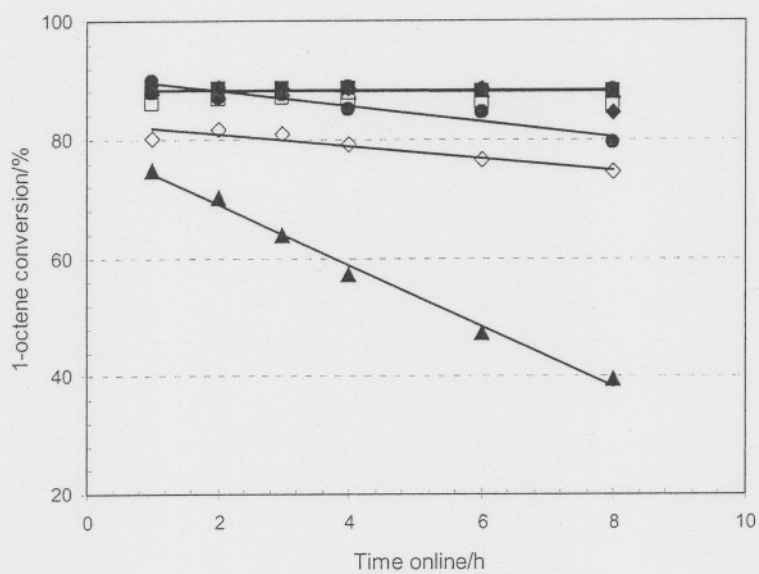


**Figure 6.8** The relationship between conversion and time online for WO<sub>3</sub>/SiO<sub>2</sub> catalysts with different WO<sub>3</sub> loadings. Reaction conditions: 460 °C, 5.6 h<sup>-1</sup> LHSV (▲ 3 wt%; ◇ 4.5 wt%; ● 6 wt%; ◆ 7 wt%; □ 8 wt%; ○ 10 wt%; ■ 15 wt%; △ 20 wt%).

### 6.2.3 Metathesis of 1-octene with the 8 wt% WO<sub>3</sub>/SiO<sub>2</sub> catalyst

A once through reaction was conducted with the 8 wt% WO<sub>3</sub>/SiO<sub>2</sub> catalyst at 460 °C, 5 h<sup>-1</sup> LHSV with percolated 1-octene as feed. The conversion, selectivity and yield curves for the reaction are depicted in Figure 6.9.

The selectivity and yield for the reaction is low for the first hour. This corresponds to the break-in time that is characteristic for tungsten oxide on silica metathesis catalysts. The average selectivity toward the detergent range olefin product is on average, 42%. The selectivity to the primary metathesis product is low at 5%.

### 6.2.4 Metathesis of an industrial cut 1-heptene feed with the 8 wt% WO<sub>3</sub>/SiO<sub>2</sub> catalyst

A once through reaction was conducted with the 8 wt% WO<sub>3</sub>/SiO<sub>2</sub> catalyst at 460 °C, 5 h<sup>-1</sup> LHSV with a percolated, industrial cut 1-heptene feed. The feed contained 75% 1-heptene and 25% paraffins and branched olefins. The purpose of the conducting such a reaction is to determine if this industrial cut feed is suitable for the metathesis reaction and if similar results to 1-octene are obtained. The conversion, selectivity and yield curves for the reaction are depicted in Figure 6.10.

The activity of the catalyst is similar to the case with 1-octene, but lower yields and selectivities towards the detergent range olefins are obtained. The selectivity to the primary metathesis product (C<sub>12</sub>) is also low.

## 6.3 Influence of ionic modification of the catalyst with Alkali metal ions

### 6.3.1 Influence of doping with 0.1 wt% of alkali metal ions on metathesis activity and selectivity

The influence of modification of the support surface with alkali metal ions on the activity and selectivity of an 8 wt% WO<sub>3</sub>/SiO<sub>2</sub> catalyst for the metathesis of 1-octene was investigated. Most earlier work on the addition of alkali metal ions to tungsten based

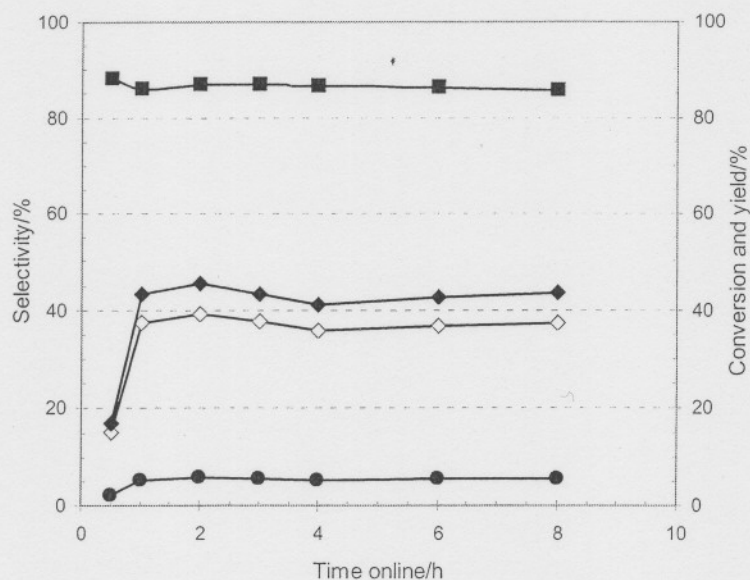


**Figure 6.9** Activity, selectivity and yield curves for the metathesis of 1-octene over the  $\text{WO}_3/\text{SiO}_2$  catalyst. Reaction conditions:  $460^\circ\text{C}$ ,  $5\text{ h}^{-1}$  LHSV (■ Conversion; ◆  $\text{C}_{10}\text{-C}_{13}$  Selectivity; ◇  $\text{C}_{10}\text{-C}_{13}$  Yield; ●  $\text{C}_{14}$  Selectivity).

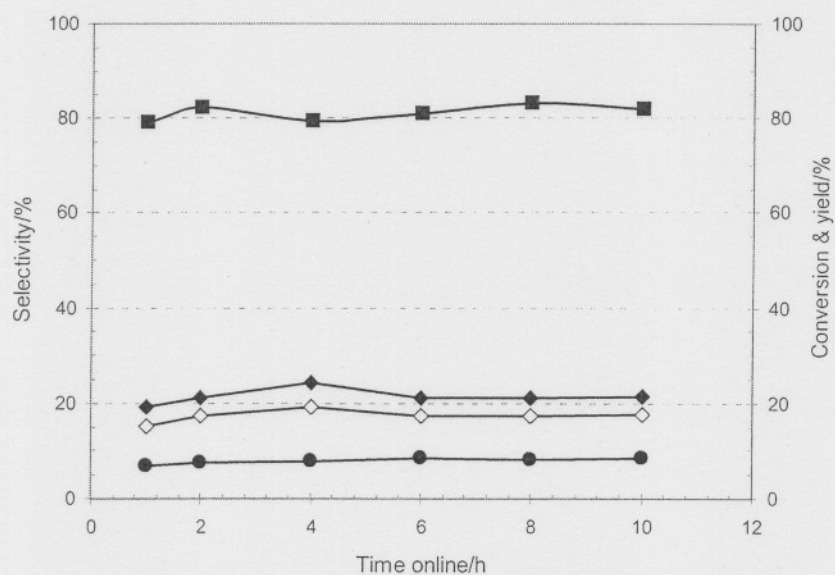


**Figure 6.10** Activity, selectivity and yield curves for the metathesis of an industrial cut 1-heptene feed over the 8 wt%  $\text{WO}_3/\text{SiO}_2$  catalyst. Reaction conditions:  $460^\circ\text{C}$ ,  $5\text{ h}^{-1}$  LHSV (■ Conversion; ◆  $\text{C}_{10}\text{-C}_{13}$  Selectivity; ◇  $\text{C}_{10}\text{-C}_{13}$  Yield; ●  $\text{C}_{12}$  Selectivity).

catalysts has been restricted to sodium and potassium ions.<sup>7</sup> The first objective of this study was to determine whether increasing the alkali metal ion size had any influence on the selectivity of the 8 wt%  $\text{WO}_3/\text{SiO}_2$  catalyst. Sodium, potassium and cesium ions were selected for testing and an arbitrary value of 0.1 wt% of each alkali metal ion was deposited onto an 8 wt%  $\text{WO}_3/\text{SiO}_2$  catalyst. The silica gel was first treated with 0.1 wt% of  $\text{M}^+\text{NO}_3^-$  ( $\text{M}^+ = \text{Na}^+, \text{K}^+, \text{Cs}^+$ ) prior to impregnation with an aqueous solution of ammonium metatungstate hydrate. These catalysts were compared to a standard unmodified catalyst in terms of conversion and selectivity. All reactions were online for 8 h and results are reported as averages over the 8 h period. Reaction conditions were 460 °C, 5.6  $\text{h}^{-1}$  LHSV and atmospheric pressure.

The addition of the alkali ions resulted in a decline in activity of the catalyst. The activities of catalysts doped with 0.1 wt% of  $\text{Na}^+$ ,  $\text{K}^+$ , and  $\text{Cs}^+$  are compared in Figure 6.11. The activity of the catalysts decreased in the order: no  $\text{M}^+ > \text{Cs}^+ \approx \text{K}^+ \approx \text{Na}^+$ .

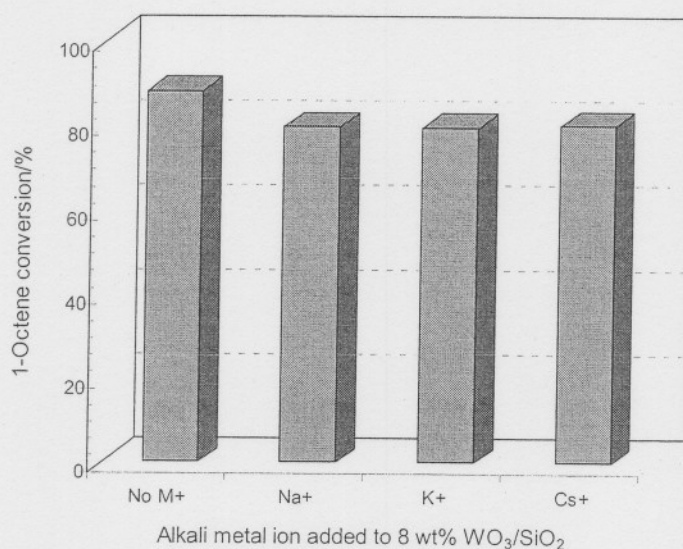


**Figure 6.11** The influence of 0.1 wt%  $\text{Na}^+$ ,  $\text{K}^+$ , and  $\text{Cs}^+$  on the activity of an 8 wt%  $\text{WO}_3/\text{SiO}_2$  catalyst for the metathesis of 1-octene (Reaction temp = 460 °C, LHSV = 5.6  $\text{h}^{-1}$ , Reaction time = 8 h).

Pre-treatment of the 8 wt%  $\text{WO}_3/\text{SiO}_2$  catalyst with the alkali ions clearly had an effect on the selectivity of the catalyst towards the desired products as can be observed in Figure 6.12. The doping of the catalyst with the alkali metal ions resulted in improved selectivity to the desired detergent olefin range ( $\text{C}_{10}\text{-C}_{13}$  linear). The order of increasing selectivity towards the  $\text{C}_{10}\text{-C}_{13}$  linear products was:  $\text{no M}^+ < \text{Na}^+ < \text{K}^+ < \text{Cs}^+$ . There was also an improvement in the selectivity toward the primary metathesis product ( $\text{C}_{14}$  linear). There was a decrease in the amount of branched olefins in both the  $\text{C}_{10}\text{-C}_{13}$  range and  $\text{C}_{14}$  range. The cesium ion doped catalyst showed the greatest increase in  $\text{C}_{10}\text{-C}_{13}$  linear selectivity, while the potassium ion doped catalyst showed the highest increase in  $\text{C}_{14}$  selectivity. The order of decreasing selectivity towards branched products was:  $\text{no M}^+ > \text{Na}^+ > \text{K}^+ > \text{Cs}^+$ .

### 6.3.2 The influence of the sequence of impregnation of alkali metal ions

The sequence of impregnation may play a role in influencing the selectivity of the catalyst and it has been reported that the order of impregnation is an important factor in the preparation of metathesis catalysts.<sup>8</sup> This postulate was tested by comparing two catalyst samples in which the sequence of impregnation was reversed. In the first sample the silica was impregnated with the tungsten salt followed by impregnation with potassium ions (normal impregnation). In the second sample the silica was impregnated with potassium ions and then impregnated with the tungsten salt (reverse impregnation). The results of this experiment are illustrated in Figure 6.13.

This study suggests that impregnation with potassium ions before impregnation with the tungsten salt (normal impregnation) results in a slight decrease in the conversion as well as a decrease in the  $\text{C}_{10}\text{-C}_{13}$  selectivity.

### 6.3.3 The influence of alkali metal loading on metathesis activity and selectivity

Different amounts of potassium ions (0.05, 0.1 and 0.5 wt%) were loaded onto the 8 wt%  $\text{WO}_3/\text{SiO}_2$  metathesis catalyst. The catalysts were then tested in a once through mode at 460 °C and 5.6  $\text{h}^{-1}$  LHSV with a percolated 1-octene feed over a period of 8 h. The influence of potassium ion loading on the activity of the 8 wt%  $\text{WO}_3/\text{SiO}_2$  metathesis catalyst is shown in Figure 6.14. The feed conversion decreases with an increase in

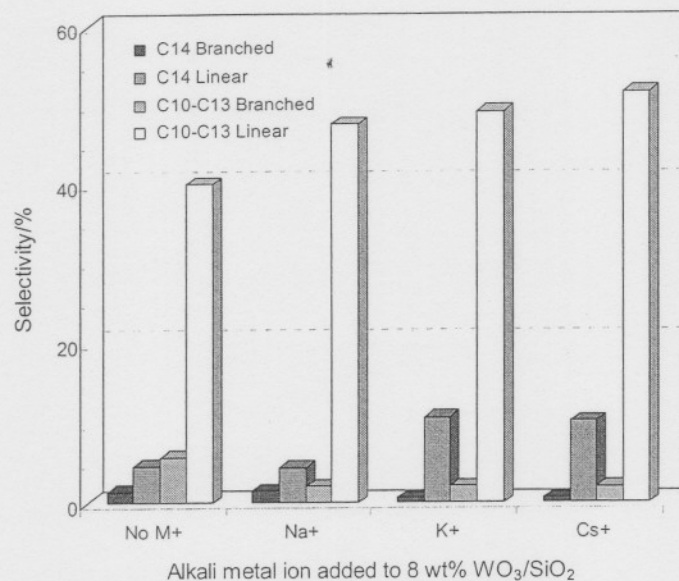


**Figure 6.12** The influence of 0.1 wt% Na<sup>+</sup>, K<sup>+</sup>, and Cs<sup>+</sup> on the selectivity of an 8 wt% WO<sub>3</sub>/SiO<sub>2</sub> catalyst for the metathesis of 1-octene (Reaction temp = 460 °C, LHSV = 5.6 h<sup>-1</sup>, Reaction time = 8 h).

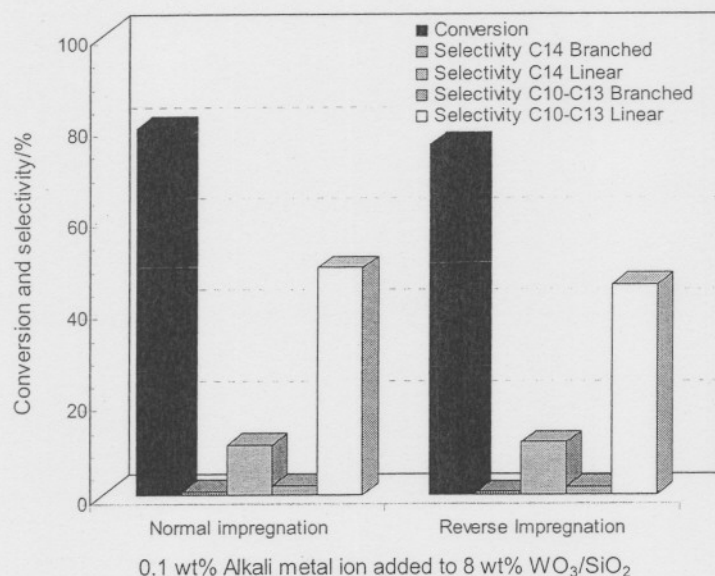


**Figure 6.13** The influence of the impregnation sequence of 0.1 wt% potassium ion and the tungsten precursor on the conversion and selectivity of the 8 wt% WO<sub>3</sub>/SiO<sub>2</sub> metathesis catalyst for the metathesis of 1-octene (Reaction temp = 460 °C, LHSV = 5.6 h<sup>-1</sup>, Reaction time = 8 h).

potassium ion loading. At 0.5 wt% K<sup>+</sup> the catalyst activity drops to around 10%. The influence of potassium ion loading on the catalyst selectivity is shown in Figure 6.15. The selectivity towards the primary metathesis product (C<sub>14</sub>) increases gradually with potassium ion loading up to 0.1 wt%. At 0.5 wt% K<sup>+</sup> there is dramatic increase in selectivity to the C<sub>14</sub> olefin product. Selectivity to the C<sub>10</sub>-C<sub>13</sub> fraction increases with increasing potassium loading up to 0.1 wt% K<sup>+</sup> after which it declines sharply.

## 6.4 Lifetime, regeneration and coking studies of the 8 wt% WO<sub>3</sub>/SiO<sub>2</sub> catalyst

### 6.4.1 Lifetime and effect of regeneration of the catalyst

Van Schalkwyk *et al.*<sup>9</sup> used an experimental design program to optimise reaction conditions for an 8 wt% WO<sub>3</sub>/SiO<sub>2</sub> catalyst using an industrial cut 1-heptene feed. It was decided to use these reported optimized conditions (LHSV = 16 h<sup>-1</sup>, temperature = 460 °C and a feed to recycle ratio of 1:5.6), for the experimental work to determine the lifetime and study the online activity changes of the catalyst. An industrial cut 1-heptene feed containing 75% 1-heptene and 25% paraffins and branched olefins was metathesized over the 8 wt% WO<sub>3</sub>/SiO<sub>2</sub> catalyst, in a recycle mode. The catalyst was run for a period of 700 h and the run was terminated after the catalyst showed signs of deactivation. The activity and selectivity of the catalyst for this run is shown in Figure 6.16.

Coke formed on the catalyst was analysed by TG and this revealed 45.7% coke. The same catalyst was then regenerated and run with 1-heptene feed. The run with the regenerated catalyst lasted 1200 h before it showed signs of deactivation. The activity and selectivity for the run is shown in Figure 6.17. The run was terminated and the catalyst was analysed again by TG and showed 46.2% mass loss due to coke burn off.

During the two runs the catalyst became more selective towards the primary metathesis products (C<sub>2</sub> and C<sub>12</sub>) with time online. The conversion is a little lower after regeneration, but the selectivity towards the C<sub>10</sub>-C<sub>13</sub> fraction is almost the same.

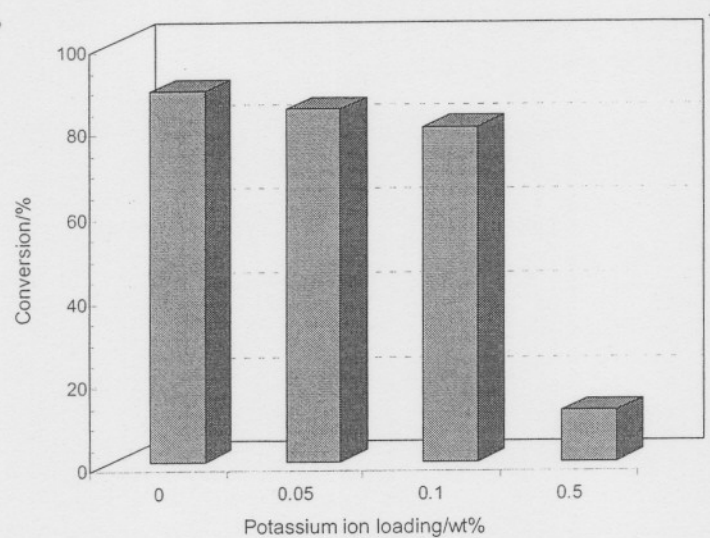


**Figure 6.14** The influence of potassium ion loading on the activity the 8 wt%  $\text{WO}_3/\text{SiO}_2$  metathesis catalyst for the metathesis of 1-octene (Reaction temp = 460 °C, LHSV = 5.6  $\text{h}^{-1}$ , Reaction time = 8 h).

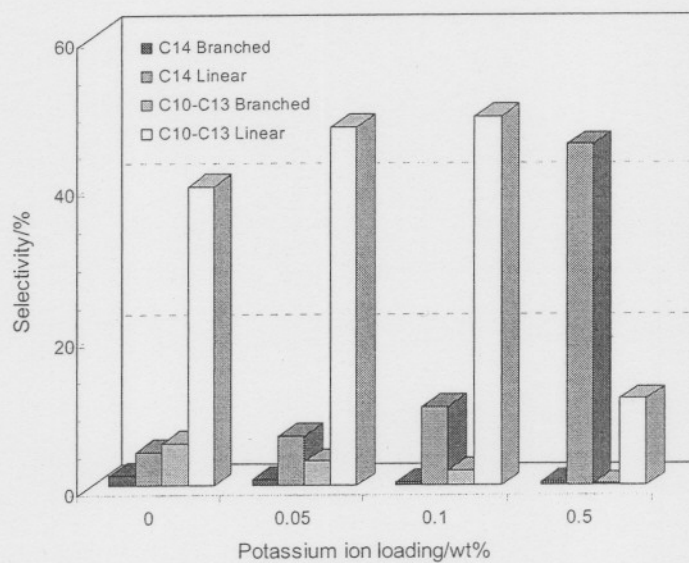


**Figure 6.15** The influence of potassium ion loading on the selectivity of the 8 wt%  $\text{WO}_3/\text{SiO}_2$  metathesis catalyst for the metathesis of 1-octene.

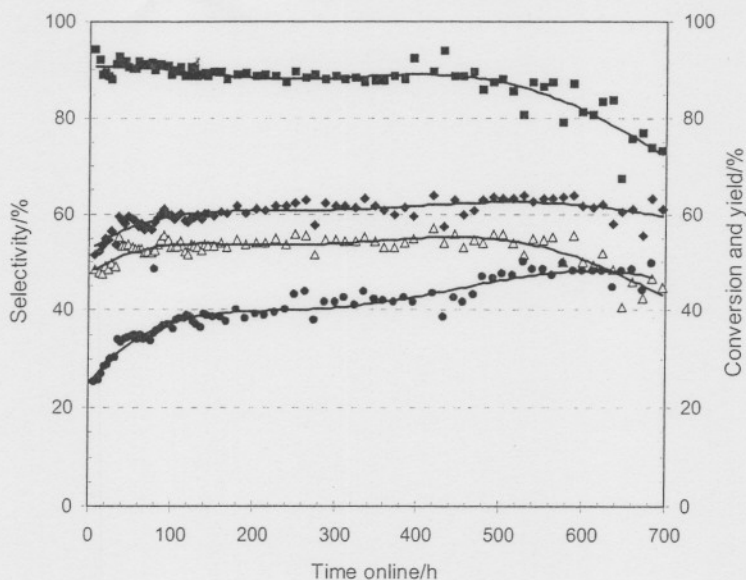


**Figure 6.16** Activity of the fresh 8 wt%  $\text{WO}_3/\text{SiO}_2$  catalyst as a function of time online. Reaction temperature = 460 °C, LHSV = 16  $\text{h}^{-1}$ , Feed: recycle ratio = 1:5.6. (■ Conversion; ◆  $\text{C}_{10}\text{-C}_{13}$  Selectivity; ◇  $\text{C}_{10}\text{-C}_{13}$  Yield; ●  $\text{C}_{12}$  Selectivity).

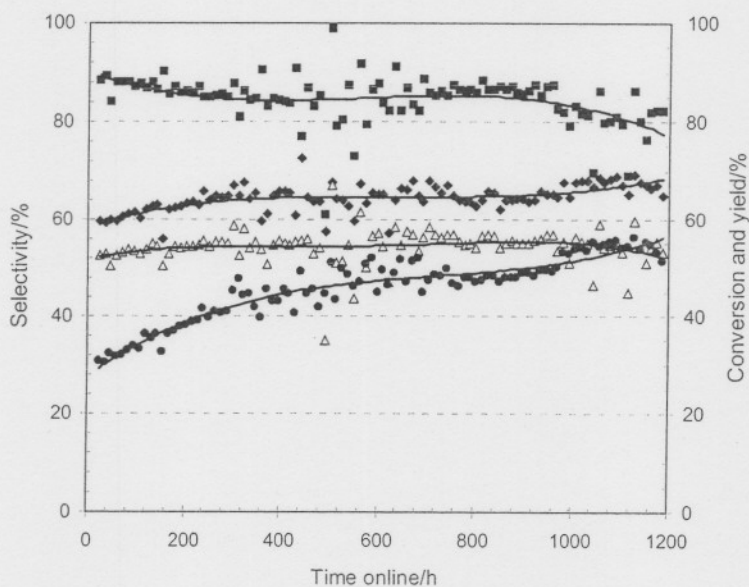


**Figure 6.17** Activity of the regenerated 8 wt%  $\text{WO}_3/\text{SiO}_2$  catalyst as a function of time online. Reaction temperature = 460 °C, LHSV = 16  $\text{h}^{-1}$ , Feed: recycle ratio = 1:5.6 (■ Conversion; ◆  $\text{C}_{10}\text{-C}_{13}$  Selectivity; ◇  $\text{C}_{10}\text{-C}_{13}$  Yield; △  $\text{C}_{12}$  Selectivity).

In order to investigate the ratio of primary to secondary metathesis, it was decided to monitor the ethene and propene selectivity. Ethene is a primary metathesis product while propene is a product of secondary metathesis (see Scheme 6.1). From Figure 6.18 it is clear that the catalyst has about the same selectivity towards propene and ethene in the initial stages. The longer the time online, the more selective the catalyst becomes towards the primary metathesis products ( $C_2$  and  $C_{12}$ ). The production of ethene increases and the production of propene decreases. This shows that the catalyst becomes selective towards metathesis and that isomerization activity is reduced.

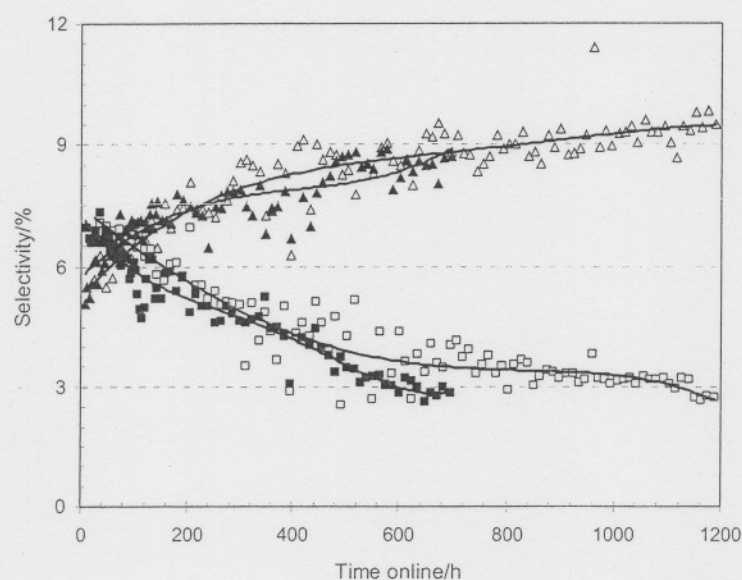


**Figure 6.18** Selectivity towards ethene and propene as a function of time for the two long runs. Reaction temperature = 460 °C, LHSV = 16h<sup>-1</sup>, Feed: recycle ratio = 1: 5.6. (▲ ethene (1 st run); △ ethene (2 nd run); ■ propene (1 st run); □ propene (2 nd run)).

#### 6.4.2 Characterisation of fresh, spent and regenerated catalysts

During the two demonstration runs, discussed in Section 6.4.1, the coke levels on the catalyst built up to 46%. This effectively means that the catalyst has doubled its mass due to coke deposition. At these high coke levels plugging may become a serious problem. This will result in a pressure drop over the catalyst bed and will cause complications

during scale-up. However no pressure drop was observed during either of the two demonstration runs. To verify this observation, a simple experiment was conducted to observe the change in bulk volume of the catalyst after the coke was burnt off. A 10 ml sample of spent catalyst, from the second run, was carefully, measured in a 10 ml measuring cylinder. The sample of catalyst was weighed and found to have a total mass of 7.01 g. The catalyst was then regenerated in an oven at 550 °C under air. After regeneration, the catalyst volume and mass was determined again. These measurements showed a mass loss of 49% with only a 1% change in bulk volume indicating that most of the coke deposits may form inside the pores of the catalyst. To confirm these observations, SEM analyses (Figures 6.19-22) were done on the fresh and spent catalyst (after being online for 1200 h).

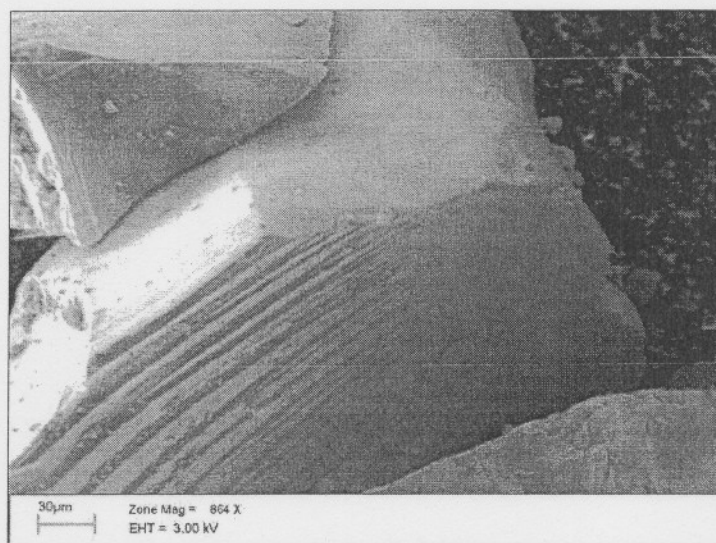


**Figure 6.19** SEM micrograph of the fresh 8 wt%  $\text{WO}_3/\text{SiO}_2$  catalyst.

A close inspection of Figure 6.19 revealed grooves in the catalyst particle that originates from the  $\text{SiO}_2$  support. These grooves were created during grinding of the support to the correct size prior to impregnation.<sup>10</sup> The grooves are still visible in the spent catalyst sample (Figure 6.20), further verifying the fact that coke formation occurs predominantly in the pores of the catalyst and not to a great extent on the outside of the particle. Further magnification of the surface of both the fresh and spent catalyst (Figures 6.21 and 6.22) revealed no cracks or damage to the surface of the catalyst. Following the

observations made from the SEM analysis, one would expect a decrease in the average pore diameter, pore size and surface area of the catalyst from the fresh to the spent catalyst. This was indeed the case as is indicated in Table 6.4. Crystallite sizes (XRD) and tungsten content determinations (ICP) were also done and are included in Table 6.4.

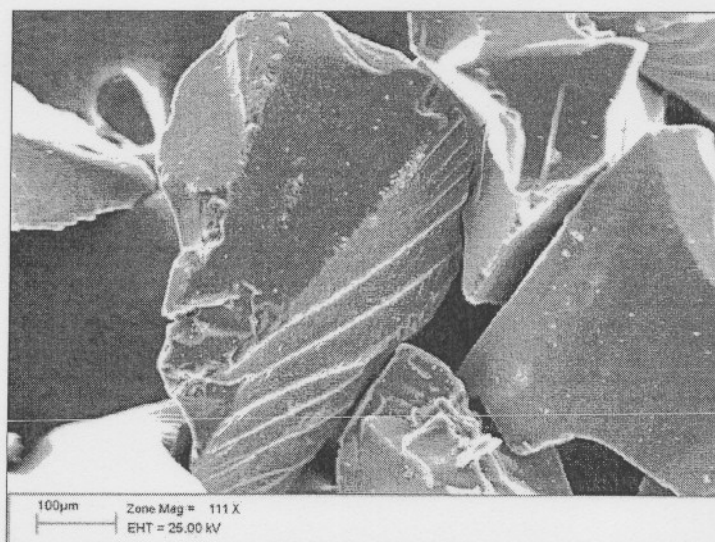


Figure 6.20 SEM micrograph of the spent 8 wt%  $\text{WO}_3/\text{SiO}_2$  catalyst.

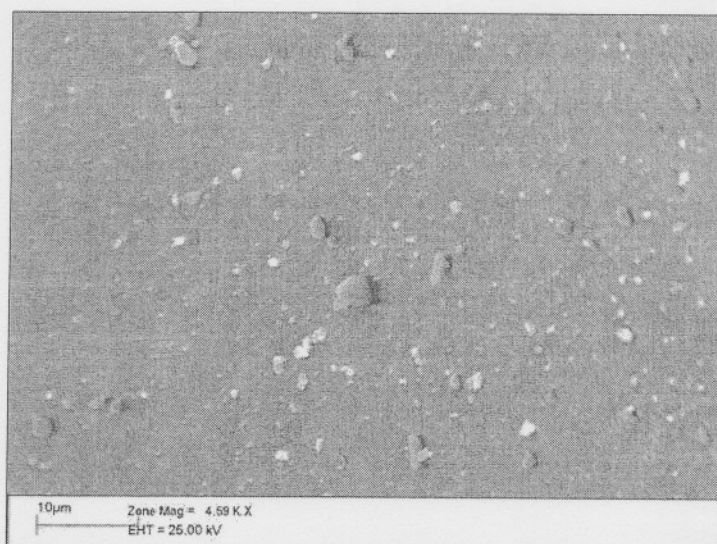


Figure 6.21 SEM micrograph of the fresh 8 wt%  $\text{WO}_3/\text{SiO}_2$  catalyst (higher magnification).



**Figure 6.22** SEM micrograph of the spent 8%  $\text{WO}_3/\text{SiO}_2$  catalyst (higher magnification).

**Table 6.4** Surface area analysis of the 8 wt%  $\text{WO}_3/\text{SiO}_2$  catalyst during different stages.

Catalyst	BET ( $\text{m}^2/\text{g}$ )	Avg. Pore Size (nm)	Pore volume ( $\text{cm}^3 \cdot \text{g}^{-1}$ )	Crystallite Size ( $\text{\AA}$ )	wt% $\text{WO}_3$ ICP analyses
Fresh*	257.74	15.65	0.98	126	8.0
Spent**	127.66	7.35	0.21	-	
Regenerated***	257.73	16.08	1.03	110	7.8

\* 8 wt%  $\text{WO}_3/\text{SiO}_2$  calcined at 550 °C in air.

\*\* deactivated 8%  $\text{WO}_3/\text{SiO}_2$  after 2 runs in the recycle reactor with  $\text{C}_7$  SLO as feed.

\*\*\* Regenerated – Spent 8%  $\text{WO}_3/\text{SiO}_2$  regenerated in air at 550 °C.

#### 6.4.3 Location of coke on the catalyst

There is a difficulty in distinguishing between carbon and silica using transmission electron microscopy methods, as they may both be amorphous in nature. High resolution transmission electron microscopy (HRTEM) can provide useful information about the location of the tungsten crystallites on the silica carrier, but will not allow one to detect coke on the catalyst. Energy Filtered Transmission Electron Microscopy (EFTEM)

provides a way for distinguishing carbon from silica. A catalyst containing 46% coke, determined by TG analysis was used for this study. This catalyst was still active for the metathesis reaction although deactivation behaviour had set in.

The HRTEM image of the coked catalyst (Figure 6.23) shows clusters of tungsten oxide (darker regions, **a**) present on the silica support (lighter regions, **b**). It is not possible to distinguish between the carbon and the silica support.<sup>11</sup>

The EFTEM technique couples normal transmission electron microscopy with a powerful energy filter. In this way a carbon map of the region was obtained. The carbon map of the catalyst (Figure 6.24) shows all of the carbon (orange region) surrounding the tungsten oxide cluster (blue cluster in centre). Carbon deposition seems to occur mostly around the clusters and does not cover them to a great extent. To ensure this observation was indeed the case and not the result of an artefact an oxygen map was also done (Figure 6.25). The catalyst was oxygen rich throughout (gold regions) as expected as it contains  $\text{WO}_3$  as well as  $\text{SiO}_2$ .

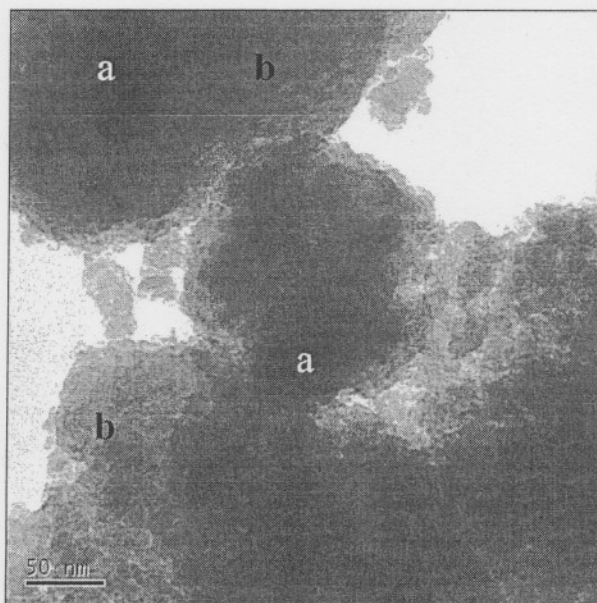


**Figure 6.23** HRTEM micrograph of an 8 wt%  $\text{WO}_3/\text{SiO}_2$  catalyst containing 46% coke.

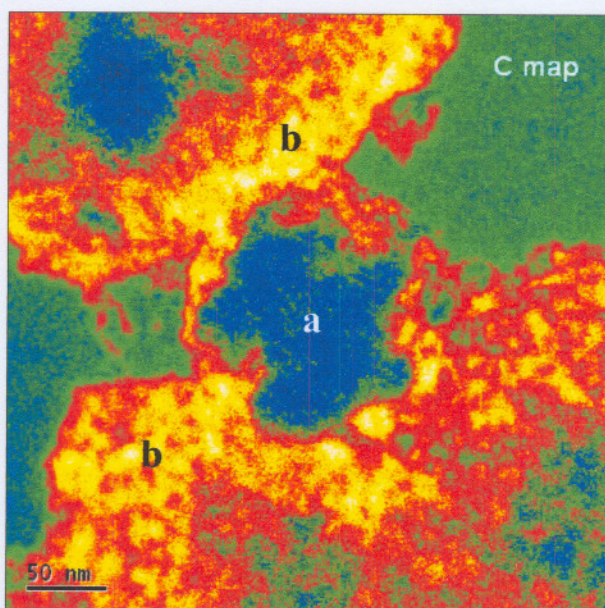


**Figure 6.24** EFTEM carbon map of an 8 wt%  $\text{WO}_3/\text{SiO}_2$  catalyst containing 46% coke.

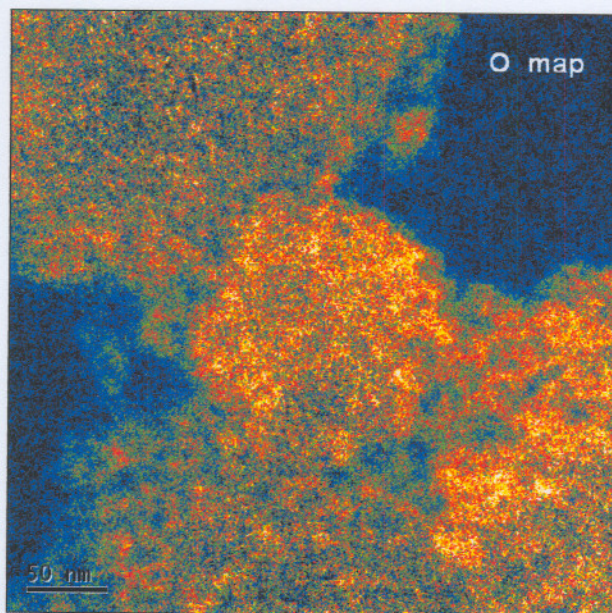


**Figure 6.25** EFTEM oxygen map of an 8 wt%  $\text{WO}_3/\text{SiO}_2$  catalyst containing 46% coke.

## 6.5 Factors effecting coke formation

### 6.5.1 Coke formation as a function of temperature

Temperature plays an important role in the formation of coke on acid catalysts.<sup>12</sup> The influence of reaction temperature was investigated with the industrial cut 1-heptene feed over the 8 wt%  $\text{WO}_3/\text{SiO}_2$  catalyst in a recycle mode. Reactions were conducted over a period of 48 h at  $16 \text{ h}^{-1}$  LHSV at temperatures of 550, 505 and 460 °C with a feed to recycle ratio of 1:5.6. The effect of temperature on coke formation is shown in Figure 6.26.

Temperature plays a major role in the formation of coke. Coke formation increases with increasing temperature. After 48 h at 550 °C the coke level on the catalyst is 23% while at 460 °C after the same time online the coke level on the catalyst is 1.5%. Working at lower temperatures is favourable in terms of reducing coke formation

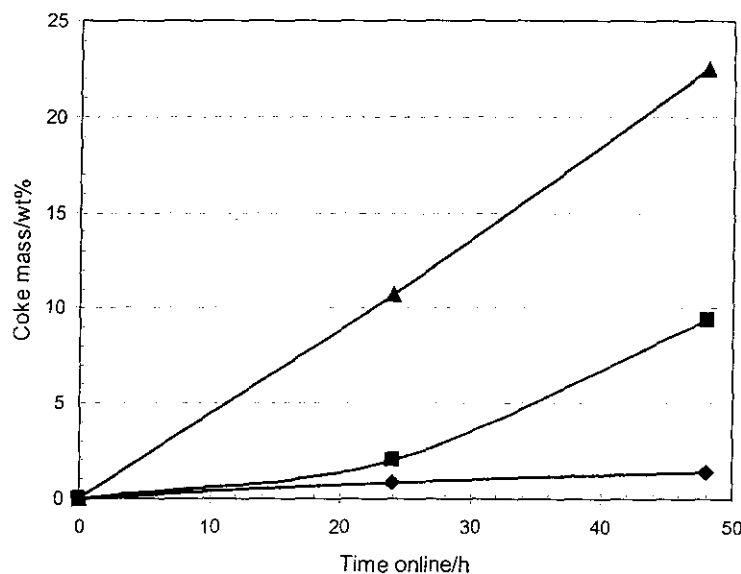


**Figure 6.26** Coke formation on an 8 wt%  $\text{WO}_3/\text{SiO}_2$  catalyst as a function of time online at different temperatures ( $\blacktriangle$  550 °C,  $\blacksquare$  505 °C,  $\blacklozenge$  460 °C).

### 6.5.2 Coke formation as a function of space velocity

The influence of space velocity was investigated with the industrial cut 1-heptene feed over the 8 wt%  $\text{WO}_3/\text{SiO}_2$  catalyst in a recycle mode. Reactions were conducted over a period of 48 h at 460 °C and at LHSV's of 4 and 16  $\text{h}^{-1}$  with a feed to recycle ratio of 1:5.6. The effect of space velocity is depicted in Figure 6.27. Coke formation increases with an increase in space velocity. The amount of coke formed is directly proportional to the amount of reactable feed per hour through the reactor. It is therefore clear that working at a lower LHSV would have a marked effect on the catalyst online lifetime by reducing the laydown of coke.

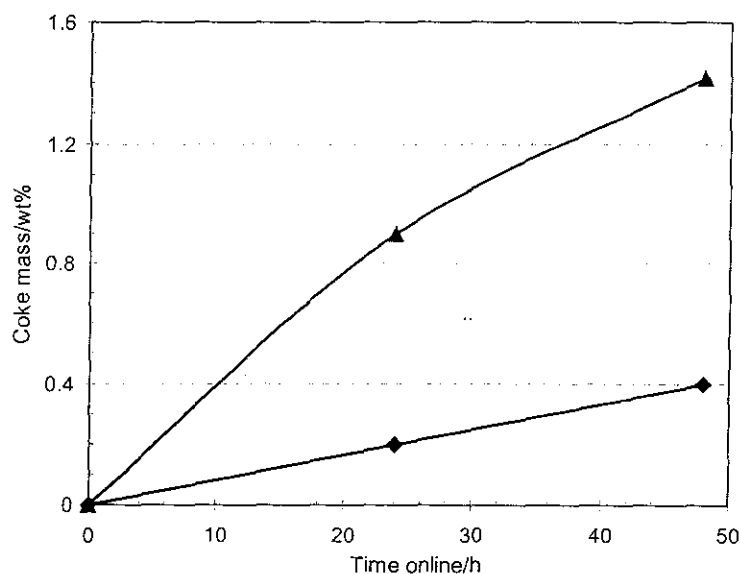


**Figure 6.27** Coke formation on an 8 wt%  $\text{WO}_3/\text{SiO}_2$  catalyst as a function of time online at different LHSV values ( $\blacktriangle$  16  $\text{h}^{-1}$ ,  $\blacklozenge$  4  $\text{h}^{-1}$ ).

### 6.5.3 Coke formation as a function of time online

A regenerated catalyst was run over different time intervals to determine the amount coke formation as a function of time. Reactions were conducted with an industrial cut 1-heptene feed at 460 °C in the recycle mode at 16  $\text{h}^{-1}$  LHSV with a feed to recycle ratio of 1:5.6.

The results are depicted in Figure 6.28. Coke formation increases almost linearly with time-on-line.

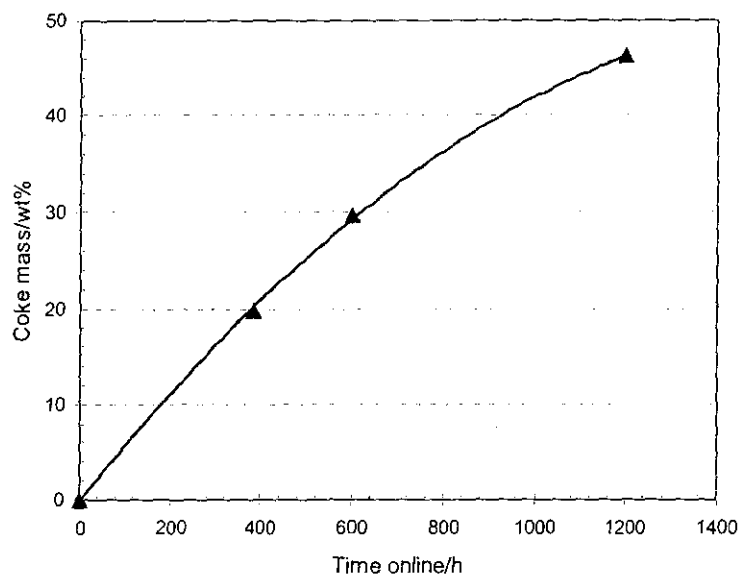


**Figure 6.28** Coke formation as a function of time online using an 8 wt%  $\text{WO}_3/\text{SiO}_2$  catalyst that was regenerated once.

#### 6.5.4 Influence of olefin content in feed

It is well known from literature that olefins coke much faster than paraffins.<sup>13</sup> The industrial cut 1-heptene feed has paraffins present (~15%). The ratio of olefin to paraffin may play a role in determining the coke formation on the catalyst. In order to investigate this, reactions were conducted with different feed mixtures of 1-octene/n-heptane. The reactions were carried out in a once through mode at 460 °C and 5 h<sup>-1</sup> LHSV for a period of 72 h. The influence of the olefin to paraffin ratio is shown in Figure 6.29.

At higher olefin to paraffin ratios the coke formation on the catalyst is greater. Coke formation is highest with a pure olefin feed while with pure paraffin feed; coke formation on the catalyst is negligible.

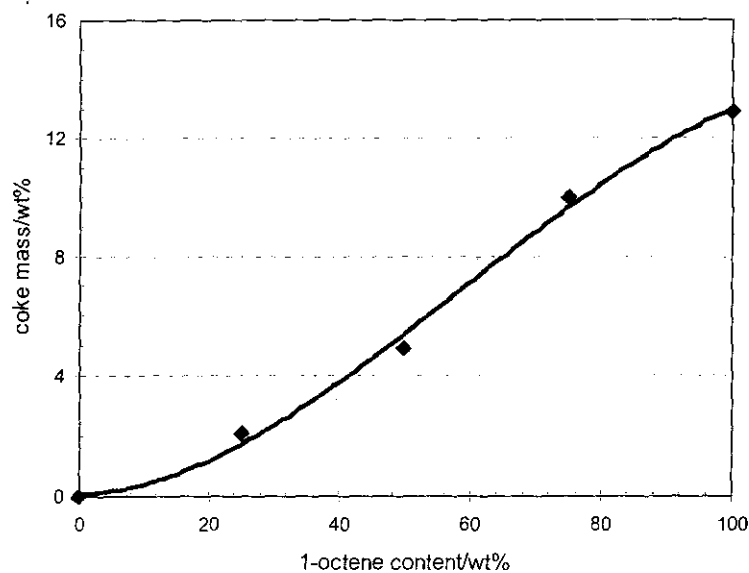


**Figure 6.29** Coke formation as a function of olefin to paraffin content in feed (Reaction conditions: 460 °C, LHSV = 5 h<sup>-1</sup> over a period of 72 h, feed = mixtures of 1-octene/n-heptane).

#### 6.5.5 Influence of oxygenated components on coke formation on the 8 wt% WO<sub>3</sub>/SiO<sub>2</sub> catalyst

Oxygenated compounds may be co-fed as coke inhibiting agents.<sup>14</sup> It was decided to add trace amounts (100 ppm) of 2-pentanone, water and butanol to the 1-octene feed stream to observe the effects of these oxygenates on coke formation. It is well known that oxygenates deactivate most heterogeneous metathesis catalysts.<sup>15</sup> However trace amounts of oxygenate may not have a negative impact on activity.

This is indeed the case as depicted in Figure 6.30. The catalyst activity does drop over the 72 h period but this also occurs with a pure 1-octene feed. This intrinsic deactivation behaviour has been observed in the once through mode for pure 1-octene feed and the low level of oxygenates introduced in the spiked feed is not responsible for the loss in activity. It can be concluded that the addition of 100 ppm of oxygenate does not significantly alter the performance of the catalyst.

As can be noted from Figure 6.31, the addition of these trace amounts of oxygenates significantly reduces the rate of coke formation. The Lewis base 2-pentanone has the greatest effect, reducing the amount of coke by almost half over a 72 h period. The Brønsted acids, butanol and water have a lesser effect. Introducing trace levels of oxygenates therefore can reduce coke formation without having any significant effect on the catalyst performance.

## 6.6 Influence of oxygenates on the 8 wt% $\text{WO}_3/\text{SiO}_2$ catalyst

### 6.6.1 Influence of Lewis bases on the activity and selectivity of the 8 wt% $\text{WO}_3/\text{SiO}_2$ catalyst

2-Pentanone, ethyl acetate and hexanal are oxygenates containing a carbonyl group and act as Lewis bases. It is well known that oxygenates are poisons for metathesis catalysts. The influence of oxygenates on the catalyst was investigated.

Percolated 1-octene was metathesized in the presence of an 8 wt%  $\text{WO}_3/\text{SiO}_2$  catalyst at 460 °C and 5 h<sup>-1</sup> LHSV, in a once-through mode. The catalyst was allowed to reach steady state activity, then a 1-octene feed containing 500 ppm of the oxygenate was introduced into the system. The catalyst was allowed to run for two hours before a step change was made to a 1-octene feed containing the next level of oxygenate. Oxygenate concentrations of 500, 1000, 2000 and 4000 ppm, if necessary, were used to determine the tolerance level of the catalyst. The activity of the catalyst was monitored during the course of the reaction. Figure 6.32 shows the influence of 2-pentanone on the activity of the catalyst.

The response variables that were used to compare the influence of different oxygenates on the metathesis activity of the catalyst were the feed conversion,  $\text{C}_{11}\text{-C}_{15}$  yield and  $\text{C}_{11}\text{-C}_{15}$  selectivity and  $\text{C}_{14}$  (primary product) selectivity. With the feed conversion it will be possible to determine the activity of the catalyst, while the  $\text{C}_{11}\text{-C}_{15}$  range contains the desired fraction for the detergent range olefins. The catalyst can tolerate 500 ppm of 2-pentanone with no adverse effect on its activity. However when 1000 ppm of 2-pentanone is introduced into the feed, after 2 h, the conversion begins to drop dramatically. The  $\text{C}_{11}\text{-C}_{15}$  yield and selectivity also decreases markedly. At 2000 ppm of 2-pentanone the catalyst conversion is below 20%.

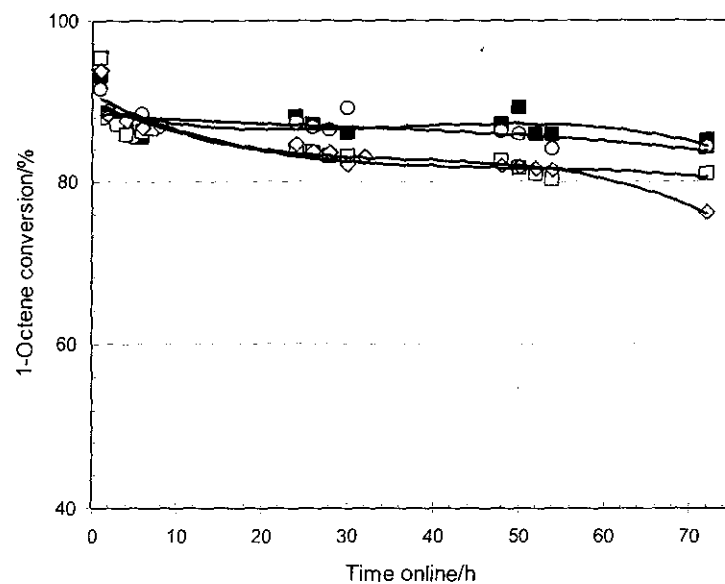


**Figure 6.30** Influence of 100 ppm of different oxygenates on the activity of an 8 wt %  $\text{WO}_3/\text{SiO}_2$  catalyst over a 72 h period. Reaction conditions: 460 °C, LHSV = 5  $\text{h}^{-1}$  (■ butanol; ◇ pure 1-octene; □ pentanone; ○ water).

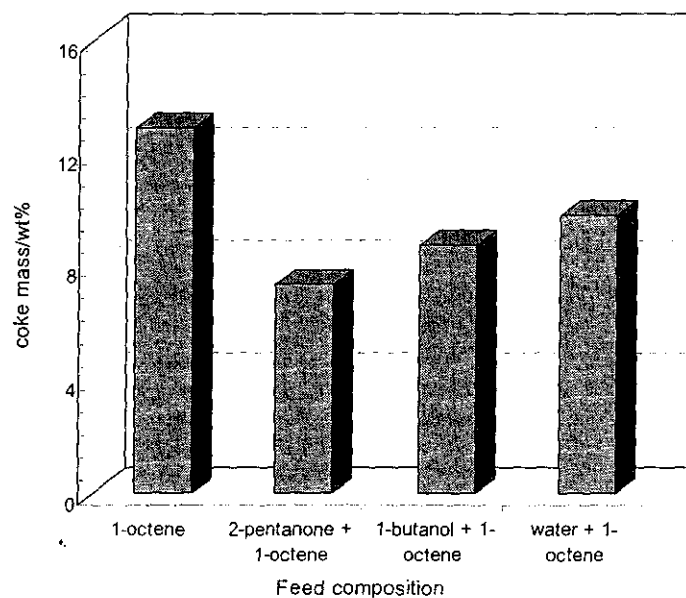


**Figure 6.31** Influence of 100 ppm of different oxygenates on coke formation on an 8 wt%  $\text{WO}_3/\text{SiO}_2$  catalyst (Reaction conditions: 460 °C, LHSV = 5  $\text{h}^{-1}$  over a 72 h period).

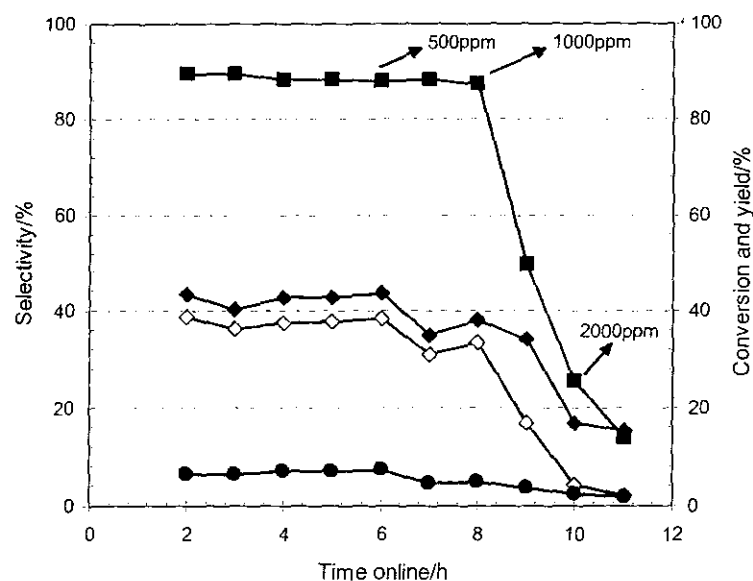


**Figure 6.32** The influence of 2-pentanone on the activity, selectivity and yield of the 8 wt%  $\text{WO}_3/\text{SiO}_2$  catalyst with a 1-octene feed. Reaction temperature =  $460^\circ\text{C}$ , LHSV =  $5\text{ h}^{-1}$  (■ Conversion; ◆  $\text{C}_{11}\text{-C}_{15}$  Selectivity; ◇  $\text{C}_{11}\text{-C}_{15}$  Yield; ●  $\text{C}_{14}$  Selectivity).

Ethyl acetate was also tested to determine its effect on the metathesis activity of the catalyst. The influence of ethyl acetate is shown in Figure 6.33. When ethyl acetate was used as the Lewis base a significant deactivation of the catalyst could be detected with the introduction of about 1000 ppm. The  $\text{C}_{11}\text{-C}_{15}$  yield steadily decreases after that point.

The catalyst is fairly resistant towards hexanal, as it shows a decrease in activity only after about 2000 ppm of hexanal was introduced to the system (Figure 6.34).

### 6.6.2 The influence of Brønsted acids on the activity and selectivity of the 8 wt% $\text{WO}_3/\text{SiO}_2$ catalyst.

Water and butanol are Brønsted acids. The influence of water on the activity and selectivity of the 8 wt%  $\text{WO}_3/\text{SiO}_2$  catalyst was determined differently than the other reactions. The solubility of water in the organic layer (1-octene) is poor. The greater polarity of water makes separation of water and the organic layer easy. 1-Octene was

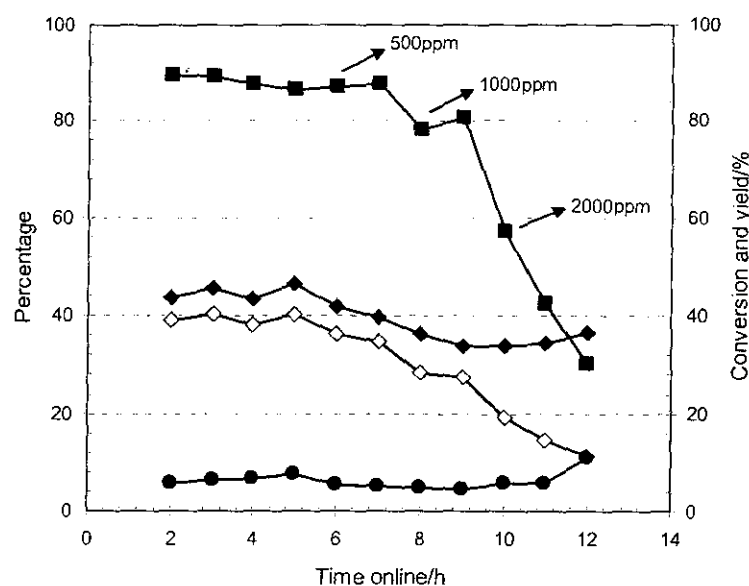


**Figure 6.33** The influence of ethyl acetate on the activity, selectivity and yield of the 8 wt%  $\text{WO}_3/\text{SiO}_2$  catalyst with a 1-octene feed. Reaction temperature =  $460^\circ\text{C}$ ,  $\text{LHSV} = 5\text{ h}^{-1}$  (■ Conversion; ◆  $\text{C}_{11}\text{-C}_{15}$  Selectivity; ◇  $\text{C}_{11}\text{-C}_{15}$  Yield; ●  $\text{C}_{14}$  Selectivity).

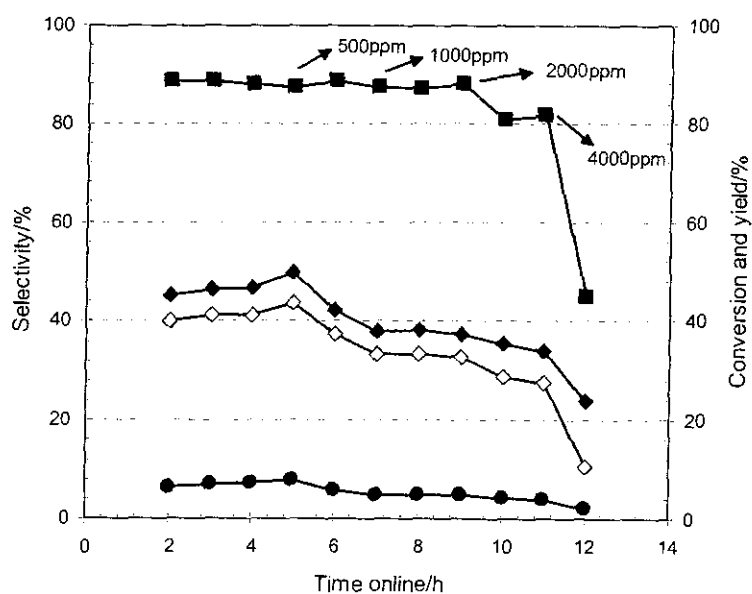


**Figure 6.34** The influence of hexanal on the activity, selectivity and yield of the 8 wt%  $\text{WO}_3/\text{SiO}_2$  catalyst with a 1-octene feed. Reaction temperature =  $460^\circ\text{C}$ ,  $\text{LHSV} = 5\text{ h}^{-1}$  (■ Conversion; ◆  $\text{C}_{11}\text{-C}_{15}$  Selectivity; ◇  $\text{C}_{11}\text{-C}_{15}$  Yield; ●  $\text{C}_{14}$  Selectivity).

saturated by adding an excess amount of water to it and stirring the mixture for 24 h. The excess water was then decanted from the mixture and the water saturated 1-octene was used as feed. Colorimetric analysis revealed that this feed contained 104 ppm of water. Figure 6.35 shows the influence of water on the catalyst. The addition of water to the reaction mixture shows no deactivation of the catalyst and a total feed conversion of about 88% could be obtained throughout the reaction. The  $C_{11}$ - $C_{15}$  selectivity and yield and  $C_{14}$  selectivity were also not influenced.

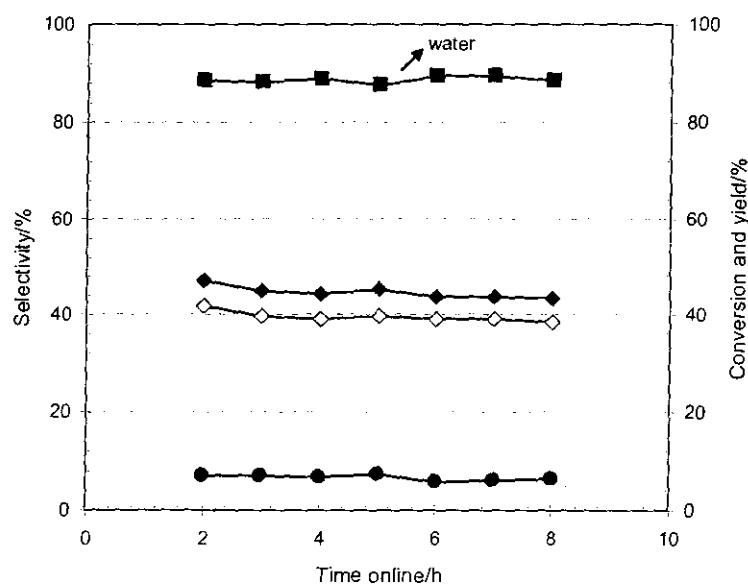


**Figure 6.35** The influence of water on the activity, selectivity and yield of the 8 wt%  $WO_3/SiO_2$  catalyst with a 1-octene feed. Reaction temperature = 460 °C, LHSV = 5 h<sup>-1</sup> (■ Conversion; ◆  $C_{11}$ - $C_{15}$  Selectivity; ◇  $C_{11}$ - $C_{15}$  Yield; ●  $C_{14}$  Selectivity).

The influence of the Brønsted acid, butanol on the activity and selectivity of the catalyst is depicted in Figure 6.36. With the introduction of 500 ppm of butanol, the feed conversion and  $C_{11}$ - $C_{15}$  selectivity and yield are not affected. When the level of butanol was increased to a 1000 ppm, a slight decrease in feed conversion and  $C_{11}$ - $C_{15}$  yield could be detected.

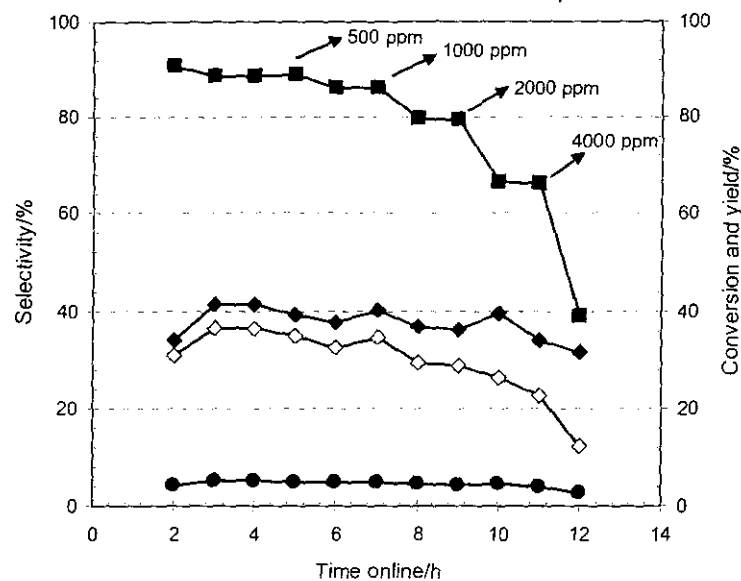


**Figure 6.36** The influence of butanol on the activity, selectivity and yield of the 8 wt%  $\text{WO}_3/\text{SiO}_2$  catalyst with a 1-octene feed. Reaction temperature = 460 °C, LHSV = 5  $\text{h}^{-1}$  (■ Conversion; ◆  $\text{C}_{11}\text{-C}_{15}$  Selectivity; ◇  $\text{C}_{11}\text{-C}_{15}$  Yield; ●  $\text{C}_{14}$  Selectivity).

### 6.6.3 The influence of oxygenates on the activity and selectivity of the 8 wt% $\text{WO}_3/\text{SiO}_2$ catalyst when operating in the recycle mode

The oxygenated components may accumulate in the second column and be recycled to the reactor (Figure 5.2). This will result in a built up of the oxygenate concentration and may have a greater impact on the catalyst activity. For this reason the effect of 2-pentanone on the catalyst was investigated in the recycle mode. The optimised reaction conditions were used and a feed containing a mixture of 85% 1-octene/15% n-heptane was used. The purpose of the inert paraffin is to ensure that the second column and recycle loop do not run dry and to simulate the industrial cut heptene feed. The reactor was started up with feed and the catalyst was allowed to reach steady state activity, before a step change to feed containing 100 ppm 2-pentanone was done. The feed was left online for 48 h before another step change to a feed containing the next level of oxygenate was done. 2-Pentanone concentrations of 100, 200, 300 and 400 ppm were used. The influence of the 2-pentanone in the recycle mode is shown in Figure 6.37. The  $\text{WO}_3/\text{SiO}_2$  catalyst shows no

sign of deactivation up to a level of about 300 ppm of 2-pentanone in the feed. When the level is increased to 400 ppm the catalyst shows a decrease in feed conversion as well as a decrease in C<sub>11</sub>-C<sub>15</sub> yield. Reintroduction of the pure feed results in the catalyst regaining its original activity. Analysis was done on the feed and the liquid samples collected as product (purge 1 and 2 in Figure 5.2) to determine the level of carbonyl content in each fraction. It was found by carbonyl analysis that with 400 ppm of 2-pentanone in the feed, the carbonyl content of purge streams 1 and 2 are 180 ppm and 210 ppm respectively.

An interesting observation was made concerning the colour of the product. The product, using a pure feed containing no oxygenates, is deep yellow. Introduction of the oxygenate into the feed stream results in a decrease in the yellow colour. This change in colour was quantified by UV-Vis spectroscopy. Due to the possible interference from olefinic material present a wavelength of 370 nm was employed. This allows good quantification of the yellowness of the product. The product reverted to its yellow colour when the pure feed was reintroduced. The influence of 2-pentanone on the colour of the product is shown in Figure 6.38.

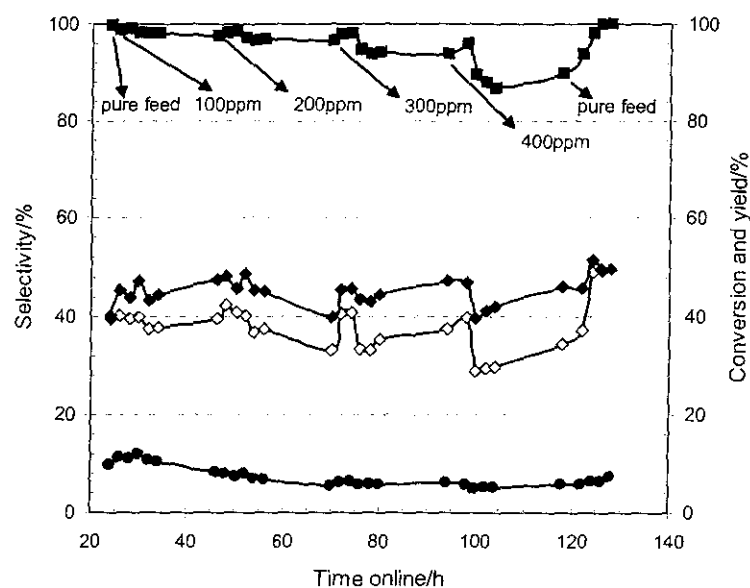


**Figure 6.37** The influence of 2-pentanone on the activity, selectivity and yield of the 8 wt% WO<sub>3</sub>/SiO<sub>2</sub> catalyst with a 1-octene/ n-heptane feed in the recycle mode at 460 °C, 16 h<sup>-1</sup> LHSV and a feed to recycle ratio of 1:5.6 (■ Conversion; ◆ C<sub>11</sub>-C<sub>15</sub> Selectivity; ◇ C<sub>11</sub>-C<sub>15</sub> Yield; ● C<sub>14</sub> Selectivity).

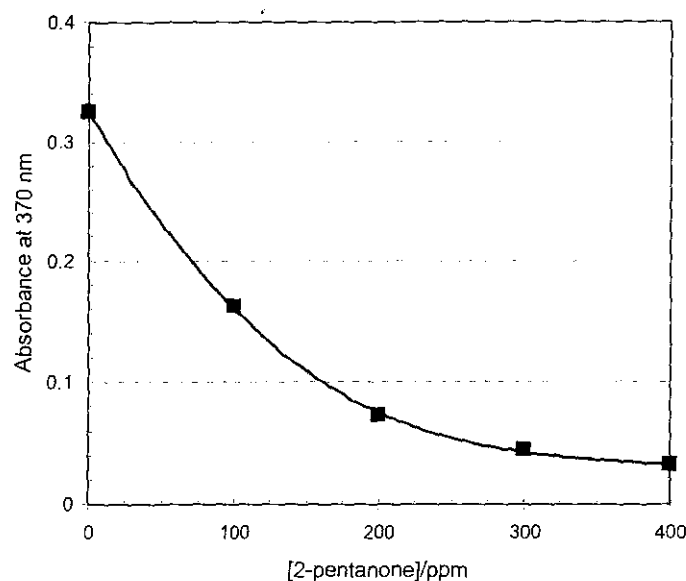


**Figure 6.38** The influence of 2-pentanone on the colour of the product produced from the metathesis of a 1-octene/n-heptane feed over an 8 wt%  $\text{WO}_3/\text{SiO}_2$  catalyst in the recycle mode at 460 °C, 16 h<sup>-1</sup> LHSV and a feed to recycle ratio of 1:5.6.

#### 6.6.4 The influence of oxygenates on the colour of the product produced *via* metathesis over the 8 wt% $\text{WO}_3/\text{SiO}_2$ catalyst

The observations made from the experiments with 2-pentanone in the recycle mode (Section 6.6.3) clearly showed that oxygenates affected the colour of the product. It was decided to investigate the influence of different oxygenates on the colour of the product obtained *via* the metathesis of 1-octene over the 8 wt%  $\text{WO}_3\text{-SiO}_2$  catalyst, in a once through mode. For these experiments concentrations of oxygenate lower than 500 ppm were used. The activity of the catalyst was also monitored. The oxygenates tested were butanol (Brönsted acid), 2-pentanone, hexanal and butanal (Lewis bases) at concentrations of 100, 200, 300 and 400 ppm.

The activity and selectivity of the catalyst and the colour of the product, when 2-pentanone is introduced into the system are illustrated in Figures 6.39 and 6.40 respectively. As expected at concentrations lower than 500 ppm the activity of the catalyst is not

significantly affected. However the colour of the product begins to decrease as the level of 2-pentanone in the feed is increased. After 1 h at a concentration of 200 ppm the absorbance of the product is decreased to more than half that with a pure feed. When a pure feed is reintroduced the absorbance of the product begins to increase indicating that the product is becoming yellow once more.

The influence of the aldehydes, hexanal and butanal on product colour was also investigated. The activity of the catalyst and the absorbance of the product are illustrated for hexanal in Figures 6.41 and 6.42. The catalyst shows no signs of deactivation up to 400 ppm of hexanal, but the colour of the product becomes clearer with the introduction of just 100 ppm of hexanal. Figures 6.43 and 6.44 show the influence of butanal on the activity of the catalyst and colour of the product. Butanal has a similar effect to hexanal. The catalyst conversion is steady up to a concentration of 400 ppm. Increasing the concentration of butanal results in a corresponding drop in the product absorbance. The Brönsted acid, butanol has a similar effect as depicted in Figure 6.45 and 6.46.

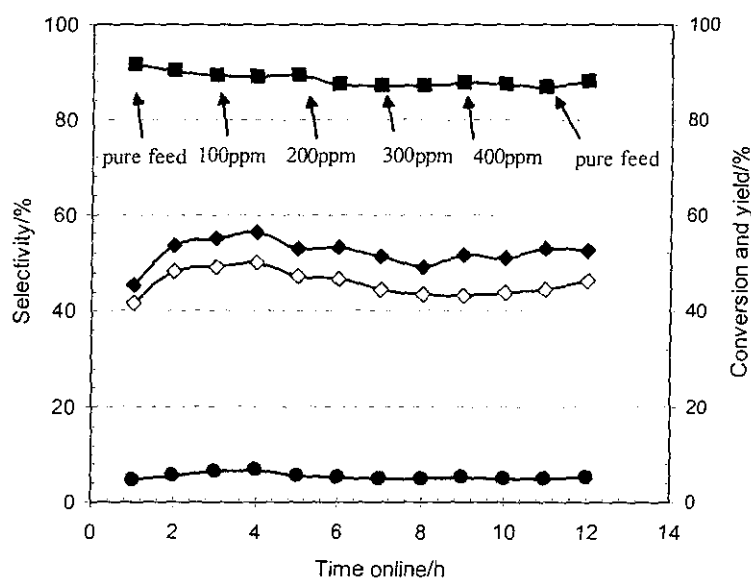


**Figure 6.39** The influence of 2-pentanone on the activity, selectivity and yield of the 8 wt%  $\text{WO}_3/\text{SiO}_2$  catalyst with a 1-octene feed. Reaction temperature = 460 °C, LHSV = 5  $\text{h}^{-1}$  (■ Conversion; ◆ C<sub>11</sub>-C<sub>15</sub> Selectivity; ◇ C<sub>11</sub>-C<sub>15</sub> Yield; ● C<sub>14</sub> Selectivity).

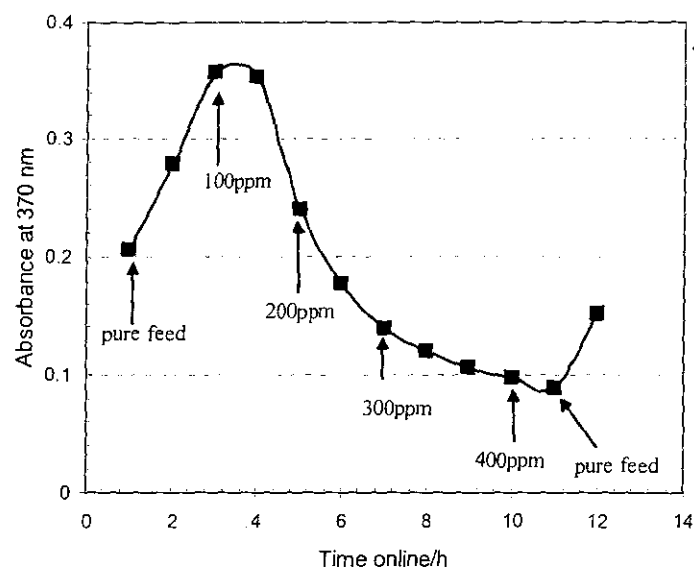


**Figure 6.40** The influence of 2-pentanone on the colour of the product produced *via* metathesis of 1-octene over the 8 wt%  $\text{WO}_3/\text{SiO}_2$  catalyst in a once through mode. Reaction temperature = 460 °C, LHSV = 5  $\text{h}^{-1}$ .

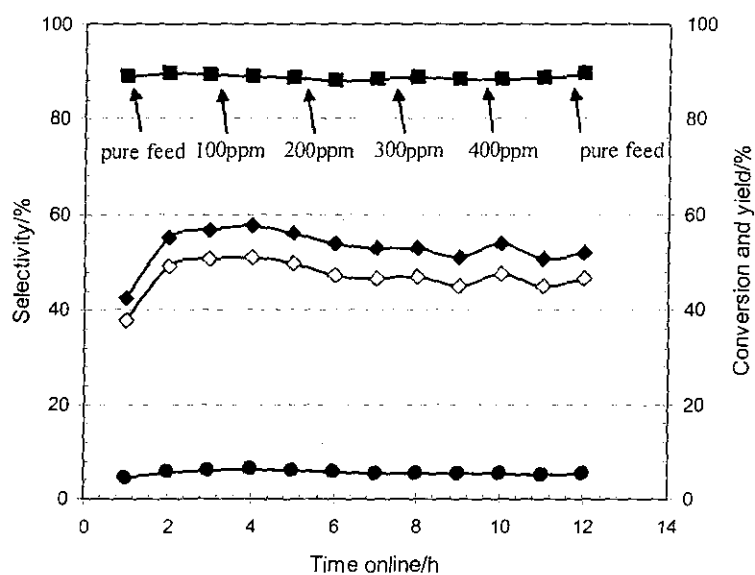


**Figure 6.41** The influence of hexanal on the activity, selectivity and yield of the 8 wt%  $\text{WO}_3/\text{SiO}_2$  catalyst with a 1-octene feed. Reaction temperature = 460 °C, LHSV = 5  $\text{h}^{-1}$  (■ Conversion; ◆  $\text{C}_{11}\text{-C}_{15}$  Selectivity; ◇  $\text{C}_{11}\text{-C}_{15}$  Yield; ●  $\text{C}_{14}$  Selectivity).

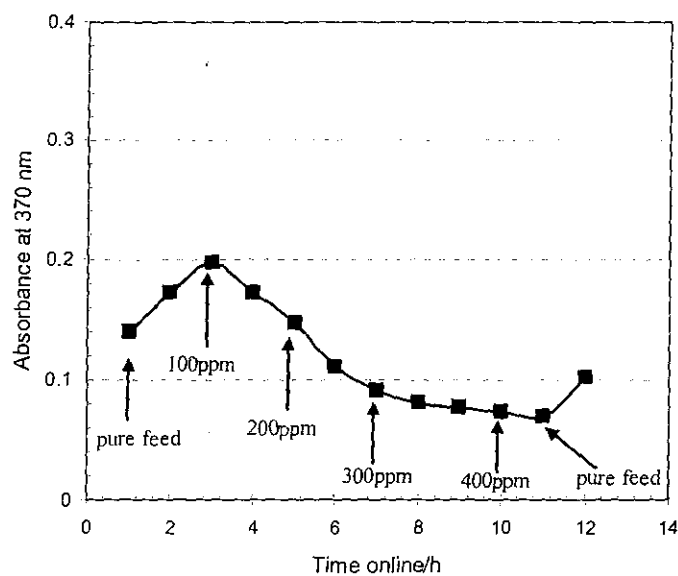


**Figure 6.42** The influence of hexanal on the colour of the product produced via metathesis of 1-octene over the 8 wt%  $\text{WO}_3/\text{SiO}_2$  catalyst in a once through mode. Reaction temperature = 460 °C, LHSV = 5  $\text{h}^{-1}$ .

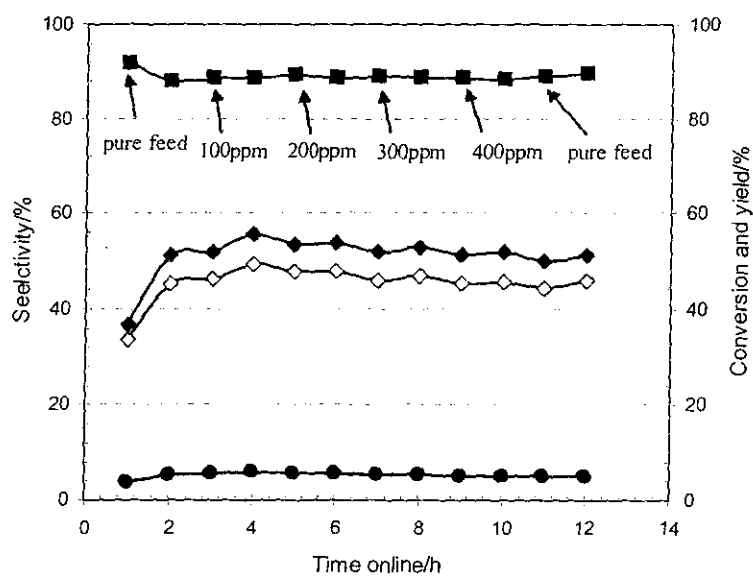


**Figure 6.43** The influence of butanal on the activity, selectivity and yield of the 8 wt%  $\text{WO}_3/\text{SiO}_2$  catalyst system with 1-octene feed. Reaction temperature = 460 °C, LHSV = 5  $\text{h}^{-1}$  (■ Conversion; ◆  $\text{C}_{11}\text{-C}_{15}$  Selectivity; ◇  $\text{C}_{11}\text{-C}_{15}$  Yield; ●  $\text{C}_{14}$  Selectivity).

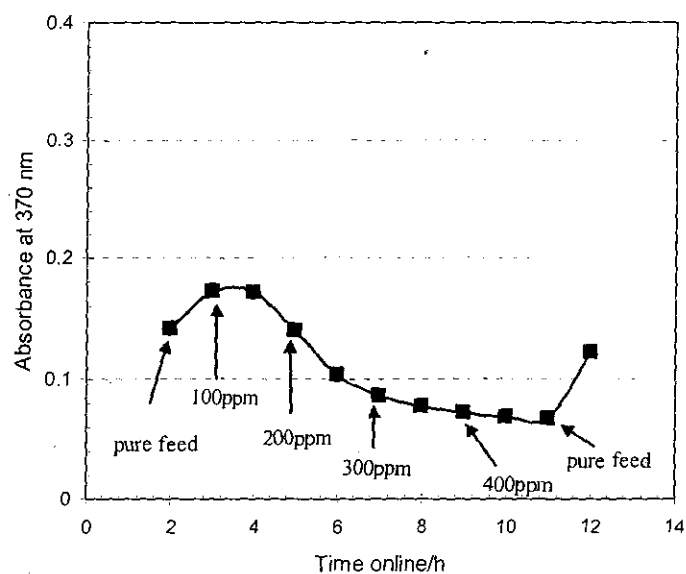


**Figure 6.44** The influence of butanal on the colour of the product produced *via* metathesis of 1-octene over the 8 wt%  $\text{WO}_3/\text{SiO}_2$  catalyst in a once through mode. Reaction temperature = 460 °C, LHSV = 5  $\text{h}^{-1}$ .

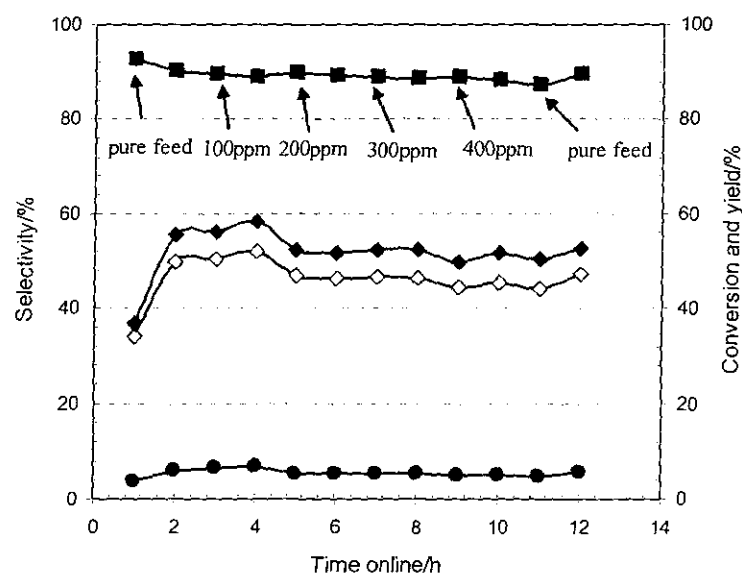


**Figure 6.45** The influence of butanol on the activity, selectivity and yield of the 8 wt%  $\text{WO}_3/\text{SiO}_2$  catalyst system with 1-octene feed. Reaction temperature = 460 °C, LHSV = 5  $\text{h}^{-1}$  (■ Conversion; ◆  $C_{11-C15}$  Selectivity; ◇  $C_{11-C15}$  Yield; ●  $C_{14}$  Selectivity).

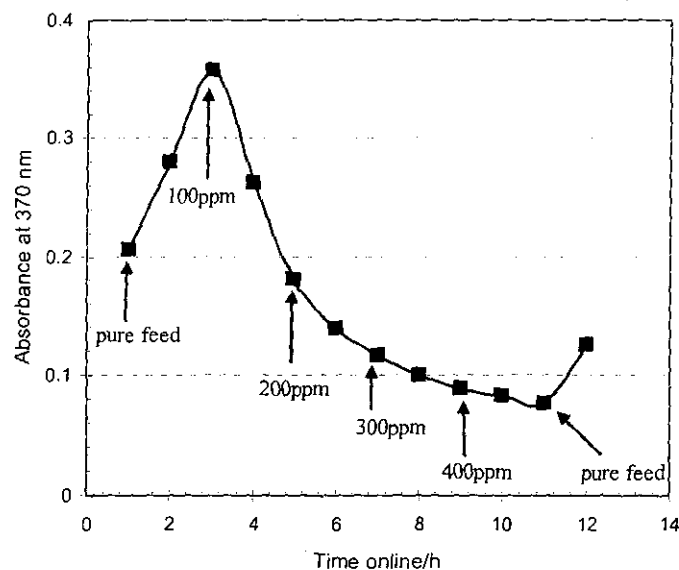


**Figure 6.46** The influence of butanol on the colour of the product produced *via* metathesis of 1-octene over the 8 wt%  $\text{WO}_3/\text{SiO}_2$  catalyst in a once through mode. Reaction temperature = 460 °C, LHSV = 5  $\text{h}^{-1}$ .

#### 6.6.5 The influence of a fixed concentration of oxygenate on the colour of the product produced *via* metathesis over the 8 wt% $\text{WO}_3/\text{SiO}_2$ catalyst

It was decided to investigate the effect of a constant amount of oxygenate on the activity of the catalyst and colour of the product. The oxygenate chosen for this experiment was 2-pentanone. The reaction was started with pure feed and the catalyst was allowed to reach steady state. A step change to a feed containing 200 ppm of 2-pentanone was done and this feed was kept on line for 20 hours. Pure feed was reintroduced into the system, thereafter. In Figure 6.47 it is clear that 2-pentanone does not have an influence on the activity or selectivity of the catalyst, but in Figure 6.48, a decrease in colour could be observed after the introduction of 2-pentanone. The product colour stabilises for a while and with the reintroduction of the pure feed, it returns to its original yellow colour.

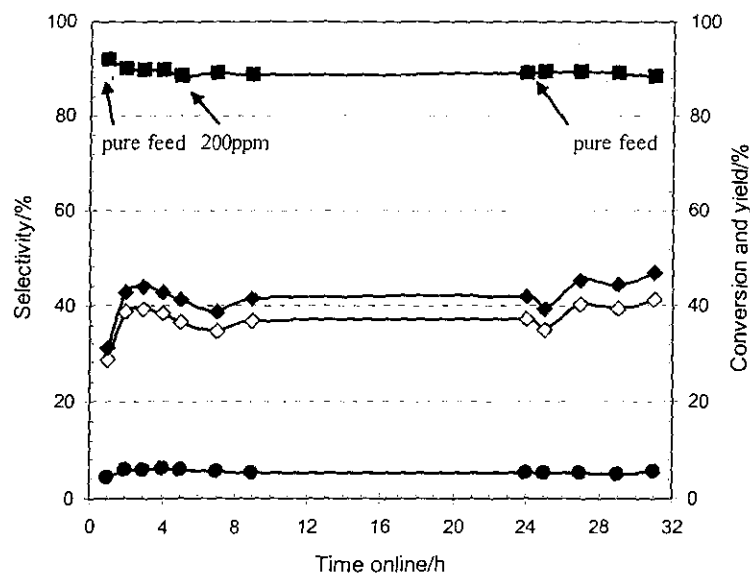


**Figure 6.47** The influence of 200 ppm 2-pentanone on the activity, selectivity and yield of the 8 wt%  $\text{WO}_3/\text{SiO}_2$  catalyst system with 1-octene feed. Reaction temperature =  $460^\circ\text{C}$ , LHSV =  $5\text{ h}^{-1}$  (■ Conversion; ◆  $\text{C}_{11}\text{-C}_{15}$  Selectivity; ◇  $\text{C}_{11}\text{-C}_{15}$  Yield; ●  $\text{C}_{14}$  Selectivity).

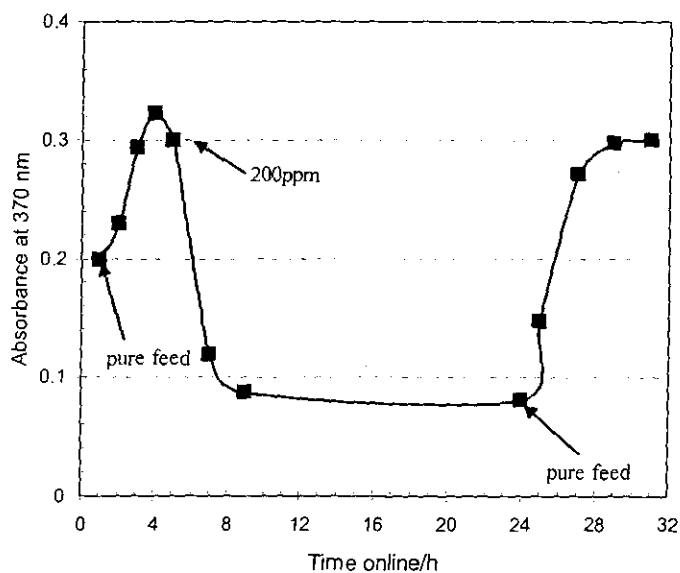


**Figure 6.48** The influence of 200 ppm on the colour of the product produced *via* metathesis of 1-octene over the 8 wt%  $\text{WO}_3/\text{SiO}_2$  catalyst in a once through mode. Reaction temperature =  $460^\circ\text{C}$ , LHSV =  $5\text{ h}^{-1}$ .

## 6.7 Summary of important results

1.  $\text{WO}_3/\text{SiO}_2$  catalysts of different tungsten loadings were prepared and characterized. LRS, XRD and TEM showed that crystalline  $\text{WO}_3$  was predominant on catalysts with higher tungsten loading, while  $\text{WO}_3$  was well dispersed on catalyst with lower loadings. A surface tungsten species was observed on catalysts with lower loadings.
2. The metathesis activity of the catalysts increased up to loading of 6 wt%  $\text{WO}_3$ . Thereafter the activity stabilised and was constant and independent of tungsten loading. Selectivity to branched products was lower with catalysts of lower tungsten loading. The stability of catalysts containing more than 7 wt%  $\text{WO}_3$  was higher.
3. Alkali metal ion doping of the catalyst resulted in lower activity and lower selectivity to branched products. Doping the catalyst with greater than 0.5 wt% of alkali metal ion resulted in a sharp drop in conversion. Reverse impregnation resulted in a loss of activity and selectivity compared to the normal impregnation technique.
4. The 8 wt%  $\text{WO}_3/\text{SiO}_2$  catalyst has a long lifetime (700 h) when operated in the recycle mode, using optimised conditions. The selectivity of the catalyst improves with time online. Regeneration of the catalyst results in a slight drop in conversion but enhanced selectivity and lifetime. There is a large amount of coke that forms inside the pores of the catalyst.
5. EFTEM was used as technique to locate carbon on coked catalysts. Carbon maps indicated that the carbon was located around the tungsten oxide clusters and were not covering them.
6. Temperature, LHSV, time-online and olefin content all play an important role in determining the rate of coke laydown on the catalyst. Trace quantities of oxygenates reduce the rate of coke laydown significantly without any adverse effect on activity and selectivity.

7. Oxygenates are responsible for catalyst deactivation if they are present in high enough concentrations. Trace quantities of oxygenates can help to reduce the colour of the final product.

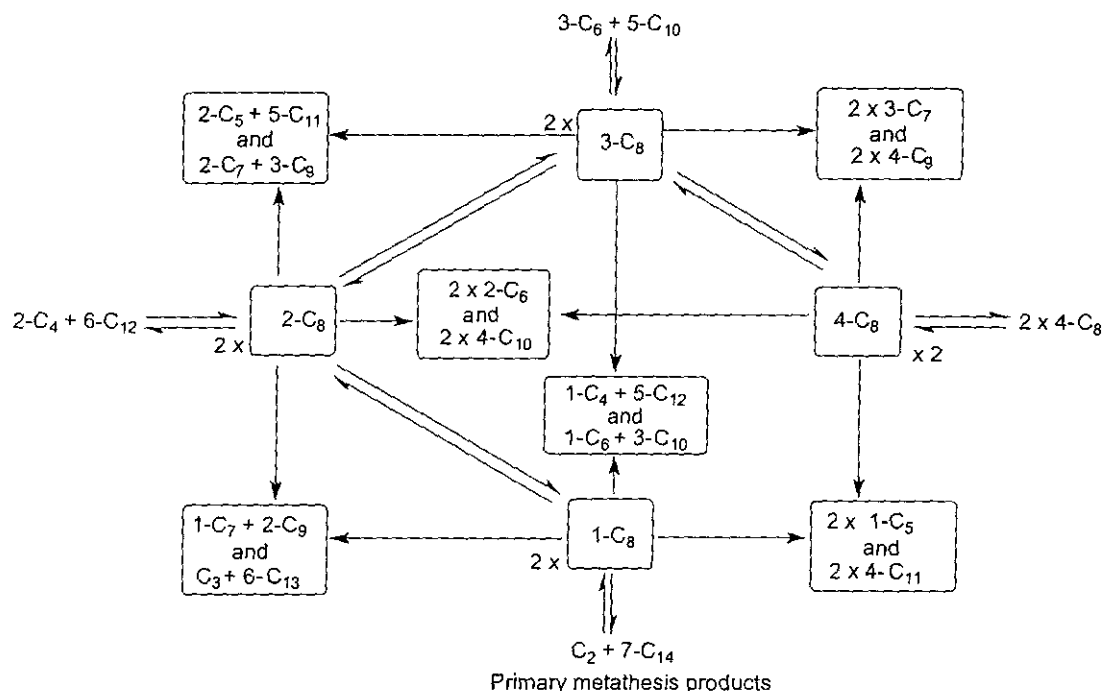
## 6.8 References

1. L. F. Heckelsburg (to Phillips Petroleum Co.), US Pat. 3365513, 1968 (23 January)
2. K. J. Ivin, J. C. Mol, *Olefin Metathesis and Metathesis Polymerization*, Academic Press (San Diego), 1997, p. 401
3. R. L. Banks, L. F. Heckelsberg, G. C. Bailey, *Ind. Eng. Chem., Prod. Res. Dev.*, 1968, **7**, 29
4. A. J. Van Roosmalen, J. C. Mol, *J. Catal.*, 1982, **78**, 17
5. R. Thomas, J. A. Moulijn, F. P. J. M. Kerkhof, *Recl. Trav. Chim. Pays-Bas*, 1977, **96(ii)**, 134
6. D. S. Kim, M. Ostromecki, I. E. Wachs, *Catal. Lett.*, 1995, **33**, 209
7. R. L. Banks in *Applied Industrial Catalysis*, Volume 3, B. E. Leach (Ed.), Academic Press (New York), 1984, p. 215
8. K. J. Ivin, J. C. Mol, *Olefin Metathesis and Metathesis Polymerization*, Academic Press (San Diego), 1997, p. 13
9. C. van Schalkwyk, A. Spamer, D. J. Moodley, T. Dube, J. Reynhardt, J. M. Botha, *Appl. Catal. A: Gen.*, 2003, article in press
10. A. Spamer, J. M. Botha, D. J. Moodley, C. van Schalkwyk, T. Dube, *Appl. Catal. A: Gen.*, 2003, article in press
11. A. K. Datye, Personal communication, 13 November 2002
12. C. H. Bartholomew, *Appl. Catal. A: Gen.*, 2001, **212**, 17
13. P. G. Menon, *J. Mol. Catal.*, 1990, **59**, 207
14. I. V. Kozhevnikov, S. Holmes, M. R. H. Siddiqui, *Appl. Catal. A: Gen.*, 2001, **214**, 27
15. J. C. Mol, *Catal. Today*, 1999, **51**, 289

## 7 CONCLUSIONS

### 7.1 Metathesis reactions over $\text{WO}_3/\text{SiO}_2$ catalysts

It has been demonstrated in this study that  $\text{WO}_3/\text{SiO}_2$  catalysts are active for olefin metathesis reactions at high temperatures. The catalyst also has appreciable isomerization activity. Primary metathesis, isomerization and secondary metathesis are the chief reactions that take place when employing a catalyst of this nature. The combination of these reactions results in a mixture of products, however this broad product spectrum (mainly  $\text{C}_{10}$ - $\text{C}_{13}$  internal olefins) is suitable for applications in detergent alcohol (DA) and linear alkyl benzene (LAB) synthesis. The formation of the reaction products when using 1-octene as a feed material is illustrated in Scheme 7.1.



**Scheme 7.1** Primary metathesis, isomerization and secondary metathesis with 1-octene as feed over  $\text{WO}_3/\text{SiO}_2$  catalysts.

## 7.2 The WO<sub>3</sub>/SiO<sub>2</sub> catalyst system

### 7.2.1 Introduction

WO<sub>3</sub>/SiO<sub>2</sub> metathesis catalysts are composed of a surface phase and crystalline trioxide. It has been proved extensively that WO<sub>3</sub> crystals are inactive in metathesis and as a consequence the catalytic sites have to be contained in the surface phase or at the boundary of the WO<sub>3</sub> crystals and the silica carrier.<sup>1</sup> Kerkhoff *et al.*<sup>2</sup> determined that crystalline WO<sub>3</sub> is not a precursor for the active site, since the measured metathesis activity of their WO<sub>3</sub>/SiO<sub>2</sub> catalysts decreased from 20 to 40 wt% WO<sub>3</sub> while the amount of crystalline material increased in this range. It was also shown that WO<sub>3</sub>/Al<sub>2</sub>O<sub>3</sub> catalysts have a high metathesis activity in spite of the fact that no crystalline material was detected by XRD.<sup>3</sup> The structure of the amorphous surface compound is still a subject of debate.<sup>4</sup>

### 7.2.1 Characterisation of WO<sub>3</sub>/SiO<sub>2</sub> catalysts with different WO<sub>3</sub> loadings

From the Raman spectra (Figure 6.2) it is evident that at low tungsten loadings, tungsten is present as a surface tungsten species as well as crystalline material. The weak Raman bands attributed to the surface tungsten species at 973 and 329 cm<sup>-1</sup> have a greater intensity at lower loadings showing a higher amount of surface tungsten species at low tungsten loadings. In catalysts with lower loading the Raman bands due to crystalline WO<sub>3</sub> (802-811, 700-718 and 271 cm<sup>-1</sup>) have a lower intensity. At high tungsten loadings this surface species is totally overshadowed by the crystalline WO<sub>3</sub> species. This observation was also made by Thomas *et al.*<sup>3</sup> The presence of this highly crystalline material indicates that for higher tungsten loadings preparation by the aqueous impregnation method gives a poorly dispersed supported tungsten oxide phase on silica.<sup>5</sup>

The XRD patterns of the 3-20 wt% WO<sub>3</sub>/SiO<sub>2</sub> catalysts (Figure 6.1) indicated the presence of crystalline WO<sub>3</sub> only if the catalyst contained more than 7 wt% WO<sub>3</sub>. Below this level the tungsten appeared to be present largely as an amorphous, surface compound. This was also observed by Kerkhof *et al.*<sup>2</sup> It was only possible to determine crystallite sizes for catalysts with loadings higher than 8 wt%. Lower loadings either had too small crystallites present or the tungsten oxide was present as an amorphous surface compound (see Table 6.2). The crystallite sizes increased from 8-20 wt% WO<sub>3</sub>/SiO<sub>2</sub>.

TEM analysis of the 20 wt% WO<sub>3</sub>/SiO<sub>2</sub> catalyst (Figure 6.5) also indicated the presence of a greater amount of larger crystallites at high loadings. The 3 wt% WO<sub>3</sub>/SiO<sub>2</sub> catalyst appeared to be well dispersed with only a few crystallites present (Figure 6.3). TEM analysis further strengthened the theory that tungsten is largely present as a surface compound at lower loadings.

### 7.3 Factors that influence the WO<sub>3</sub>/SiO<sub>2</sub> catalyst

#### 7.3.1 Influence of WO<sub>3</sub> loading on the metathesis activity and selectivity of an 8 wt% WO<sub>3</sub>/SiO<sub>2</sub> catalyst

When evaluating the analytical and experimental results it becomes clear that there is a strong relationship between the surface tungsten species and the conversion and selectivity observed.

At lower loadings of tungsten, conversion is low probably due to the small quantity of active surface species present. Increasing tungsten loading leads to an increase in conversion, which reaches a maximum and stabilises at around 6 wt% WO<sub>3</sub> (Figure 6.6). At about this particular WO<sub>3</sub> loading, the tungsten surface compound must reach its maximum level. Increasing the loading further (>6 wt% WO<sub>3</sub>) results in further growth of the crystalline WO<sub>3</sub> that has no or very little effect on catalytic activity. The fact that Kerkhof *et al.*<sup>3</sup> observed a decline in conversion after about a 20 wt% WO<sub>3</sub> loading can be related to WO<sub>3</sub> crystallite growth starting to cover the active surface compound.

Selectivity is also directly related to the tungsten loading. It is evident that selectivity to the linear C<sub>14</sub> (primary metathesis product) is higher at the low tungsten loadings (Figure 6.7). The selectivity towards the secondary metathesis products (C<sub>10</sub>-C<sub>13</sub>) is also higher at the lower loadings (< 8 wt%), which indicates a higher degree of isomerization. At lower WO<sub>3</sub> loadings Brønsted acidity is still relatively low. The presence of tungsten surface compounds however create Lewis acidity while no or very little Brønsted acidity is present, indicating possible double bond isomerization of the feed according to an allylic mechanism.<sup>6</sup> The selectivity of the catalyst towards the branched products, C<sub>10</sub>-C<sub>13</sub> and C<sub>14</sub> branched (skeletal isomerization activity), increases with loading up to a maximum of 1% for the 8 wt% catalyst and stabilises thereafter. From a selectivity point of view a

catalyst with lower tungsten loadings will be favourable for our applications as it gives high selectivities to the linear C<sub>14</sub> and C<sub>10</sub>-C<sub>13</sub> and lower selectivities to branched olefins.

### 7.3.2 Influence of metal loading on the stability of the catalysts

It was found during this study that catalysts with lower WO<sub>3</sub> loadings show relatively lower stability in comparison to 8 wt% WO<sub>3</sub>/SiO<sub>2</sub> and higher, where high stability was observed (Figure 6.8). As was indicated with both XRD and TEM, low WO<sub>3</sub> loadings appear to be present as highly dispersed, small crystallites on the support material while larger clusters of crystalline material also starts appearing from around 8 wt% WO<sub>3</sub>. It can thus be that the presence of crystalline material has a stabilising effect on the tungsten surface compound. The active tungsten surface compound has a very strong interaction with the support and is also very difficult to reduce. The crystalline WO<sub>3</sub> on the other hand is easily reducible. During the metathesis reaction the precursor to the active species is reduced by the olefinic feed to the desired oxidation state.<sup>7</sup> Over-reduction of the active species however can result in deactivation of the catalyst.<sup>8</sup> The presence of crystalline material can thus protect the active surface tungsten species from deactivation by being the preferred species for over-reduction.<sup>3</sup> In terms of catalyst stability using a catalyst with around 8 wt% WO<sub>3</sub> loading will give longer lifetimes.

### 7.3.3 Influence of alkali metal doping on metathesis activity

Treatment of the 8 wt% WO<sub>3</sub>/SiO<sub>2</sub> with 0.1 wt% of alkali ion (Na<sup>+</sup>, K<sup>+</sup> and Cs<sup>+</sup>) had an influence on the metathesis activity and selectivity of the catalyst (Figure 6.11, 6.12). In all cases the metathesis activity was hampered by addition of the alkali metal ions. The conversion of the different alkali-doped samples however was almost identical at around 80%.

Previous work done on heterogeneous rhenium catalysts showed a strong correlation between the ionic radii of the dopant alkali metal ion and the activity and selectivity of the catalysts.<sup>9</sup> In this case, there was no distinct correlation between the size of ionic radii of the cation and the behavior of the catalyst (Table 7.1). However it was observed that the

alkali metal ions with larger ionic radii ( $K^+$  and  $Cs^+$ ) behaved slightly differently to  $Na^+$ , which has a smaller ionic radius.

The most notable difference between the alkali metal ion doped and standard catalysts were the selectivity to both primary and secondary metathesis products (Table 7.1). If only the selectivity to one of the primary metathesis products, i.e. 7-tetradecene, is studied it is quite clear that doping with cesium and potassium ions does indeed increase the selectivity to primary metathesis products. If the selectivity to secondary metathesis products is however compared the observation is made that selectivity actually increases to secondary metathesis products.

If the percentage branched metathesis products are also compared it becomes clear that alkali doping reduces the branched products considerably. Branched metathesis products are the result of skeletal isomerization of the feed.<sup>11</sup> Skeletal isomerization occurs on acid sites displaying acidity higher than that needed for *cis-trans* isomerization and double bond isomerization.<sup>12</sup> It is expected that skeletal isomerization will occur on stronger acid sites than double bond isomerization. Doping of the catalyst with alkali metal ions targets the stronger acid sites first. The results (Figure 6.12) show that skeletal isomerization and hence branched products, is dramatically reduced by alkali doping.

This is an important observation, as it is well known that branched olefins need to be limited for LAB production. Alkylation of branched olefins lead to LAB's with low biodegradability.<sup>13</sup>

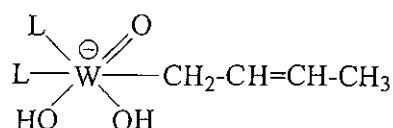
#### 7.3.4 Influence of alkali metal ion loading of metathesis activity

When a 8 wt%  $WO_3/SiO_2$  catalyst is doped with increasing amounts of potassium (Figure 6.15), skeletal isomerization and thus branched metathesis products immediately decrease, while linear  $C_{10}-C_{13}$  metathesis products do not show any significant decrease but rather an increase (between 0.05 wt%  $K^+$  and 0.1 wt%  $K^+$ ). Conversion also declined slowly (Figure 6.16). It is only when large amounts of potassium (0.5 wt%  $K^+$ ), are added to the catalyst that both conversion and selectivity to  $C_{10}-C_{13}$  metathesis products decrease significantly.

**Table 7.1** Influence of 0.1 wt% alkali ion doping on the selectivity of an 8 wt% WO<sub>3</sub>/SiO<sub>2</sub> catalyst for the metathesis of 1-octene.

Alkali metal ion added	No M <sup>+</sup>	Na <sup>+</sup>	K <sup>+</sup>	Cs <sup>+</sup>
Ionic Radius <sup>10</sup> /Å	-	1.02	1.38	1.67
Selectivity C <sub>14</sub> Branched/%	1.4	1.5	0.5	0.5
Selectivity C <sub>14</sub> Linear/%	4.6	4.4	10.6	10.2
Selectivity C <sub>10</sub> -C <sub>13</sub> Branched/%	5.7	2.0	2.0	1.9
Selectivity C <sub>10</sub> -C <sub>13</sub> Linear/%	40.0	47.6	49.2	51.6
% branched C <sub>10</sub> -C <sub>13</sub>	14.3	4.1	4.0	3.7
% branched C <sub>14</sub>	30.4	7.4	4.7	4.9

The proposals of Van Roosmalen and Laverty *et al.*<sup>14,15</sup> will be used to explain the formation of active metathesis centres (see Section 4.4.1). Proton donation occurs by the Lewis acid site-olefin complexes (Scheme 7.2) to tetravalent tungsten followed by reaction of the tungsten hydrides with the olefin. It seems that excessive doping of the catalyst with potassium will result in destruction of the Lewis acidity associated with the tungsten surface compound. The large decrease in linear C<sub>10</sub>-C<sub>13</sub> metathesis products with excessive potassium doping then possibly corresponds to a Lewis catalyzed (allylic) isomerization mechanism.



**Scheme 7.2** The Lewis acid site-olefin complex.

### 7.3.5 The influence of sequence of impregnation of alkali metal ions

Reverse impregnation (first with potassium and then with the tungsten precursor) resulted in a slight decrease in conversion as well as a decrease in selectivity to linear C<sub>10</sub>-C<sub>13</sub> metathesis products (Figure 6.13). This may be further indication that an allylic mechanism

for double bond isomerization is present as potassium probably destroyed Lewis acidity present on the support before impregnation with the tungsten precursor. This could have led to the observed decrease in conversion and double bond isomerization as both these reactions are reliant on Lewis acidity for activity. However, it should be noted that the changes in the activity of the normal and reverse impregnation catalyst are very small and no definite conclusions on the impact of the two techniques can be drawn.

## 7.4 Lifetime, regeneration and coking studies

### 7.4.1 Lifetime and effect of regeneration of the catalyst

The  $\text{WO}_3/\text{SiO}_2$  catalyst has been the subject of many studies; however the longest lifetime indicated in literature is 48 h.<sup>16</sup> Moreover most work on the catalyst has been done with shorter chain olefins.<sup>3</sup> Due to the ease of regeneration and high activity obtained after regeneration, it is possible that the catalysts are regenerated after being online for 48 h. The long run conducted with a fresh 8 wt%  $\text{WO}_3/\text{SiO}_2$  catalyst showed that the catalyst has an online lifetime of around 500 h (Figure 6.16). The run was terminated after the catalyst showed a 10% drop in conversion, but the catalyst was still active at the point of termination. The selectivity towards the primary metathesis products increases with time online as observed by an increase in 7-tetradecene and ethene selectivity (Figure 6.16 and 6.18).

Regeneration of the catalyst results in a slight loss in activity but an increase in selectivity towards the desired products (Figure 6.17). Heckelsberg<sup>17</sup> also reported that the selectivity of the  $\text{WO}_3/\text{SiO}_2$  catalyst towards propene could be improved (with a slight drop in conversion) during the metathesis of 2-butene with ethene after regeneration. This behaviour was also observed by Basrur *et al.*<sup>18</sup> and they concluded that a change in the catalyst structure facilitates this decrease in conversion and increase in selectivity. Reduction of tungsten oxides is known to proceed through intermediate phases which include the  $\text{W}_{20}\text{O}_{58}$ , and  $\text{W}_{18}\text{O}_{49}$  phases.<sup>19</sup> Electron spin resonance (ESR) studies done by Basrur *et al.*<sup>18</sup> indicated that at least some of the  $\text{WO}_3$  that was reduced to a lower state during the reaction could not readily be re-oxidized to  $\text{W}^{6+}$  during regeneration and thus appeared to be in a stabilized non-stoichiometric state. These conclusions show that in a

regenerated catalyst, tungsten oxide is present in at least two different oxidation states and this results in an enhancement of selectivity when the catalyst is regenerated.

The regeneration procedure may also result in a better dispersion of the tungsten oxide on the silica carrier. Spamer *et al.*<sup>20</sup> showed that it is possible that migration of the tungsten occurs on the silica support. Crystallite size analyses (Table 6.4) also show that there are smaller crystallites present on the regenerated catalyst, indicating the possibility of greater dispersion. The acidity of the catalyst seems to be lowered after regeneration. Van Roosmalen and Koster<sup>21</sup> showed that acidity is low on well-dispersed  $\text{WO}_3/\text{SiO}_2$  catalysts. The regenerated catalyst requires twice as long as the fresh catalyst to build up the same amount of coke and this points to a loss of acidity after the regeneration stage.

#### 7.4.2 Characterisation of fresh, spent and regenerated catalysts

A large amount of coke forms inside the pores of the  $\text{WO}_3/\text{SiO}_2$  catalyst during the long runs. All indications are that this coke is predominantly forming inside the pores of the catalyst and not on the surface where the active species are present. Surface area and pore volume measurements (Table 6.4) confirmed that coke occurs primarily in the pores of the catalyst. The pore volume of the catalyst is reduced by a factor of 5.

This excessive build-up of coke inside the pores of the catalyst does not seem to cause any cracking or break-up of the catalyst and is easily removed by regeneration treatment. SEM analysis of the fresh and spent catalyst (Figure 6.21, 6.22) show that the catalyst does not lose its structural integrity even after it accumulates more than 45% coke. There are no cracks visible on the surface of the spent catalyst. Indications are that coke is formed inside the pores of the catalyst, as grooves created by grinding the catalyst are still visible on a catalyst with more than 45% coke (Figure 6.19, 6.20).

#### 7.4.3 Location of coke on the catalyst

EFTEM can be a useful tool for locating the carbon on a coked catalyst. The technique provides a way for differentiating between silica and carbon. A carbon map was done on

the catalyst (Figure 6.24) and it indicated that most of the carbon was located around the tungsten oxide cluster and did not cover it to a great extent.

This observation can offer an explanation for the long lifetime of the catalyst. Thomas *et al.*<sup>3</sup> proposed that active sites may be located at the boundary of the tungsten oxide crystallite and the silica. The carbon map shows that at even high coke levels the tungsten oxide is still exposed. The active sites present in this boundary region may be still able to metathetically convert reactant olefins. It is expected that as coke levels increase, these sites will eventually be blocked by coke and catalyst deactivation will consequently result.

#### 7.4.4 Factors effecting coke formation

##### 7.4.4.1 Coke formation as a function of temperature

As can be seen from Figure 6.26, coke formation increases with an increase in reaction temperature. This result is expected because the formation of coke is thermodynamically favoured at higher temperatures.<sup>22</sup>

It is therefore favourable to work at lower temperatures to reduce the rate of coke laydown. However if much lower temperatures are employed this may result in lower tolerance levels towards typical catalyst poisons.<sup>23</sup> At high temperatures, there is enough energy available to keep the catalyst from deactivating. Also lower temperatures may result in loss in activity as it has been reported that temperature is related to the activity.<sup>24</sup>

##### 7.4.4.2 Coke formation as a function LHSV

It can be concluded from Figure 6.27 that increasing the LHSV increases the rate of coke formation. The greater the LSHV, the higher the amount of reactable feed passing through the catalyst bed. This shows that the rate of coke formation is related to the amount of olefin feed, rather than the contact time.

Working at lower LHSV will be useful in reducing coke formation on the catalyst. However decreasing the LHSV will increase the contact time of the feed with the catalyst

and will enhance side reactions such as isomerization. At lower LHSV's, a high conversion but poor selectivity toward the primary metathesis product will be obtained.

#### **7.4.4.3 Coke formation as a function of time on-line**

The rate of coke formation increases almost linearly with time online as shown in Figure 6.28. This may provide an explanation for the change in selectivity of the catalyst with increasing time online. Coke formation results as a consequence of side reactions catalyzed by acid sites.<sup>22</sup> The coke formed may cover these acid sites resulting in loss of isomerization activity of the catalyst.<sup>25</sup> As a result of this, the selectivity toward the primary metathesis product will increase. Eventually coke deposits will cover all the active sites and result in catalyst deactivation.

#### **7.4.4.4 Influence of olefin content in feed on coke formation**

Figure 6.29 shows that the rate of coke formation increased with increasing olefin to paraffin content in the feed. This implies that olefins have a faster rate of coking than paraffins. This was demonstrated by Panchenkov *et al.*<sup>26</sup> with silica-alumina cracking catalysts.

The industrial cut heptene feed has 15% n-heptane present. It is possible to tailor the ratio of olefin to paraffin in the feed depending on the desired rate of coke laydown. It is not practical to work with 100% olefin feed as this will result in faster deactivation of the catalyst by coke deposition.

#### **7.4.4.5 Influence of oxygenates on coke formation on the 8 wt% $WO_3/SiO_2$ catalyst**

Various additives may be used to reduce coke on acid catalysts.<sup>27</sup> The addition of alkali metal ions to acid catalysts is known to reduce coke formation but this may also result in loss of activity.<sup>28</sup> Hydrogen is used as an important coke retarding reactant in several hydrocarbon conversion processes such as FCC (Fluid catalytic cracking) and catalytic reforming.<sup>22</sup> However the optimal amount of hydrogen must be employed or the catalyst may be deactivated by over-reduction.<sup>8</sup>

Kozhevnikov *et al.*<sup>29</sup> showed that oxygenates can be used as coke inhibiting agents for a silica-supported heteropoly acid catalyst used in propene oligomerization. The addition of water, methanol and acetic acid to the propene flow reduced coking. Water was reported as the most effective inhibitor.

The addition of 100 ppm of butanol, water and 2-pentanone had a significant influence on the rate of coke formation (Figure 6.31), without affecting the activity of the  $\text{WO}_3/\text{SiO}_2$  catalyst (Figure 6.30). The Lewis base 2-pentanone had the greatest effect on coke formation and resulted in reducing the rate of coke formation by almost half. Water and butanol also reduced the amount of coke formed.

The oxygenates may reduce coke formation by blocking acid sites which catalyze side reactions that lead to coke. This is an important result as it provides a way to reduce coke formation on the catalyst without affecting the catalyst performance significantly.

## **7.5 Influence of oxygenates on the activity and selectivity of the 8 wt% $\text{WO}_3/\text{SiO}_2$ catalyst**

### **7.5.1 Influence of Lewis bases on the activity and selectivity of the 8 wt% $\text{WO}_3/\text{SiO}_2$ catalyst**

The 8 wt%  $\text{WO}_3/\text{SiO}_2$  catalyst operates at high temperatures and as a consequence higher tolerance towards poisons is expected. However it has been reported in literature that oxygenated components are catalyst poisons.<sup>30</sup> The oxygenates act as temporary poisons and the reintroduction of a pure feed stream results in the gain of initial activity.

The Lewis bases, 2-pentanone, ethyl acetate and hexanal were used to test the tolerance levels of the catalyst. The maximum tolerance levels for these components are shown in Table 7.2. The selectivity of the catalyst towards the detergent range olefins decreased after the maximum tolerance level of Lewis base as indicated in Figures 6.32-34.

The 8 wt%  $\text{WO}_3/\text{SiO}_2$  catalyst has the same maximum tolerance level for the ketone, 2-pentanone and ester ethyl acetate. However the catalyst could tolerate a greater level of the aldehyde. These results are different from those obtained by du Plessis *et al.*<sup>9</sup> with a low

temperature heterogeneous  $\text{Re}_2\text{O}_7/\text{Al}_2\text{O}_3$  catalyst system. They showed that ketones have a greater effect on the catalyst than esters. The  $\text{WO}_3/\text{SiO}_2$  catalyst however operates at much higher temperatures and consequently the reactivity of these poisons will not be the same.

**Table 7.2** The maximum tolerance level for Lewis bases over an 8 wt%  $\text{WO}_3/\text{SiO}_2$  catalyst.

Lewis bases	Maximum tolerance level (ppm)
2-Pentanone	500
Ethyl acetate	500
Hexanal	1000

A possible explanation for the higher resistance towards aldehydes is that they may undergo aldol condensation reactions, effectively decreasing the carbonyl concentration. In aldol condensation reactions, a simple aldehyde may be converted to an aldol (a molecule containing both aldehyde and alcoholic groups).<sup>31</sup> The case is illustrated for acetaldehyde in Scheme 7.3. Moggi and Albanesi<sup>32</sup> showed that gas phase aldol condensation readily proceeds over  $\text{WO}_3/\text{SiO}_2$  catalysts.

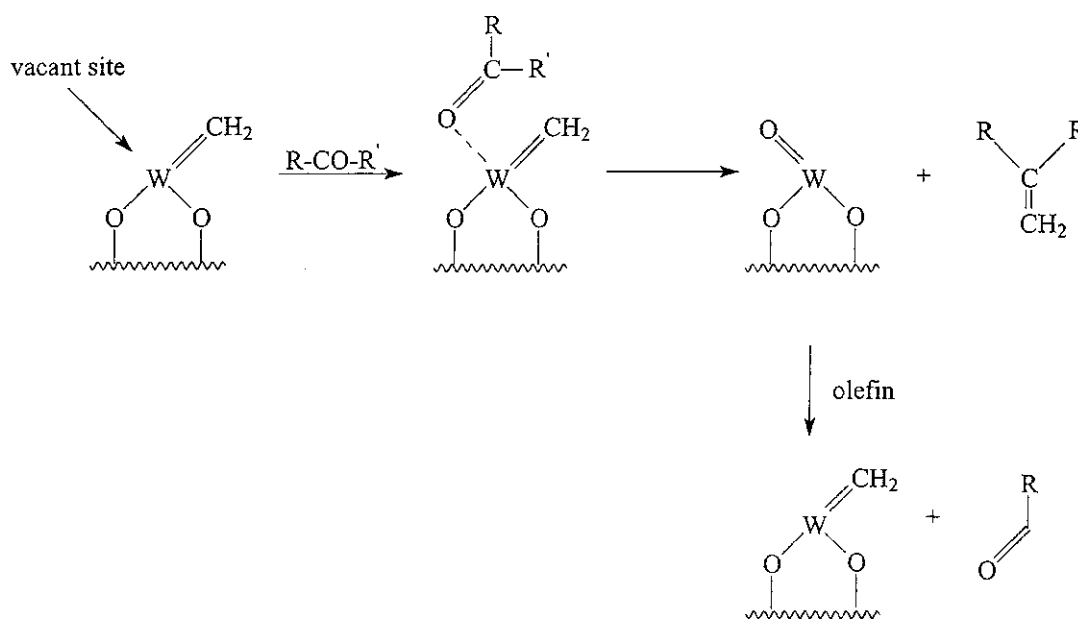


**Scheme 7.3** The aldol condensation reaction of acetaldehyde.

#### 7.5.1.1 The mechanism of deactivation by Lewis bases

It is generally accepted that the metal carbene moiety is the active species for the olefin metathesis reaction.<sup>1</sup> 2-Pentanone, ethyl acetate and hexanal are Lewis bases containing a carbonyl group. The oxygen atom of the carbonyl group on the Lewis base has two lone pairs of electrons that could be donated to the empty orbital on the metal centre. Therefore it is possible for the Lewis base to react with the metal carbene in a Wittig-type fashion.<sup>33</sup>

It is therefore proposed that the Lewis base can undergo a “hetero-atom metathesis” reaction that involves exchange of an oxygen atom between the metal carbene of the tungsten catalyst and the carbonyl group of the Lewis base. The requirement of such a reaction is that both molecules contain a double bond. The proposed mechanism of this reaction is illustrated in Scheme 7.4. The Lewis base deactivates the catalyst to an inactive oxide state. The catalyst can then be reactivated by reintroduction of pure feed.



**Scheme 7.4** Mechanism of deactivation by Lewis bases.

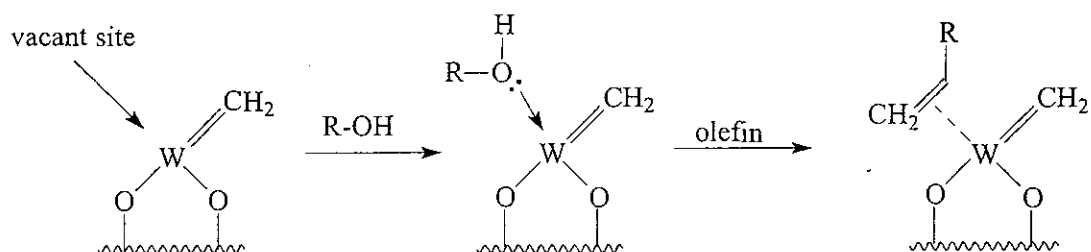
### 7.5.2 Influence of Brönsted acids on the activity and selectivity of the 8 wt% WO<sub>3</sub>/SiO<sub>2</sub> catalyst

Brönsted acids like water and butanol are known catalyst poisons.<sup>30</sup> The catalyst was able to easily tolerate water at the saturation level (104 ppm) in the feed (Figure 6.35). The catalyst activity and selectivity was not affected at all by this level of water. The tolerance level for butanol was 500 ppm (Figure 6.36).

#### 7.5.2.1 Mechanism of deactivation by Brönsted acids

The effect of Brönsted acids may be due to blocking of active sites (Scheme 7.5). The alcohol and the olefin compete for the same active site on the metal centre. If the active

sites are blocked by the presence of the alcohol, the high temperature of the reaction and the excess of olefin feed could remove it. The metal centre will then be available for coordination of the olefin. The effect of the Brönsted acid is therefore reversible.



**Scheme 7.5** Mechanism of deactivation by Brönsted acids.

### 7.5.3 The influence of oxygenates on the activity and selectivity of the 8 wt% $\text{WO}_3/\text{SiO}_2$ catalyst in the recycle mode

The influence of 2-pentanone on the activity of the catalyst in the recycle mode is shown in Figure 6.37. The maximum tolerance level towards the oxygenate is 300 ppm. This indicates that oxygenates do build up concentration in the recycle loop as the tolerance to oxygenates is 500 ppm in the once through mode.

The boiling point of 2-pentanone is 102 °C and it is expected that this component will be separated in the first column at 220 °C, pass through to the second column and be collected at purge 2. However analysis revealed that carbonyls were present in both purge 1 and 2. This indicates that 2-pentanone is converted to longer or shorter analogues and this could result from the proposed mechanism in Scheme 7.5. Reintroduction of pure feed results in the catalyst regaining its original activity, indicating that this mode of deactivation is reversible, again supporting the proposed mechanism.

### 7.5.4 The influence of oxygenates on the colour of the product

Observations made from the addition of oxygenates in the recycle (Figure 6.38) and once through mode (Figures 6.40, 6.42, 6.44, 6.46) show that trace amount of oxygenates can be used to significantly reduce the colour of the product. Brönsted acids and Lewis bases

result in a reduction of colour in the product. Reintroducing the pure feed causes the colour to increase. The activity and selectivity of the catalyst is not effected by the addition of a maximum level of 400 ppm of these oxygenates (Figure 6.39, 6.41, 6.43, 6.45).

The influence of a fixed concentration of 2-pentanone is shown in Figure 6.47. The activity and selectivity of the catalyst is not significantly affected. The colour of the product decreases when 2-pentanone is introduced (Figure 6.48). The colour increases upon the introduction of pure feed. This confirms that the effect of the oxygenate is reversible.

A clearer product is desirable as it increases the product quality and hence the value. A clearer product is advantageous from a marketing point of view.<sup>34</sup>

It is known that highly conjugated molecules and polyaromatic compounds appear coloured.<sup>35</sup> Mechanistically, colour is the result of excitation of electrons in the molecular orbitals to new temporary states.<sup>36</sup> Excitation occurs in the highest occupied molecular orbital (HOMO) to a higher unoccupied state, i.e., the lowest unoccupied molecular orbital (LUMO). The greater the number of  $\pi$ -electrons, the greater the number of resulting molecular orbitals and the smaller the HOMO – LUMO gap. This explains why simple aromatics are essentially colourless and polyaromatics, which have extended conjugated system of  $\pi$ -electrons, appear coloured.<sup>37</sup> Trace quantities of these components may cause colouration.

It is proposed that the yellow colour is imparted to the product due to the formation of polyaromatic compounds. These polyaromatic compounds result as a consequence of side reactions on acid sites (reactions that lead to coke formation) as shown in Scheme 3.10. The oxygenates may act by blocking the acid sites that lead to the eventual formation of these components. It is therefore possible to use oxygenates as additives to enhance the colour of the product.

Oxygenates are present in most Fischer-Tropsch derived feed streams.<sup>38</sup> Expensive feed preparation routes (extractive distillation) are generally required to remove all the oxygenates. Allowing trace amounts of oxygenates in the feed (below the maximum tolerance level of 300 ppm) may be less costly in terms of feed preparation and at the same time advantageous towards that colour of the product.

## 7.6 Summary

During this investigation it was found that the 8 wt%  $\text{WO}_3/\text{SiO}_2$  catalyst was effective for the metathetical conversion of 1-octene or 1-heptene to longer chain internal olefins in the detergent range. Various factors were investigated and the following conclusions were drawn:

- (a) Characterisation of catalysts with different metal loadings showed that crystalline  $\text{WO}_3$  is the predominant species on catalyst with higher loadings. The  $\text{WO}_3$  is well dispersed at lower loadings and is present a surface species. The activity of the catalyst increase with loading up to 6 wt% and is independent of any further increase in metal loading. This gives an indication that crystalline material does not contribute significantly to the metathesis activity. The stability of the catalysts is greater at loadings of 8 wt% and higher which suggests that crystalline material may play a stabilising role by preventing over-reduction of the active species.
- (b) Alkali metal ion doping can be used to significantly reduce the formation of branched metathesis products and is thus useful for curbing skeletal isomerization activity. Excessive doping ( $> 0.5\%$ ) results in loss of Brønsted acidity and hence a dramatic loss of metathesis activity.
- (c) The 8 wt%  $\text{WO}_3/\text{SiO}_2$  catalyst has a long lifetime (700 h) when operating in the recycle mode using the optimised conditions used (460 °C, 16  $\text{h}^{-1}$  and 1:5.6 feed: recycle ratio). Regeneration of the catalyst results in a longer lifetime (1200 h) suggesting a decrease in acidity or better dispersion. Coke formation seems to be the cause of deactivation. The catalyst seems to coke from inside the pores and these act as reservoirs for the deposits.
- (d) Carbon maps (EFTEM) of the coked catalyst showed that carbon was located around the  $\text{WO}_3$  clusters and did not cover them. This explains why the catalyst is still active even after the accumulation of excessive amounts of coke
- (e) Coke formation is dependent on a number of factors including temperature, time online, LHSV and amount of olefin. Trace quantities of oxygenates (100 ppm) can

be used as coke retarding additives. These may act by blocking acid sites that result in reactions that lead to coke formation.

- (f) The catalyst is sensitive to the typical oxygenates (300 ppm in the recycle mode) present in an FT-derived feed stream however the effect of these poisons is reversible upon reintroduction of a pure feed stream. The oxygenates lower the intensity of the yellow colour of the product which is believed to be caused by polyaromatics. This effect may prove to be beneficial in terms of the quality of the final product.

## 7.7 References

1. J. C. Mol in *Handbook of Heterogeneous Catalysis*, Volume 5, G. Ertl, H. Knozinger, J. Weitkamp (Eds.), Wiley-VCH (Weinheim), 1997, p. 2387
2. F. P. J. M. Kerkhof, R. Thomas, J. A. Moulijn, *Rec. Trav. Chim. Pays-Bas*, 1977, **96**, M121
3. R. Thomas, J. A. Moulijn, F. P. J. M. Kerkhof, *Rec. Trav. Chim. Pays-Bas*, 1977, **96**, M134
4. W. Grunert, *Indian J. Technol.*, 1992, **30**, 113
5. A. J. van Roosmalen, J. C. Mol, *J. Chem. Soc., Chem. Commun.*, 1980, 704
6. N. C. Ramani, D. L. Sullivan, J. R. Ekerdt, *J. Catal.*, 1998, **173**, 105
7. A. Andreini, J. C. Mol, *J. Chem. Soc., Faraday Trans. 1*, 1985, **81**, 1705
8. K. J. Ivin, J. C. Mol, *Olefin Metathesis and Metathesis Polymerization*, Academic Press (London), 1997
9. J. A. K. du Plessis, A. Spamer, H. C. M. Vosloo, *J. Mol. Catal. A: Chem.*, 1998, **133**, 175
10. R. D. Shannon, *Acta Cryst.*, 1976, **A32**, 751
11. S. van Donk, J. H. Bitter, K. P. de Jong, *Appl. Catal. A: Gen.*, 2001, **212**, 97
12. J. P. Damon, B. Delmon, J. M. Bonnier, *J. Chem. Soc., Faraday Trans. 1*, 1977, **73**, 372
13. C. Perego, P. Ingallina, *Catal. Today*, 2002, **73**, 3
14. A. J. van Roosmalen, J. C. Mol, *J. Mol. Catal.*, 1982, **78**, 17
15. D. T. Lavery, J. J. Rooney, A. Stewart, *J. Catal.*, 1976, **45**, 110
16. E. D. Oliver, *Butylenes; SRI report no. 71*, October 1971, p. 145
17. L. F. Heckelsberg (to Phillips Petroleum Co.), US Pat. 3365513, 1968 (3 January)
18. A. G. Basrur, S. R. Patwardan, S. N. Vyas, *J. Catal.*, 1991, **127**, 86
19. S. Venables, M. E. Brown, *Thermochim. Acta*, 1997, **291** (1-2), 131
20. A. Spamer, J. M. Botha, D. J. Moodley, C. van Schalkwyk, T. Dube, *Appl. Catal. A: Gen.*, 2003, article in press
21. A. J. van Roosmalen, D. Koster, J. C. Mol, *J. Phys. Chem.*, 1980, **84**, 3075
22. J. R. Rostrup-Nielsen, *Catal. Today*, 1997, **37**, 225
23. P. Forzatti, L. Letti, *Catal. Today*, 1999, **52**, 165.
24. A. J. Moffat, A. Clark, *J. Catal.*, 1970, **17**, 264.
25. E. E. Wolf, F. Alfani, *Catal. Rev. Sci. Eng.*, 1982, **24**, 239.

26. G. M. Panchenkov, M. E. Levinter, M. A. Tanatarov, B. F. Moroziv, *Int. Chem. Eng.*, 1968, **8**, 582.
27. K. Tanabe, *New Solid Acids and Bases; Their Catalytic Properties, Studies in surface science and catalysis*, Volume 51, Kodansha (Tokyo), 1989, 204.
28. W. D. Mross, *Catal. Rev. Sci. Eng.*, 1983, **25** (4), 591.
29. I. V. Kozhevnikov, S. Holmes, M. R. H. Siddiqui, *Appl. Catal. A: Gen.*, 2001, **214**, 27
30. R. L. Banks in *Applied Industrial Catalysis*, Volume 3, B. E. Leach (Ed.), Academic Press (New York), 1984, p. 215
31. J. March, *Advanced Organic Chemistry*, Wiley (New York), 1984, p. 830
32. P. Moggi, G. Albanesi, *Appl. Catal.*, 1991, **68**, 285
33. A. Agüero, J. Kress, J. A. Osborn, *J. Chem. Soc., Chem. Commun.*, 1986, 531
34. Shell Chemicals, 2003, Neodol Detergent Alcohols, <http://www.shellchemicals.com/neodol/1,1098,876,00.html>, 23 June 2003
35. R. P. Bauman, *Absorption Spectroscopy*, Wiley (New York), 1962, p. 315
36. C. N. R. Rao, *Ultra-Violet and Visible Spectroscopy: Chemical Applications*, Butterworths (London), 1975, p. 13
37. C.E. Wallace, 2000, UV Visible Spectroscopy, [http://websites.anderson.edu/~cewallace/class%20info/org\\_spec/UV/UV.ppt](http://websites.anderson.edu/~cewallace/class%20info/org_spec/UV/UV.ppt), 23 June 2003
38. A. P. Steynberg, R. L. Espinoza, B. Jager, A. C. Vosloo, *Appl. Catal. A: Gen.*, 1999, **186**, 41

## SUMMARY

---

In this study,  $\text{WO}_3/\text{SiO}_2$  catalysts were investigated for the metathesis of 1-octene or  $\text{C}_7$  SLO (an industrial cut 1-heptene) to longer chain internal olefins in the detergent range. The catalysts were active for metathesis at high temperature (460 °C). The catalyst has appreciable isomerization activity and this facilitates secondary metathesis reactions, which results in a broad product spectrum.

$\text{WO}_3/\text{SiO}_2$  catalysts of different  $\text{WO}_3$  loadings were prepared and characterized by BET, XRD, TEM and LRS. The catalysts having lower metal loadings showed better  $\text{WO}_3$  dispersion on the support and seemed to be composed mainly of the surface tungsten compound. Catalysts with higher loadings had mainly crystalline material present. These results are in agreement with literature. The metathesis activity increases up to a loading of 6 wt%, stabilizes and is constant independent of further  $\text{WO}_3$  loading. Selectivity to branched metathesis products is lower on catalysts with lower metal loading while selectivity towards the primary metathesis products increases. The stability of the catalysts containing more than 7 wt%  $\text{WO}_3$  was higher.

Doping of the 8 wt%  $\text{WO}_3/\text{SiO}_2$  catalyst with 0.1 wt% of alkali metal ion resulted in a decrease in both the metathesis activity and selectivity towards unwanted branched products. Doping of the catalyst with more than 0.5 wt% of alkali metal ion resulted in a sharp decrease in the conversion. There was no definite correlation between the size of the alkali metal ion and the activity of the catalyst. There were no major differences in the catalyst behavior when using the reverse and normal impregnation techniques.

The lifetime of the catalyst was approximately 700 h when using the original optimized conditions (460 °C, 16  $\text{h}^{-1}$  LHSV, 1:5.6 feed to recycle ratio). An appreciable amount of coke (46%) built up on the catalyst during the run. Regeneration of the catalyst resulted in a longer lifetime (1200 h) and the catalyst took twice as long to build up the equivalent amount of coke. The regenerated catalyst showed a higher selectivity indicating a change in morphology and a possible lowering of acidity. Most of the coke formed on the catalyst seems to be located in the pores. EFTEM showed that carbon was deposited around the

WO<sub>3</sub> clusters and did not cover them. Some active sites are still exposed which could explain the activity of the catalyst even when coke levels are high.

Coke formation increases with time online, LHSV, temperature and olefin content in the feed. Inhibition of coke formation, without significant loss of activity can be achieved by co-feeding 100 ppm of oxygenated components, e.g. 100 ppm of 2-pentanone decreased coke formation considerably. The oxygenates may inhibit coke formation by blocking active sites that catalyze side reactions that lead to coke formation.

The catalyst is deactivated by typical oxygenates present in a Fischer-Tropsch derived feed stream. Both Brønsted acids and Lewis bases are responsible for deactivation of the catalyst. The maximum tolerance for the oxygenates was 500 ppm in the once through mode and 300 ppm in the recycle mode. The effect of the oxygenates is reversible when a pure feed is reintroduced. Trace quantities of oxygenates may be used to reduce the yellow colour of the product thus enhancing product quality.

## OPSOMMING

---

### **Die metatieseaktiwiteit en deaktivering van heterogene metaaloksiedkatalisatorsisteme**

In hierdie studie is 'n  $\text{WO}_3/\text{SiO}_2$ -katalisator ondersoek vir die metatiese van 1-okteen of C7 SLO ('n industriële 1-hepteensnit) na 'n langer ketting interne olefien in die wasmiddelgebied. Die katalisator was by hoë temperature aktief ( $460\text{ }^\circ\text{C}$ ) vir metatiese. Die katalisator het merkbare isomerisasie-aktiwiteit en dit fasiliteer sekondêre metatesereaksies wat tot a breë produkspektrum aanleiding gee.

$\text{WO}_3/\text{SiO}_2$  katalisatore met verskillende  $\text{WO}_3$ -ladings is berei en met behulp van BET, XRD, TEM en LRS gekarakteriseer. Die katalisatore met laer  $\text{WO}_3$ -ladings toon 'n beter verspreiding van die metaal op die ondersteuningsmateriaal en dit wil voorkom asof dit hoofsaaklik uit die oppervlak wolframkompleks saamgestel is. Katalisatore met hoër ladings bevat hoofsaaklik kristallyne materiaal. Die resultate stem ooreen met dit wat in die literatuur gevind word. Die metatieseaktiwiteit neem toe tot by 'n lading van 6 massa % waarna dit stabiliseer en konstant bly ongeag of die lading verhoog word. By laer ladings neem die selektiwiteit ten opsigte van vertakte metateseprodukte af, terwyl die selektiwiteit tot die primêre metateseprodukte toeneem. Die stabiliteit van die katalisatore wat meer as 7 massa % bevat het was hoër.

Behandeling van die 8 massa %  $\text{WO}_3/\text{SiO}_2$ -katalisator met 'n 0.1 massa % alkali-metaalioon veroorsaak 'n afname in beide die metatieseaktiwiteit en selektiwiteit ten opsigte van die ongewenste vertakte produkte. Behandeling van die katalisator met meer as 0.5 massa % alkalimetaalioon het tot 'n drastiese afname in die omsetting gelei. Daar was geen onderlinge verband tussen die grootte van die alkalimetaalioon en die aktiwiteit van die katalisator nie. Daar was geen verskille in die katalisatorgedrag indien 'n normale of 'n omgekeerde impregneringsmetode gebruik is nie.

Die leeftyd van die katalisator was ongeveer 700 h indien die oorspronklike geoptimeerde reaksiekondisies ( $460\text{ }^\circ\text{C}$ ,  $16\text{ h}^{-1}$  LHSV, 1:5.6 voer-tot-hersikuleer-verhouding)

gebruik is. 'n Merkbare hoeveelheid kooks (46%) het tydens die lopie op die katalisator opgebou. Regenerering van die katalisator het tot 'n langer leeftyd (1200 h) aanleiding gegee en die katalisator het tweekeer langer geneem om dieselfde hoeveelheid kooks op te bou. Die geregenereerde katalisator het 'n hoër selektiwiteit vertoon wat op 'n verandering in morfologie en die moontlike verlaging van die suurhied dui. Meeste van die kooks wat op die katalisator gevorm het, blyk in die porieë gekonsentreer te wees. EFTEM het getoon dat die koolstof rondom die  $WO_3$ -trosse gedeponeer is en dit nie bedek nie. Sommige van die aktiewe punte is nog steeds oop wat die aktiwiteit van die katalisator verduidelik selfs waneer die kooksvlakke hoog is.

Kooksvorming neem toe met 'n toename in aanlyntyd, LHSV, temperatuur en olefieninhoud van die voer. Onderdrukking van kooksvorming, sonder 'n beduidende verlies aan aktiwiteit, kan verkry word deur 100 dpm suurstofbevattende bymiddels by die voer te voeg. Byvoorbeeld, 100 dpm 2-pentanoon het kooksvorming aansienlik laat afneem. Die oksigenate kan kooksvorming onderdruk deur die aktiewe punte, wat newereaksies kataliseer, te blokkeer.

Die katalisator word gedeaktiveer deur die tipiese oksigenate wat in 'n Fischer-Tropsch-afgeleide voerstroom voorkom. Beide Brönsted-sure en Lewis-basisse is verantwoordelik vir die deaktivering van die katalisator. Die maksimum bestandheid teen oksigenate was 500 dpm in die eenmaal-deurmetode en 300 dpm in die hersikuleringsmetode. Die effek van die oksigenate is omkeerbaar indien skoon voer weer gebruik word. Spoorhoevelhede oksigenate kan gebruik word om die geel kleur van die produk te verminder en sodoende die kwaliteit van die produk te verhoog.

## ACKNOWLEDGMENTS

---

First and foremost I want to thank the Lord Jesus Christ for granting me His grace to complete this study.

I would like to extend my gratitude to my supervisor and co-supervisor, Prof. H.C.M Vosloo and Dr C. van Schalkwyk for their guidance. My appreciation also goes to the High temperature Metathesis Group at Sasol Technology especially Dr. J.M Botha, Dr. A. Spamer and Mr. T. Dube for their valuable contributions. I would like to acknowledge Prof. Abhaya Datye of the University of New Mexico for the EFTEM work. I would also like to thank SASOL for funding this study.

To my parents, Ronnie and Savy, my sister, Camy and my fiancée Prabashini, thank you for all your love and support.